ISTANBUL TECHNICAL UNIVERSITY ★ GRADUATE SCHOOL

INVESTIGATION OF INTERACTING MULTIPLE FATIGUE CRACKS PROPAGATION USING TWO-DIMENSIONAL BOUNDARY CRACKLET METHOD

Ph.D. THESIS

Talal AHMED

Department of Aeronautics and Astronautics Engineering

Aeronautical and Astronautical Engineering Programme

APRIL 2021

ISTANBUL TECHNICAL UNIVERSITY ★ GRADUATE SCHOOL

INVESTIGATION OF INTERACTING MULTIPLE FATIGUE CRACKS PROPAGATION USING TWO-DIMENSIONAL BOUNDARY CRACKLET METHOD

Ph.D. THESIS

Talal AHMED
(511172126)

Department of Aeronautics and Astronautics Engineering

Aeronautical and Astronautical Engineering Programme

Thesis Advisor: Prof. Dr. Halit S. TÜRKMEN
Thesis Co-Advisor: Prof. Dr. Abdülkadir YAVUZ

APRIL 2021

İSTANBUL TEKNİK ÜNİVERSİTESİ ★ LİSANSÜSTÜ EĞİTİM ENSTİTÜSÜ

İKI BOYUTLU SINIR ÇATLAK ELEMANI YÖNTEMI (BOUNDARY CRACKLET METHOD) KULLANILARAK ETKILEŞIMLI ÇOKLU YORULMA ÇATLAKLARININ İLERLEMESININ ARAŞTIRILMASI

DOKTORA TEZİ

Talal AHMED
(511172126)

Uçak ve Uzay Mühendisliği Anabilim Dalı
Uçak ve Uzay Mühendisliği Programı

Tez Danışmanı: Prof. Dr. Halit S. TÜRKMEN
Eş Danışman: Prof. Dr. Abdülkadir YAVUZ

NİSAN 2021

Talal AHMED, a Ph.D. student of İTU Graduate School student ID 511172126, successfully defended the thesis/dissertation entitled "INVESTIGATION OF INTERACTING MULTIPLE FATIGUE CRACKS PROPAGATION USING TWO-DIMENSIONAL BOUNDARY CRACKLET METHOD", which he prepared after fulfilling the requirements specified in the associated legislations, before the jury whose signatures are below.

Thesis Advisor :	**Prof. Dr. Halit S. TÜRKMEN** Istanbul Technical University	....
Co-advisor :	**Prof. Dr. Abdülkadir YAVUZ** Higher Colleges of Technologies (HCT) Abu-Dhabi, UAE	....
Jury Members :	**Prof. Dr. Şafak YILMAZ** Istanbul Technical University	....
	Prof. Dr. Şenol ATAOĞLU Istanbul Technical University	....
	Prof. Dr. Haydar LİVATYALI Yıldız Technical University	....
	Assoc. Prof. Dr. Mesut KIRCA Istanbul Technical University	....
	Asst. Prof. Dr. Üyesi Sedat SÜSLER Kocaeli University	....

Date of Submission : 13 March 2021
Date of Defense : 28 April 2021

To my beloved parents

FOREWORD

All praises and thanks be to Almighty Allah, the most beneficent and the most merciful, Who enabled me to complete this research work successfully.

I would like to thank my both advisors, Dr. Halit S. TÜRKMEN and Dr. Abdülkadir YAVUZ for all their help and technical guidance during my entire research work. Without their support, it will not be possible for me to complete this research. I also thank all the jury members for their valuable suggestions and guidance during my research work.

I want to acknowledge the financial support of this research from the scientific research projects unit (BAP), Istanbul Technical University under Project No. MDK-2020-42460 and like to acknowledge the National Center for High Performance Computing of Turkey (UHeM) for providing the computing resources for this work under grant number 1008652020.

I also wish to offer my humble gratitude to my parents and like to thank them for their unconditional love and support in every field of my life. I am also extremely thankful to all my friends and colleagues for their help and support.

In the end, I would like to thank my wife and children for all their love and friendship which kept me motivated throughout my graduate study.

March 2021 Talal AHMED

TABLE OF CONTENTS

Page

ABBREVIATIONS

BCM	**:** Boundary cracklet method
ED	**:** Edge dislocation
EDD	**:** Edge dislocation distribution
FCG	**:** Fatigue crack growth
FCP	**:** Fatigue crack propagation
MSED	**:** Minimum strain energy density
MTS	: Maximum tangential stress
ODPs	**:** Opening displacement profiles
SIFs	**:** Stress intensity factors

SYMBOLS

a	: Crack length
a_0	: initial crack length
b_1, b_2	: Burger's vectors in tangential and normal direction respectively
C	: Paris equation constant
Δc	: Crack incremental length
da/dN	: Crack growth rate
E	: Elastic modulus of material
G	: Shear Modulus of the material
$K_{I,II}$	: Stress intensity factor for crack opening mode I and II, respectively
$\Delta K_{I,II}$	: Stress intensity range for crack opening mode I and II, respectively
L	: Specimen length
m	: Paris equation exponent
N	: Number of loading cycles
R	: Stress ratio (σ_{min} / σ_{max})
t	: CPU time (hours)
W	: Specimen width
YCF	: Yavuz's fatigue computational efficiency factor
α	: Crack position angle
β	: Crack orientation angle
λ	: biaxiality stress ratio (σ_x / σ_y)
ρ	: Eigen value
ν	: Poisson's ratio
σ	: Stress
Δσ	: Stress range
ω	: Wedge angle

LIST OF TABLES

Page

LIST OF FIGURES

Page

INVESTIGATION OF INTERACTING MULTIPLE FATIGUE CRACKS PROPAGATION USING TWO-DIMENSIONAL BOUNDARY CRACKLET METHOD

SUMMARY

Aircraft structures experience fatigue loading emanating from different sources e.g. variation of aerodynamic loads on wings and repetitive pressurizing and depressurizing the cabin of the aircraft etc. It is a well-known fact that fatigue loading is more responsible for the failure of aircraft structures as compared to static loading because a single surface crack can lead to a catastrophic failure due to fatigue loading. At the early stages of the life of aircraft, these surface cracks have no effect on the structural integrity of the aircraft, but with the passage of time, environmental effect, and nature of loading these cracks propagate and interact with each other. These cracks propagate, up to the point where the remaining cross-section of the component is not being capable of carrying the loads and the component will be subjected to sudden fracture.

The failures due to fatigue usually start at small surface cracks which act as local stress raisers and propagate and interact with each other and turn into large damage-producing cracks. In practice, these micro surface cracks are always likely to be present in many aircraft structural components even the newly made components can have these cracks due to certain imperfections in machining processes during the manufacturing of aircraft. To produce a damage tolerance design and to meet the certain requirements of certifications applicable in the aerospace industry, it becomes very important to know the behaviour of aerospace structures in the presence of these inevitable surface cracks under fatigue loading. Thus, a fast and accurate method of predicting the behaviour of these cracks under fatigue loading plays a vital role. This fact forces engineers to develop new methods and models which can simulate the effects of existing cracks so that they can predict the remaining useful life of aircraft structure more accurately. Such methods and simulation techniques not only reduce the high cost of physical testing of the aerospace structures but also play a crucial role in producing a better design of these structures.

For the analysis of planar cracks, different commercial tools are available, which are mostly based on the analytical formulations and different handbook solutions e.g. NASGRO and AFGROW. These software packages can simulate the fatigue crack growth (FCG) problems of predefined cracks under mode-I loading conditions only, but most of the real problems in the industry are under the influence of mix mode loading where crack tip grows under the effect of both mode-I and mode-II loading conditions. Therefore, these software packages cannot handle such complex problems of mix mode crack growth. Finite element methods are also being used from a long time for the study of FCG. These methods can simulate the interactions of cracks with reasonably good accuracy. But, due to the requirement of fine mesh at the crack tip, generation of a representation of the crack advancement and regeneration of FE mesh after each iteration of FCG, make these methods challenging to adopt. To overcome

these difficulties of FEM, in 1999, a mesh-independent method called Extended-FEM (XFEM) with minimal re-meshing was developed and since then a continuous improvement has been seen in the implementation of these methods. However, the accuracy of these methods decreases as the complexity of the problem increases and still a lot of research efforts are underway to overcome this shortcoming.

By considering the above-mentioned limitations of the conventional methods to analyse the FCG of problems involving multiple cracks under mixed-mode conditions, there is always room to develop such methods which can mitigate the deficiencies of these methods. Recently, in 2006, a fast and accurate semi-analytical method called Boundary Cracklet Method (BCM) is developed by Prof. Dr. A. K. Yavuz (co-advisor of this study) and Prof. Dr. S. L. Phoenix at Cornell University, to find the overall stress field and the stress intensity factor (SIF) for crack tips and crack singular wedges at the crack kinks. This method is based on the dislocation distribution approach which approximates the crack opening displacement profiles by using certain power series that satisfy the traction-free condition on crack faces. Unlike the conventional mesh dependent methods, where a very fine mesh is required to overcome the stress singularities around crack tips, BCM takes care of crack tip singularities by including wedge eigenvalues in power series and makes sure that all integrals necessary to calculate stress fields are in closed form to give fast solutions. The solution of these integrals is the most time-consuming part in other mesh-dependent methods such as FEMs and BEMs. Moreover, only a few numbers of allocation points are used around the crack tips to satisfy traction-free boundary conditions instead of using more elements. These factors make the algorithm of BCM more reliable and fast as compared to other methods and enable us to solve difficult fatigue crack growth problems. Therefore, the main objective of this thesis is to analyse the multiple cracks interaction under mix mode fatigue loading by using BCM in the two-dimensional domain and to show the accuracy and versatility of the method to different fatigue crack growth problems that are difficult to solve by using the conventional methods.

Throughout the thesis, it has been proved that the proposed scheme is a reliable and accurate method to simulate the fatigue crack propagation (FCP) involving multiple cracks in complex plate geometries under different conditions of fatigue loading. The accuracy of the method is established through the results presented by different researchers which were already available in the literature. Crack tip SIFs, fatigue crack propagation paths and the number of loading cycles required to produce a given crack length extension are used as a parameter for the comparison. A good agreement among the results of each mentioned parameter is achieved for every problem.

Further, this proposed method is used to simulate the FCP in different plate geometries involving single as well as multiple cracks under different conditions of fatigue loading which are typical and difficult problems to solve in aerospace structural components. For this purpose, three different studies are conducted, and the findings of each study are published in different international prestigious forums.

In the first study, fatigue crack growth in an infinite plate having two rivet holes separated at some distance and crack emanating from a certain location and orientation from one hole are analyzed under three different far-field fatigue loadings i.e. loading in X-direction, loading in Y- direction and shear loading. The maximum tangential stress (MTS) criterion is used to predict the trajectories of crack growth. Paris's Law along with the approach of equivalent stress intensity factor is used to compute the number of loading cycles to produce a required crack length. It is concluded that after some initial number of loading cycles, the fatigue crack growth path becomes perpendicular to the direction of applied loading in case of far-field applied tensile stress (whether in X or Y direction), and similarly, in the case of shear loading, cracks propagate perpendicular to the direction of maximum principal stress. Almost ten times fewer loading cycles are required to reach at a certain crack size under shear loading as compared to the normal applied stress, which shows that the rate of crack propagation is ten times higher under shear stress. Therefore, among the given three loading conditions, cycling shear stress is the worst one and needs more attention while designing the structures having rivet holes.

In the second study, fatigue crack growth simulations of interacting multiple cracks in perforated plates with multiple holes are discussed. To show the versatility of the proposed method, emphasis is given to study such complicated problems which cannot be solved by conventional methods to analyse the FCG. Three different studies with multiple cases of initial cracks emanating from side edges, the center of the plate and the outer periphery of holes in the plate at different orientations are simulated. It has been concluded that the FCG of complicated problems e.g. plate with six holes having seven pre-cracks can be computed fast by the proposed scheme. The conventional methods of analysing FCG have limitations in solving such complex problems. Moreover, the effect of a newly added crack in the vicinity of already present crack is also analyzed and concluded that when two coplanar cracks approach each other, they exhibit an over-constraining phenomenon, which causes the near-tip stress field to be significantly higher than that near a single crack and hence ultimately increases the rate of crack growth. To show the efficiency of a computational method in fatigue problems a new and very useful parameter is also introduced: Yavuz's fatigue computational efficiency factor, $Y_{CF} = \mu N/t$, which is the number of computed million loading cycles per hour (CPU time).

In the third study, FCG behaviour of symmetric cracks emanating at different locations at the outer periphery of the hole in an infinite plate with different orientations under in-phase tension-tension biaxial loading is presented. As the effects of initial crack orientation under uniaxial fatigue loading are well reported in the literature but the same under the effect of different conditions of biaxial loading has not been investigated. The rate of FCG is computed using Walker's equation, whereas the direction of propagation of crack tip is predicted using the minimum strain density (MSED) criterion. Our results show that BCM is equally effective in predicting the FCG behaviour under complex cases of fatigue loading. It is concluded that cracks tend to propagate perpendicular to the direction of dominant stress in the case of biaxial load where biaxiality ratio $\lambda \neq 1$ and there is no effect of location and orientation of initial crack on the crack trajectory. For equibiaxial loading where $\lambda = 1$, the crack tends to propagate diagonally, and its path depends upon the location and orientation of the initial pre-crack. As far as the number of loading cycles for a given crack extension are concerned, equal load cycles are computed for $\lambda = 0, 0.5, 1$ whereas it is concluded that for $\lambda = 1.5$, the rate of crack growth increases, and fewer loading cycles are required to produce the given crack length. It is also concluded that there is no change in crack trajectories under different stress ratios (R). For a given effective stress intensity factor (ΔK_{eff}) the rate of crack propagation is increased with the increase in R, but for a given value of stress, the value of ΔK_{eff} is lower for a higher R-value, which results in a higher number of required loading cycles to produce the same crack extension.

.

İKI BOYUTLU SINIR ÇATLAK ELEMANI YÖNTEMI (BOUNDARY CRACKLET METHOD) KULLANILARAK ETKILEŞIMLI ÇOKLU YORULMA ÇATLAKLARININ İLERLEMESININ ARAŞTIRILMASI

ÖZET

Uçak yapıları, kanatlar üzerine gelen aerodinamik yüklerin değişimi ve kabin basıncının değişimi gibi çeşitli nedenlerden dolayi yorulma yüklemesi etkisi altında kalır. Yorulma yüklemesinin, statik yüklemeye kıyasla uçak yapılarının hasar görmesinde daha fazla sorumlu olduğu iyi bilinen bir gerçektir; çünkü yorulma yüklemesinin meydana getireceği tek bir yüzey çatlağı kazaya neden olabilecek bir hasara neden olabilir. Uçağın ömrünün ilk aşamalarında, bu yüzey çatlaklarının uçağın yapısal bütünlüğü üzerinde hiçbir etkisi yoktur, ancak zamanın geçişi, çevresel etki ve bu çatlakların yükleme etkisiyle yayılması ve birbirleriyle etkileşime girmesi olasıdır. Bu çatlaklar, yapı bileşeninin kesitinin yükleri taşıyamayacağı noktaya kadar yayılır ve söz konusu bileşen ani kırılmaya maruz kalır.

Yorulmadan kaynaklanan hasarlar genellikle yerel gerilme arttırıcılar olarak hareket eden, yayılan, birbirleriyle etkileşime giren ve büyük hasar meydana getiren çatlaklara dönüşen küçük yüzey çatlaklarıyla başlar. Uygulamada, bu mikro yüzey çatlaklarının her zaman birçok hava taşıtı yapısal bileşeninde mevcut olması muhtemeldir, hatta yeni imal edilen yapısal bileşenlerde bile, uçak üretimi sırasında işleme proseslerindeki bazı kusurlar nedeniyle bu çatlaklar olabilir. Bir hasar toleransı ile tasarlanan yapıyı imal etmek ve havacılık endüstrisinde geçerli olan sertifikaların belirli gereksinimlerini karşılamak için, yorulma yüklemesi altında bu kaçınılmaz yüzey çatlaklarının varlığında havacılık yapılarının davranışını bilmek çok önemli hale gelir. Bu nedenle, söz konusu çatlakların yorulma yüklemesi altındaki davranışını tahmin etmenin hızlı ve doğru bir yöntemi hayati bir rol oynar. Bu gerçek, mühendisleri, uçak yapısının kalan faydalı ömrünü daha doğru bir şekilde tahmin edebilmeleri için mevcut çatlakların etkilerini simüle edebilen yeni yöntemler ve modeller geliştirmeye zorlamaktadır. Bu tür yöntemler ve simülasyon teknikleri, yalnızca havacılık ve uzay yapılarının yüksek fiziksel test maliyetini düşürmekle kalmaz, aynı zamanda bu yapıların daha iyi tasarlanmasında çok önemli bir rol oynar.

Düzlemsel çatlakların analizi için, çoğunlukla analitik formülasyonlara ve farklı el kitabı çözümlerine dayanan farklı ticari yazılımlar mevcuttur, örneğin NASGRO ve AFGROW. Bu yazılım paketleri, yalnızca mod-I yükleme koşulunda önceden tanımlanmış bir çatlak ilerlemesi (FCG) sorununu simüle edebilir, ancak endüstrideki gerçek sorunların çoğu, çatlak ucunun her ikisinin de etkisi altında ilerlediği karışım modu(mod-I ve mod-II yükleme koşulları) yüklemesinin etkisi altındadır. Bu nedenle, söz konusu yazılım paketleri, karışım modu çatlak ilerlemesi gibi karmaşık sorunları çözemez. FCG çalışması için uzun zamandan beri sonlu eleman yöntemleri de kullanılmaktadır. Söz konusu yöntemler, çatlakların etkileşimlerini oldukça iyi bir doğrulukla simüle edebilir. Ancak, çatlak ucunda daha fazla eleman gereksinimi nedeniyle, FCG'nin her yinelemesinden sonra FE ağının çatlak ilerlemesi ve rejenerasyonunun bir temsilinin oluşturulması, bu yöntemlerin benimsenmesini

zorlaştırır. FEM'in bu zorluklarının üstesinden gelmek için, 1999'da, minimum yeniden ağ oluşturma ile Genişletilmiş-FEM (XFEM) adı verilen ağdan bağımsız bir yöntem geliştirilmiş ve o zamandan beri bu yöntemlerin uygulanmasında sürekli bir gelişme görülmüştür. Bununla birlikte, problemdeki karmaşıklık arttıkça bu yöntemlerin doğruluğu azalmaktadır ve söz konusu eksikliğin üstesinden gelmek için hala birçok araştırma çalışması devam etmektedir.

Karışık mod koşulları altında çok sayıda çatlak içeren problemlerin FCG'sini analiz etmek için geleneksel yöntemlerin yukarıda bahsedilen sınırlamaları dikkate alındığında, bu yöntemlerin eksikliklerini azaltabilecek yöntemleri geliştirmek için her zaman bir çalışma alanı vardır. Son zamanlarda, 2006 yılında, Cornell Üniversitesi'nde Prof. Dr. Abdulkadir Yavuz (bu tezin eş danışmanı) ve Prof. Dr. S. L Phoenix tarafından, çatlak uçları için genel gerilme alanı, gerilme yoğunluğu faktörü (SIF) ve çatlak kıvrımlarında tekil kamaları hesaplamak için, Boundary Cracklet Method (BCM) adı verilen hızlı ve guvenilir bir yarı analitik yöntem geliştirilmiştir. Bu yöntem, çatlak yüzeylerindeki çekmesiz durumu sağlayan belirli üstel fonksiyon serilerini kullanarak çatlak açılım yer değiştirme profillerine yaklaşan dislokasyon yayılımı yaklaşımına dayanmaktadır. Çatlak uçları etrafındaki gerilme tekilliklerinin üstesinden gelmek için çok ince bir ağın gerekli olduğu geleneksel ağa bağlı yöntemlerin aksine, BCM, üstel fonksiyon serilerine kama özdeğerlerini dahil ederek çatlak ucu tekilliklerini giderir ve gerilim alanlarını hesaplamak için gerekli tüm integrallerin içinde olmasını ve hızlı çözüm vermek için kapalı formda bir çözüm sağlar. Bu integrallerin çözümü, FEM'ler ve BEM'ler gibi diğer ağa bağlı yöntemlerde en çok zaman alan kısımdır. Ayrıca, daha fazla eleman kullanmak yerine serbest sınır koşullarını sağlamak için çatlak uçlarının çevresinde yalnızca birkaç tahsis noktası kullanılır. Bu faktörler, BCM algoritmasını diğer yöntemlere göre daha güvenilir ve hızlı hale getirir ve zorlu yorulma çatlak ilerleme problemlerini çözmemizi sağlar. Bu nedenle, bu tezin temel amacı, BCM'yi iki boyutlu alanda kullanarak karışım modlu yorulma yüklemesi altında çoklu çatlak etkileşimini analiz etmek ve yöntemin doğruluğu ve çok yönlülüğünü, geleneksel yöntemleri kullanarak çözülmesi zor olan farklı yorulma çatlak ilerleme problemlerinde göstermektir.

Bu çalışmada, iki boyutlu alanda BCM kullanılarak karışım modlu yorulma yüklemesi altında çoklu çatlak etkileşimini analiz eden yeni bir yöntem sunulmuştur. Tez boyunca, önerilen yöntemin, farklı yorulma yüklemesi koşulları altında karmaşık plak geometrilerinde çoklu çatlakları içeren yorulma çatlak ilerlemesini (FCP) simüle etmek için güvenilir ve doğru bir yöntem olduğu kanıtlanmıştır. Yöntemin doğruluğu, literatürde halihazırda mevcut olan farklı araştırmacılar tarafından sunulan sonuçlarla karşılaştırılarak belirlenmiştir. Karşılaştırma için bir parametre olarak çatlak ucu SIF'leri, yorulma çatlak yayılma yolları ve belirli bir çatlak uzunluğunda ileretmek için gerekli yükleme çevrimlerinin sayısı kullanılmıştır. Her bir problem için bahsedilen her bir parametrenin sonuçları arasında iyi bir uyum sağlanmıştır.

Ayrıca önerilen yöntem, havacılık ve uzay yapısal bileşenlerinde çözülmesi tipik ve zor problemler olan farklı yorulma yüklemesi koşulları altında tekli ve çoklu çatlakları içeren farklı plak geometrilerinde FCP'yi simüle etmek için kullanılır. Bu amaçla üç farklı çalışma yapılmıştır ve her bir çalışmanın bulguları farklı uluslararası prestijli dergilerde yayınlanmıştır.

İlk çalışmada, bir mesafeden ayrılmış iki perçin deliğine sahip sonsuz bir plakdaki yorulma çatlağı ilerlemesi ve bir delikten belirli bir yerden kaynaklanan çatlak ve yönelim, üç farklı uzak alan yorulma yüklemesi, yani X yönünde yükleme, Y'de yükleme, basma ve kesme yükü. Çatlak büyümesinin yörüngelerini tahmin etmek için maksimum teğetsel gerilme (MTS) kriteri kullanılmıştır. Paris yasası ve eşdeğer gerilme yoğunluğu faktörü yaklaşımı, gerekli çatlak ilerleme uzunluğunu meydana getirmek için yükleme çevrimlerinin sayısını hesaplamak için kullanılmıştır. İlk birkaç yükleme çevriminden sonra, yorulma çatlağı ilerleme yolunun, uzak alana uygulanan çekme gerilmesi (X veya Y yönünde) durumunda ve benzer şekilde kesme yükü, çatlaklar durumunda uygulanan yükleme yönüne dik hale geldiği, yani maksimum temel gerilme yönüne dik olarak yayıldığı sonucuna varılmıştır. Uygulanan normal gerilme ile karşılaştırıldığında, kesme yükü altında belirli bir çatlak boyutuna ulaşmak için neredeyse on kat daha az yükleme döngüsü gerekmekte, bu da kayma gerilmesi altında çatlak yayılma hızının on kat daha yüksek olduğunu göstermektedir. Bu nedenle, verilen üç yükleme koşulu arasında, çevrimsel kayma gerilmesi en kötüsüdür ve perçin delikli yapıları tasarlarken daha fazla dikkat gerektirir.

İkinci çalışmada, çoklu delikli perfore plaklarda çoklu çatlakların etkileştiği yorulma çatlağı ilerleme simülasyonu tartışılmıştır. Önerilen yöntemin çok yönlülüğünü göstermek amacıyla, FCG'yi analiz etmek için geleneksel yöntemlerle çözülemeyen bu tür karmaşık sorunların incelenmesine önem verilmektedir. Yan kenarlardan, plağın merkezinden ve plakdaki deliklerin dış çevresinden farklı yönelimlerde ortaya çıkan birden fazla ilk çatlak durumuyla üç farklı problem simüle edilmiştir. Karmaşık sorunların FCG'si örneğin yedi ön çatlağa sahip altı delikli plak, önerilen yöntem kullanılarak hızlı bir şekilde hesaplanmıştır. Geleneksel FCG analiz yöntemlerinin bu tür karmaşık problemleri çözmede sınırlamaları vardır. Ayrıca, halihazırda mevcut çatlağın yakınında yeni eklenen çatlağın etkisi de analiz edilmiş ve iki düzlemsel çatlak birbirine yaklaştığında aşırı sınırlayıcı bir fenomen sergiledikleri sonucuna varılmıştır. Yorulma problemlerinde bir hesaplama yönteminin verimliliğini göstermek için yeni ve çok kullanışlı bir parametre de sunulmuştur: "Yavuz" yorulma hesaplama verimliliği faktörü, $YCF = \mu N / t$, saat başına hesaplanan milyon yükleme çevrimi sayısıdır (CPU zamanı).

Üçüncü çalışmada, faz içi gerilme-gerilme çift eksenli yükleme altında farklı yönelimlere sahip sonsuz bir plakda deliğin dış çevresinde farklı yerlerde ortaya çıkan simetrik çatlakların FCG davranışı sunulmuştur. Tek eksenli yorulma yüklemesi altında ilk çatlak oryantasyonunun etkileri literatürde iyi bilindiğinden, farklı çift eksenli yükleme koşullarının etkisi altında aynı durum araştırılmamıştır. FCG oranı, Walker denklemi kullanılarak hesaplanırken, çatlak ucunun yayılma yönü minimum gerinim yoğunluğu (MSED) kriteri kullanılarak tahmin edilmiştir. Sonuçlarımız, BCM'nin karmaşık yorulma yüklemesi durumlarında FCG davranışını tahmin etmede eşit derecede etkili olduğunu göstermektedir. Çatlakların, çift eksenlilik oranının $\lambda \neq 1$ olduğu ve çatlak yörüngesi üzerindeki ilk çatlağın konumu ve oryantasyonunun hiçbir etkisinin olmadığı çift eksenli yük durumunda, baskın gerilme yönüne dik yayılma eğiliminde olduğu sonucuna varılmıştır. Eş eksenli yükleme için $\lambda = 1$ olduğunda, çatlak çapraz olarak yayılma eğilimindedir ve yolu, ilk çatlağın konumuna ve yönüne bağlıdır. Belirli bir çatlak uzaması için yükleme çevrimi sayısı söz konusu olduğunda, eşit yük çevrimleri $\lambda = 0, 0.5, 1$ için hesaplanırken, $\lambda = 1.5$ için çatlak ilerleme hızının arttığı ve verilen çatlak uzunluğunu meydana getirmek için daha az yükleme çevrimi gerektiği sonucuna varılmıştır. Ayrıca, farklı gerilme oranları (R) altında çatlak yörüngelerinde hiçbir değişiklik olmadığı sonucuna varılmıştır. Belirli bir etkili gerilme yoğunluğu faktörü (ΔK_{eff}) için çatlak yayılma hızı R'deki artışla artar, ancak belirli bir gerilme değeri için ΔK_{eff} değeri daha yüksek bir R değeri için daha düşüktür ve bu da aynı çatlak uzunluğunu meydana getirmek için daha yüksek çevrim sayısında yükleme ile sonuçlanır.

1. INTRODUCTION

Aircraft structures experience fatigue loading emanating from different sources e.g. variation of aerodynamic loads on wings and repetitive pressurizing and depressurizing the cabin of the aircraft etc. It is a well-known fact that fatigue loading is more responsible for the failure of aircraft structures as compared to static loading because a single surface crack can lead to a catastrophic failure due to fatigue loading [1]. At the early stages of the life of aircraft, these surface cracks have no effect on the structural integrity of the aircraft, but with the passage of time, environmental effect, and nature of loading these cracks propagate and interact with each other. These cracks propagate, up to the point where the remaining cross-section of the component is not being capable of carrying the loads and the component will be subjected to sudden fracture [2].

The failures due to fatigue usually start at small surface cracks which act as local stress raisers and propagate and interact with each other and turn into large damage producing cracks [1]. In practice, these micro surface cracks are always likely to be present in many aircraft structural components even the newly made components can have these cracks due to certain imperfections in machining processes during the manufacturing of aircraft. To produce a damage tolerance design and to meet the certain requirements of certifications applicable in the aerospace industry, it becomes very important to know the behaviour of structures in the presence of these inevitable surface cracks under fatigue loading. Thus, a fast and accurate method of predicting the behaviour of these cracks under fatigue loading play a vital role. This fact forces engineers to develop new methods and models which can simulate the effects of existing cracks so that they can predict the remaining useful life of aircraft structure more accurately. Such methods and simulation techniques not only reduce the high cost of physical testing of the aerospace structures but also play a crucial role in producing a better design of these structures.

Several two-dimensional methods and software packages are available in the literature to investigate fatigue crack propagation. These methods include analytical, finite element methods (FEM), extended finite element methods (XFEM), boundary element methods (BEM) and many more. Each one has its advantages as well as limitations and drawbacks considering the preparation of the model, the accuracy of the method, capabilities to solve a complex problem and required computation time.

For the analysis of planar cracks different commercial tools are available, which are mostly based on the analytical formulations and different handbook solutions e.g. NASGRO [3] and AFGROW [4]. These software packages can simulate the FCG problems of predefined cracks under mode-I loading conditions only, but most of the real problems in the industry are under the influence of mix mode loading where crack tip grows under the effect of both mode-I and mode-II loading conditions. Therefore, these software packages cannot handle such complex problems of mixed-mode loading.

Finite element methods are also being used for a long time for the study of FCG. These methods can simulate the interactions of cracks with reasonably good accuracy. But, due to the requirement of fine mesh at the crack tip, generation of a representation of the crack advancement [5] and regeneration of FE mesh after each iteration [6] of FCG, make these methods challenging to adopt. To overcome these difficulties of FEM, in 1999, Belytschko and Black presented a mesh-independent method with minimal re-meshing for elastic crack growth [7]. Since then, continuous improvement has been seen in the implementation of these methods. However, the accuracy of these methods decreases as the complexity of the problem increases and still a lot of research efforts are underway to overcome this shortcoming [8].

By considering the above-mentioned limitations of the conventional methods to analyse the FCG of problems involving multiple cracks under mixed-mode conditions, there is always room to develop such methods which can mitigate the deficiencies of these methods. Recently in 2006, a fast and accurate semi-analytical method called Boundary Cracklet Method (BCM) is developed by Prof. Dr. A.K. Yavuz (co-advisor of this study) and Prof. Dr. S.L. Phoenix at Cornell University, to find the overall stress field and the stress intensity factor (SIF) for crack tips and crack singular wedges at the crack kinks. This method is based on the dislocation distribution approach which approximates the crack opening displacement profiles by using certain power series that satisfy the traction-free condition on crack faces. Unlike the conventional mesh dependent methods, where a very fine mesh is required to overcome the stress singularities around crack tips, BCM takes cares of crack tip singularities by including wedge eigenvalues in power series and makes sure that all integrals necessary to calculate stress fields are in closed form to give fast solutions. The solution of these integrals is the most time-consuming part in other mesh dependent methods such as FEMs and BEMs. Moreover, only a few numbers of allocation points are used around the crack tips to satisfy traction free boundary conditions instead of using more elements. These factors make the algorithm of BCM more reliable and fast as compared to other methods and enable us to solve difficult fatigue crack growth problems. Therefore, the main objective of this thesis is to use the same method to analyse the multiple cracks interaction for the difficult fracture problems with complex geometry, orientation and number of pre-cracks in the model and nature of fatigue loading, in a two-dimensional domain.

1.1 Purpose of Thesis

The main purpose of this thesis is to analyse and simulate the complex phenomenon of interacting multiple cracks under mixed-mode fatigue loading by using the Boundary Cracklet Method (BCM) in a two-dimensional domain. The accuracy of the method is established through the results presented by different researchers which were already available in the literature. Crack tip SIFs, fatigue crack propagation paths and the number of loading cycles required to produce a given crack length extension are used for the comparison. Further, the proposed method is used to simulate the fatigue crack propagation (FCP) in different plate geometries which are typical and difficult problems to analyse in aerospace structural components involving single as well as multiple cracks under different conditions of fatigue loading. For this purpose, three different studies are conducted, and the findings of each study are published in different international prestigious journals.

1.2 Unique Aspects of the Thesis

Fatigue crack growth (FCG) analysis and simulation of the interaction of multiple cracks have been a key issue for decades. In this study, a method of simulating the complex phenomenon of the interaction of multiple cracks under fatigue loading is presented: Boundary Cracklet Method (BCM). BCM was developed as a semi-analytical method to calculate the overall stress field and the stress intensity factors (SIFs) for crack tips under static loads before.

In this study, BCM is used for the first time to simulate the interacting multiple cracks under mix-mode fatigue loading. Further, the proposed scheme is used to analyse and simulate the typical and complicated FCG problems of the aerospace industry which cannot be solved by conventional methods of FCG analysis. For this purpose, three different studies were conducted, and the findings of each study are published in different international prestigious journals.

In the first study, fatigue crack growth in a plate having two rivet holes separated at some distance and crack emanating from a certain location and orientation from one hole is analysed under three different far-field fatigue loadings i.e. loading in X-direction, loading in Y- direction and shear loading. The purpose of this study was to determine that what are the trajectories of crack propagation under different loading conditions, which kind of loading is worst for these common rivet structures and what are the effects of initial crack length on the FCG behaviour. It is concluded that after some initial number of loading cycles, the FCG path becomes perpendicular to the direction of applied loading in the case of far-field applied loading and this path does not depend upon the initial size of the crack. Among the given three loading conditions, cycling shear stress is the worst one and needs more attention while designing the structures having rivet holes.

In the second study, fatigue cracks growth simulations of the complex geometry of problems that cannot be solved by conventional methods to analyse the FCG. Three different studies with multiple cases of initial cracks emanating from side edges, the center of the plate and the outer periphery of holes in a plate at different orientations are simulated. It has been concluded that the FCG of such complicated problems e.g. plate with six holes having seven pre-cracks can be computed fast by the proposed scheme. Moreover, the effect of the newly added crack in the vicinity of the already present crack is also analyzed and concluded that when two coplanar cracks approach each other, they exhibit an over-constraining phenomenon, which causes the near-tip stress field to be significantly higher than that near a single crack and hence ultimately increases the rate of crack growth.

In the third study, the FCG behaviour of symmetric cracks emanating at different locations at the outer periphery of the hole in an infinite plate with different orientations under in-phase tension-tension biaxial loading is shown. The main objective of this study was to examine the effects of initial crack orientation on FCG behaviour under different conditions of biaxial loading because the effects of initial crack orientation under uniaxial fatigue loading are well reported in the literature but the same under the effect of biaxial loading has not been investigated. It is concluded that cracks tend to propagate perpendicular to the direction of dominant stress in the case of biaxial load where biaxiality ratio $\lambda \neq 1$ and there is no effect of location and orientation of initial crack on the crack trajectory. For equibiaxial loading where $\lambda = 1$, the crack tends to propagate diagonally, and its path depends upon the location and orientation of the initial pre-crack. As far as the number of loading cycles for a given crack extension are concerned, equal load cycles are computed for $\lambda = 0, 0.5, 1$ whereas it is concluded that for $\lambda = 1.5$, the rate of crack growth increases. It is also concluded that there is no change in crack trajectories under different stress ratios (R). For a given ΔK_{eff} the rate of crack propagation is increased with the increase in R, but for a given value of maximum cyclic stress σ_{max} the value of ΔK_{eff} is lower for a higher R-value, which results in a higher number of required loading cycles to produce the same crack extension.

1.3 Scope of Thesis

The scope is of this study is limited to Linear Elastic Fracture Mechanics (LEFM) in the two-dimensional domain. For the analysis, elastic and isotropic materials are considered. The FCG behaviour is predicted by computing mode-I and mode-II stress intensity factors (SIFs) with the help of the Boundary Cracklet Method (BCM). Different criteria available in literature e.g. Maximum tangential stress (MTS) criterion, minimum strain energy density (MSED) criterion and maximum energy release rate (MERR) criterion are used to determine the direction of propagation of cracks, whereas to compute the fatigue lives of structures, Paris-Erdogan law and Walker’s model are used in this study.

Chapter 2 begins with the literature review and details of different methods and techniques to simulate the interaction of multiple cracks is presented. The advantages, as well as the limitation of each method, are discussed in detail.

In chapter 3, the methodology of the boundary cracklet method (BCM) is explained in detail and how this method helps us to find the stress intensity factors (SIFs) at crack tips and stress field in the whole cracked plate.

In chapter 4, the modelling of the geometry of the problem and the implementation of BCM to simulate the interaction of multiple cracks are discussed in detail.

In chapter 5, the accuracy of the proposed method is shown by comparing computed FCG behaviours from different methods already mentioned in the literature.

Chapter 6 comprises different applications of BCM in which different aspects of fatigue crack growth are investigated in typical aerospace structures involving single as well as multiple cracks.

Conclusions drawn from this study and the relevant potential studies which can be performed in future are presented in chapter 7.

2. LITERATURE REVIEW

The phenomenon of multiple interacting cracks is very common in most engineering structures especially in ageing aircraft, marine hulls and composites materials. In this chapter, an overview of different methods available in the literature to study the interacting multiple cracks is presented.

2.1 Solution Methods Available in Literature

There are several two-dimensional methods and techniques available to study single as well as multiple cracks interactions and their propagation under fatigue loading. Some of them are as follows:

- Analytical methods
- Finite element methods (FEM)
- Extended finite element methods (XFEM)
- Boundary Element Methods (BEM)
- Different hybrid methods

A brief detail of each method is given as follows:

2.1.1 Analytical methods

Numerous analytical or semi-analytical methods are available in the literature to study the fatigue cracks interaction and their propagation. Most of these analytical methods are based on superposition law, in which the problem is split into two sub-problems. The first sub-problem plate is modelled under the specified loading and study without any crack, this part of the problem is called the Trivial problem. In the second sub-problem which is called the Auxiliary problem, the plate is modelled with a crack but without any far-field loading, and loading is applied as prescribed traction at the crack face. The sum of these two problems gives the results to the original problem.

In analytical methods, an approach of traction-based influence function method is often used to study crack problems. Several different forms of these methods can be found in the literature [9-13]. A detailed review of traction-based analytical methods for the multiple crack interaction in two and three -dimensional is given can be found in [14,15].

There are analytical methods based on dislocation distribution, in which crack opening displacements are unknown and are modelled as dislocation distributions i.e. the derivatives of opening displacements. These methods were first developed by Bilby and Eshelby in 1968 [16]. A detailed overview of dislocation-based methods is given in [17,18].

To find the stress intensity factor for the complex loading cases, a weighted function approach presented by Bueckner [19] can also be used. In this approach, first, a weighted function which is a Green function is determined for given geometry under a simple loading case and then to find the stress intensity factor for any arbitrary and relatively complex loading case this weighted function is multiplied by the applied traction and then integrating the whole product over the crack line. Detail of this approach is mentioned in [20,21]. A detailed review of analytical methods based on traction-based influence function method and dislocation distribution along with other techniques can be found in [22,23].

2.1.2 Finite element methods

Finite element methods are often used for the study of multiple crack growth and interaction, but due to the requirement of the fine-meshed crack tip, generation of a representation of the crack advancement and regeneration of FE mesh after each iteration make this method challenging to adopt. But the technique suggested by Kantorovich and Krylov in 1964 tries to solve these problems [24]. In this method, a linear superposition technique is used to solve multiple cracks interaction.

In 1969, Watwood predicted the crack propagation behaviour of cantered and side crack plate using FEM [25], and in 1970, Chan et al. studied fracture behaviour of compact tension and rotating specimen using FEM [26]. [25,26] are considered as the early applications and utilization of FEM in linear fracture mechanics, they also showed that stress singularity at the crack tip cannot be achieved by using linear elements. So, to overcome this difficulty, Byskov in 1970 [27] developed a triangular crack tip element containing necessary shape functions to accurately model the singularity at the crack tip, and later on, in 1973 Wilson [28] used circular element and Hardy [29] used rectangular element for this purpose. The singular tip elements are also very common in solving crack problems [30], but these elements also require a very fine mesh near the crack tips and wedges and hence increase the computational requirement. A review by Banks-Sills [31]also compares some other methods based on finite element methods e.g. M -integral and displacement extrapolation methods to determine the stress intensity factors for mixed-mode deformation.

2.1.3 Extended finite element methods

The extended finite element method (XFEM), also known as generalized finite element method (GFEM) or partition of unity method (PUM) is a numerical technique that evolved in the last two decades, makes it easier to solve problems with localized features that are not efficiently resolved by mesh refinement and need re-meshing by using standard FEM. There are many applications of this method but one of the initial applications was the modelling of cracks in homogeneous materials by Belytschko and Black [7] in 1999. Soon after this, Moës et al. [32] developed a method based on FEM to study the crack growth without re-meshing with an enriched displacement field near the crack tip. Many enrichment functions are developed with time for crack propagation in isotropic material [33]. Réthoré gave an energy-conserving scheme for dynamic crack growth using the extended finite element method [34]. Later on, in 2007 Grégoire presented a comparison between experiments and X-FEM simulations of dynamic crack propagation under mixed-mode loading [35].

In the recent past, several investigations have been carried out to study crack propagation using XFEM [36,37]. Multiple crack propagation in linear elastic and homogeneous material based on minimum potential energy concept using XFEM is presented in [38-40]. In 2017, to improve the computational speed of XFEM, a novel computational method called decomposed updating reanalysis (DUR) method is developed by Zhenxing et al. [41]. Thus, nowadays, XFEM is considered the most popular numerical method for crack propagation simulation due to its superiority in modelling both strong and weak discontinuities within a standard FE framework. A detailed review of fatigue crack propagation modelling techniques using FEM and XFEM can also be found [8].

2.1.4 Boundary Element Method (BEM)

Boundary Element Method is a widely used numeric technique for simulation of crack propagation problems because it is better than domain-type methods such as the finite element method (FEM) since in these methods only the boundary of the problem is meshed rather than the whole domain. As a result, BEM requires less computational resources to generate new elements for the modelling of crack propagation. In fracture mechanics problem due to the overlapping of upper and lower crack surfaces results in the degenerated formulation of BEM [42,43]. However, many researchers have developed several special methods for handling stress singularities at the cracked surfaces, such as the Green's function method [44,45], the sub-regional method [46-49], and the displacement discontinuity method [50-52]. A dual boundary element method (DBEM) is given by Portela et al., in which singular and hyper-singular integral equations are written for collocation points positioned at the opposite crack surfaces [53]. Simulations of multiple crack-hole interactions and multiple cracks interaction using BEM are presented in [54,55] and [56-59] respectively. Recently, nonlinear crack propagation solution techniques based on the use of tangent operators have been proposed in [60-62]. These nonlinear solution techniques take a smaller number of iteration and are more stable and accurate than the classical techniques. Due to the limitation of the displacement discontinuity method where every boundary element has approximately equal length, a proper selection of minimum crack growth increment is key for effectively modelling multiple-crack growth. To overcome this difficulty a useful technique was developed by Yan [63], which enabled the user to automatically select a desired crack length increment at the beginning of each simulation.

2.1.5 Different hybrid methods

In addition to the above-mentioned methods, there are some meshless methods to simulate the crack propagation problems. Some of them are the combination of the above-mentioned method. A hybrid between finite and boundary element methods, e.g. the Symmetric Galerkin Boundary Element Method – Finite Element Method (SGBEM-FEM) [64] and the Scaled Boundary Finite Element Method (SBFEM) [65,66]. Some of the other numerical methods to simulate the crack propagation process are the meshless methods [67-69], edge-based finite element method (ES-FEM) [70,71] and numerical manifold method (NMM) [72,73].

2.2 Crack Propagation Criteria

All the above-mentioned methods need a certain criterion to determine the direction of crack propagation. In literature variety of fatigue crack propagation criterion are present. One can divide them into three different categories i.e. energy-based criteria, stress-based criteria, and strain-based criteria. Energy-based criteria are accurate as compared to the other groups of criteria [74] as they use the energy dissipated around the crack tip to determine the crack growth direction and give more consistent results with the experimental results. In 1920, Griffith proposed the first energy-based criterion [75-76]. According to this criterion, the crack will propagate when the decrease in elastic strain energy that occurs due to crack growth is at least equal to the increase in surface energy due to the creation of cracks. In 1957, Irwin generalized the theory proposed by Griffith by introducing a term i.e. energy release rate G, which represents the energy available for a unit extension of the crack and is responsible for the crack growth [77]. Hussain et al. [90] proposed the Maximum Energy Release Rate (MERR) criterion to determine crack paths under combine mode I and mode II loading. The minimum Strain Energy Density (SED) criterion proposed by Sih [89] is also a very commonly used energy-based criterion.

Once the stress intensity factors and the stress fields are known around a crack tip, one can find the direction of crack propagation by implementing any of the stress-based criteria. Among the stress-based criteria, the Maximum Tangential Stress (MTS), proposed by Erdogan and Sih [88] is the simplest and most widely used criterion. According to this, it is considered that the crack will propagate from its tip in the direction along which the maximum tangential or hoop stress. In this study, Maximum Tangential Stress (MTS) and Minimum Strain Energy Density (SED) criteria are used to predict the fatigue crack growth paths. The details of these two criteria and their implementation in the analysis are discussed in chapter 4 of this thesis. In addition to energy-based and stress-based criteria, there are strain-based criteria available in the literature that also provide a better representation of fracture in certain materials. Maximum tangential strain (MTSN) by Chang [77] and its modified form proposed by Mirsayar as extended maximum tangential strain criterion ((EMTSN) [74] by including the effect of T-strain can be consider some examples of strain-based criterion.

2.3 Fatigue Crack Growth Models

To compute the rate of fatigue crack propagation, mostly Paris's law proposed by Paris and Erdogan [84] is used. Forman et al. improved the theory presented by Paris and Erdogan by including the variation in the crack-growth rate owing to the load ratio and the instability of the crack growth when the value of the maximum stress-intensity factor approaches the fracture toughness of the material [85]. It was further proved that crack propagation is influenced by the stress ratio of the applied load, therefore in 1970, Walker proposed the modified form of the Paris equation by incorporate the effect of stress ratio R on FCG rate [86]. All these models are used in this study and are discussed in chapter 4. NASGRO equation [3] is the most common fatigue crack growth equation and can be applied to all the regions of crack growth. For the cases where a large-scale yielding is produced, and the SIF does not remain valid, a different model based on J-integral is used which is proposed by Dowling and Begley [79]. One can find different model available in the literature for constant as well as variable amplitude fatigue loading [6].

3. METHODOLOGY OF BOUNDARY CRACKLET METHOD (BCM)

In this chapter, the details of the methodology of the Boundary cracklet method (BCM) will be discussed. The basic concepts and different terminologies used in the implementation of the method are also explained.

3.1 History of Boundary Cracklet Method (BCM)

The boundary cracklet method (BCM) is a dislocation-based semi-analytical method to find the overall stress field and the stress intensity factor (SIF) for crack tips and crack singular wedges at the crack kinks. This method was developed by Dr. A. K. Yavuz (co-advisor of this thesis study) and Dr. S. L. Phoenix at Cornell University, back in 2006. Through several publications by Yavuz et. al, it is proven that BCM is a fast and accurate method to compute the SIFs and stress field at crack tips and crack singular wedges at the crack kinks [80-82]. Like most of the other analytical techniques, BCM is also based on superposition law, in which the problem is split into two sub-problems: one is called **Trivial problem** (TP) and the other is called **Auxiliary problem** (AP). The first sub-problem plate is modelled under the specified loading and analyse without any crack, this part of the problem is called the Trivial problem. In the second sub-problem which is called the Auxiliary problem, the plate is modelled with a crack but without any far-field loading, and loading is applied as prescribed traction at the crack face. The sum of these two problems gives the results to the original problem. In the application of this method, all the external boundaries and internal cracks are represented by certain lines and are called "**Cracklets**".

BCM is based on a dislocation distribution approach that approximates the crack opening displacement profiles by using certain power series that satisfy the traction-free condition on crack faces. Unlike the conventional mesh dependent methods, where a very fine mesh is required to overcome the stress singularities around crack tips, BCM takes care of crack tip singularities by including wedge eigenvalues in power series and makes sure that all integrals necessary to calculate stress fields are in closed form to give fast solutions. The solution of these integrals is the most time-consuming part in other mesh dependent methods such as FEMs and BEMs. Moreover, only a few numbers of allocation points are used around the crack tips to satisfy traction free boundary conditions instead of using more elements. These factors make the algorithm of BCM more reliable and fast as compared to other methods and enable us in this study to solve difficult fatigue crack growth problems.

3.2 Cracklet Types and Construction of ODP

To understand the basic of BCM, three types of cracklets are shown in Figure 3.1. In the 2-D problems, these cracklets have their own **Opening Displacement Profiles (ODPs)** i.e. a vectorial display of top to the bottom distance between points originally coinciding on the faces of the undeformed crack segment under given boundary conditions. ODP of each cracklet type is represented by an opening profile approximation function (**b**). These ODPs are considered in both for tangential and normal direction and denoted, respectively, as $\mathbf{b}_1^{\mathrm{I}}$ and $\mathbf{b}_2^{\mathrm{I}}$ and also called Burger's vectors, corresponding to the individual crack segments i=1.....C. These functions are approximated by some rational-power series i.e. polynomial series P (t^N, N = 0,1,2,...) and wedge series W ($t^{\rho+M}$, $0 < \rho < 1$, and M = 0,1,2,...) where t is a local coordinate directed along the crack line from a tip, a kink, or a branch point and N and M are degrees of polynomial and wedge series respectively. These rational powers are eigenvalues (ρ) and are calculated from Williams Wedge Analysis [83]. The number of eigen values used for the analysis is depicted by the wedge angle (ω) as shown in Figure 3.1. As discussed earlier that it becomes a boundary value problem (BVP) with two sub-problems; Trivial problem and Auxiliary problem. To solve this BVP the common approach of super-position of the solution discussed in [22] is implied. The key to select the terms of polynomial and wedge series and their exponents lies in the fact that the tractions on the crack faces are virtually zero as compared to the far-field loading. By applying the mentioned method, we got a set of linear algebraic equations to solve for the weighting coefficients of the terms in the ODP power series. The fact that these eigenvalues are approximated by a ratio to evaluate all integrals analytically instead of calculating them numerically makes this algorithm fast as compared to the other analytical methods.

The three typical cracklets (shown in Figure 3.1) and the details of their approximation functions of opening displacement profiles (ODP) are given below.

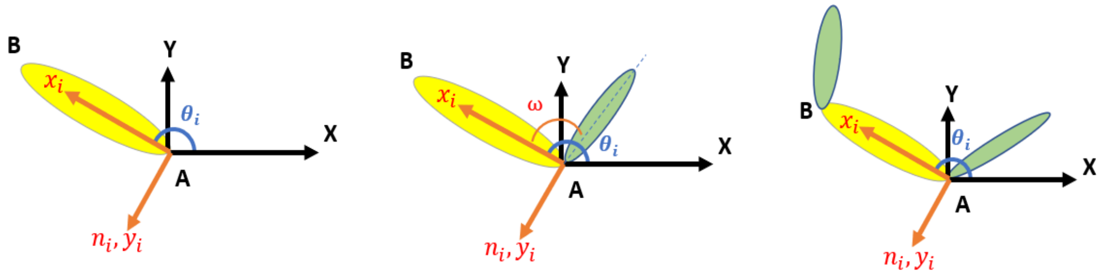

Figure 3.1 : Cracklet types; (A) C1 Cracklet, (B) C2 Cracklet, (C) C3 Cracklet.

3.2.1 Cracklet type C1

The configuration of C1 type cracklet is shown in Figure 3.2 and it is represented by a single straight line. At the tip of the crack, the value of eigenvalue remains ½, so two wedge functions (one for each tip end at point A and B) with the power of ½ are used and are given in equation (3.1).

$$b_j^{(i)}(t) = W_{\frac{1}{2}j}^{A(i)}\left(\frac{t}{a_i}\right) + W_{\frac{1}{2}j}^{B(i)}\left(1-\frac{t}{a_i}\right) \tag{3.1}$$

where wedge subfunction family (each has M-1 coefficients) for the crack tip end is given by equation (3.2).

$$W_{\frac{1}{2}j}(\eta) = \sum_{l=0}^{M-2} W_{\frac{1}{2}jl}\left[\eta^{\left(\frac{1}{2}+l\right)} - (M-1)\eta^{\left(\frac{1}{2}+M-l\right)} + (M-l-1)\eta^{\left(\frac{1}{2}+M\right)}\right] \tag{3.2}$$

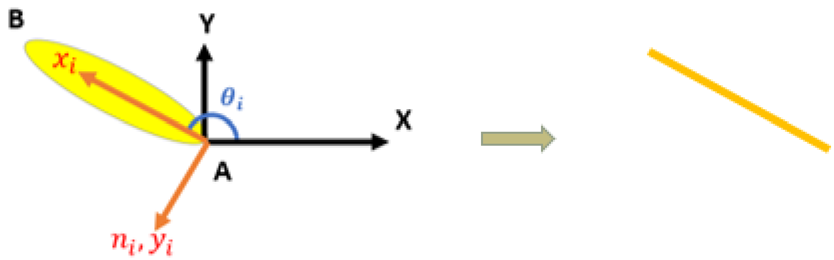

Figure 3.2 : Cracklet type C1 and its representation by a straight line.

3.2.2 Cracklet type C2

In Figure 3.3, the configuration of the C2 type cracklet and its simple representation as a straight line is shown. It is represented with one wedge end and one tip end. At the tip of the crack at point B, the value of the wedge eigenvalue is ½, so one wedge subfunction family is required. For crack end at point A, one polynomial subfunction values and two wedge subfunction families are required, each with M-1 coefficients is used. The ODP for C2 type cracklet is given in equation (3.3)

$$b_j^{(i)}(t) = P_j^{A(i)}\left(\frac{t}{a_i}\right) + \mathrm{W}^{\mathrm{A(i)}}_{\rho_1^{\mathrm{A}}\mathrm{j}}\left(\frac{t}{a_i}\right) + \mathrm{W}^{\mathrm{A(i)}}_{\rho_2^{\mathrm{A}}\mathrm{j}}\left(\frac{t}{a_i}\right) + \mathrm{W}^{\mathrm{B(i)}}_{\frac{1}{2}\mathrm{j}}\left(1 - \frac{t}{a_i}\right) \tag{3.3}$$

where polynomial and wedge subfunctions family for C2 cracklet type are in equations (3.4) and (3.5) respectively.

$$P_j(\eta) = \sum_{k=0}^{N-2} P_{jk}\left[\eta^{(k)} - (N-k)\eta^{(N-l)} + (N-k-1)\eta^{(N)}\right] \tag{3.4}$$

$$W_{\rho j}(\eta) = \sum_{l=0}^{M-2} W_{\rho jl}\left[\eta^{(\rho+l)} - (M-1)\eta^{(\rho+M-l)} + (M-l-1)\eta^{(\rho+M)}\right] \tag{3.5}$$

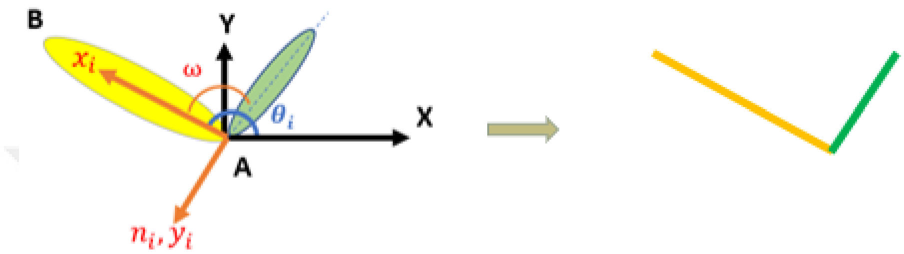

Figure 3.3 : Cracklet type C2 configuration and is represented by an orange straight line with another green line representing C2 type cracklet.

3.2.3 Cracklet type C3

Figure 3.4 shows the configuration of the C3 type cracklet which is a kinked crack and is represented by three cracklets. It's opening profile approximation (b) may have three to five subfunction families depending on the wedge angle at the end points A and B and is given by equation (3.6), where the polynomial subfunction family for cracklet type C3 with each one having (N+1) coefficients has the form mentioned in equation (3.7).

$$b_j^{(i)}(t) = P_j^{AB(i)}\left(\frac{t}{a_i}\right) + \mathrm{W}^{\mathrm{A(i)}}_{\rho_1^{\mathrm{A}}\mathrm{j}}\left(\frac{t}{a_i}\right)\langle+\mathrm{W}^{\mathrm{A(i)}}_{\rho_2^{A}\mathrm{j}}\left(\frac{t}{a_i}\right)\rangle + \mathrm{W}^{\mathrm{B(i)}}_{\rho_1^{\mathrm{B}}\mathrm{j}}\left(1 - \frac{t}{a_i}\right)\langle+\mathrm{W}^{\mathrm{B(i)}}_{\rho_2^{\mathrm{B}}\mathrm{j}}\left(1 - \frac{t}{a_i}\right)\rangle \tag{3.6}$$

$$P_j^{AB}(\eta) = \sum_{k=0}^{1} P_{jk}\left[\eta^{(k)} - (N-k)\eta^{(N-1)} + (N-k-1)\eta^{N}\right] + \sum_{k=0}^{N-2} P_{j(k+2)}\left[(1-\eta)^{k} - (N-k))(1-\eta)^{N-1} + (N-k-1)(1-)\eta^{N}\right] \tag{3.7}$$

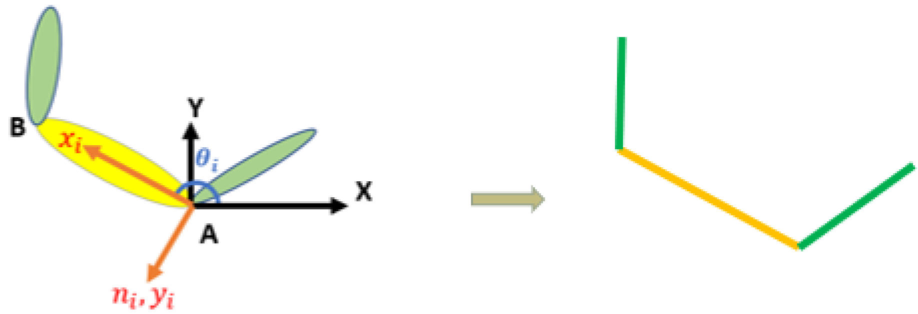

Figure 3.4 : Cracklet type C3 configuration and is represented by an orange straight line with another two green lines representing C2 type cracklets.

The most general form of these ODPs for a crack segment *i* can be written in the form mentioned in equation (3.8) in terms of distance t along the crack length when distances are measured from the left end of the crack.

$$b_j^{(i)}(t) = P_j^{1(i)}\left(\frac{t}{a_i}\right) + W^{1(i)}_{\rho_1^{1(i)}j}\left(\frac{t}{a_i}\right) + W^{1(i)}_{\rho_2^{1(i)}j}\left(\frac{t}{a_i}\right) + P_j^{2(i)}\left(1-\frac{t}{a_i}\right) + W^{2(i)}_{\rho_1^{2(i)}j}\left(1-\frac{t}{a_i}\right) + W^{2(i)}_{\rho_2^{2(i)}j}\left(1-\frac{t}{a_i}\right) \tag{3.8}$$

Where $P_j^{r(i)}$ represents the polynomial series and $W^{r(i)}_{P_k^{r(i)}j}$ represents either a tip series (ρ = 1/2) or a wedge series (1/2 < ρ < 1) for the i^{th} crack segment. Here j represents the direction of the ODP, j = 1 represents the ODP in tangential, whereas J = 2 represents the normal opening. r = 1, 2 shows that whether the series will start from the left or the right end of the crack segment, respectively as adjusted by replacing t with $a_i - t$.

The general form of approximated polynomial and the wedge series are given in equations (3.9) and (3.10) respectively, with η is equal to either t/a or $1 - t/a$, when used in equation (3.8). More details of these ODPs, analytical and computational aspects of the method can be found in [80-82].

$$P_j(\eta) = \sum_{k=0}^{N-1} P_{jk}\left[\eta^{(k)} - (N-k)\eta^{(N-1)} + (N-k-1)\eta^N\right] \tag{3.9}$$

$$W_{\rho j}(\eta) = \sum_{l=0}^{M-2} W_{\rho jl}\left[\eta^{(\rho+l)} - (M-1)\eta^{(\rho+M-l)} + (M-l-1)\eta^{(\rho+M)}\right] \tag{3.10}$$

3.3 Dislocation Based Influence Fields

The derivatives of ODPs are called **edge dislocation distributions (EDDs)**, as discussed earlier that these ODPs are selected such that the generated crack-face tractions should almost satisfying those prescribed in the AP. To understand, consider an infinite plate as shown in Figure 3.5 and imagine a local Cartesian x-y coordinate system along the crack segment. Consider an edge dislocation ED formed along a slit coincident with the positive x-axis, which causes a relative displacement (u^+- u^-) in both tangential (along x-axis) and normal (along y-axis) directions. These ED are defined by a Burger's vector (**b**) at the origin, with tangential (**b₁**) and normal (**b₂**) components representing glide and climb dislocation components, respectively. The stress (σ) and displacement (u)fields induced by these EDs are given in [17] and are represented by equations (3.11) and (3.12).

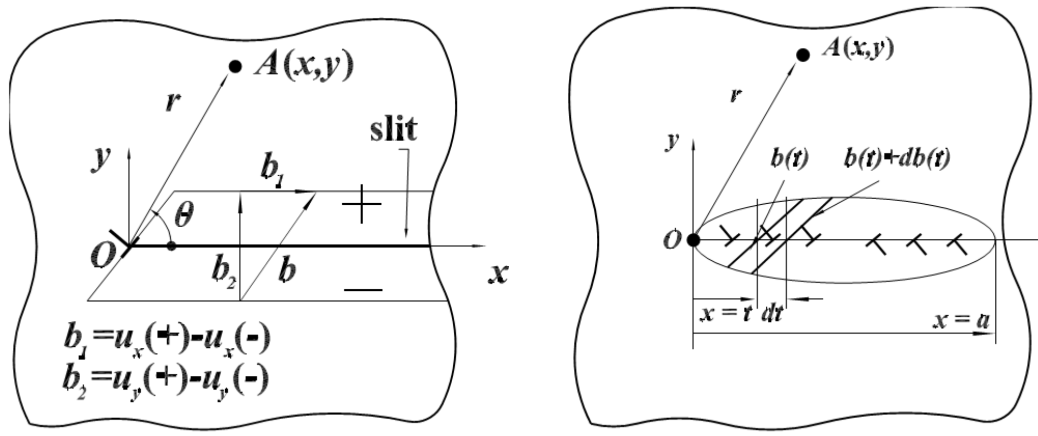

Figure 3.5 : EDD concept: (Left) a single ED producing an OPD (**b)** and (Right) a distribution of ED in an infinite plate under far-field loading.

Stress field: $$\begin{Bmatrix}\sigma_{xx}\\ \sigma_{yy}\\ \sigma_{xy}\end{Bmatrix} = \frac{2G}{\pi\,(\kappa+1)r^4}\begin{bmatrix}(3x^2+y^2)y & -(x^2-y^2)x\\ -(x^2-y^2)y & -(x^2+3y^2)x\\ -(x^2-y^2)x & -(x^2-y^2)y\end{bmatrix}\begin{Bmatrix}b_1\\ b_2\end{Bmatrix} \tag{3.11}$$

Displacement Field : $\begin{Bmatrix}u_x\\ u_y\end{Bmatrix} =$

$$\frac{1}{2\pi\,(\kappa+1)r^4}\begin{bmatrix}(\kappa+1)(\pi-\theta)-\frac{2xy}{r^2} & -(\kappa-1)\ln(r/r_{c)})+2\left(\frac{x}{r}\right)^2\\ -(\kappa-1)\ln(r/r_{c)})+2\left(\frac{y}{r}\right)^2 & (\kappa+1)(\pi-\theta)+\frac{2xy}{r^2}\end{bmatrix}\begin{Bmatrix}b_1\\ b_2\end{Bmatrix} \tag{3.12}$$

where r = $\sqrt{x^2+y^2}$ and $k = 3-4v$ for plane strain, $k = \frac{3-v}{1+v}$ for plane stress in terms of Poisson's ratio v and G is the shear modulus.

The infinitesimal distribution of Burgers vectors is captured in the dislocation distribution weighting function defined as:

$$\mu(t) = \frac{db(t)}{dt} \tag{3.13}$$

Replacing b by db(t) in equations (3.11) and (3.12) and integrating it in t along the crack segment, gives the stress and displacement fields resulting from the crack segment ODP and are given in the complex form ($z = x + iy$) in equations (3.14) and (3.15) respectively.

$$\begin{Bmatrix} \sigma_{xx} \\ \sigma_{yy} \\ \sigma_{xy} \end{Bmatrix} = \frac{2G}{\pi\,(\kappa+1)r^4} \begin{bmatrix} Re\{Z_2^1\} + yIm\{Z_1^1\} - yRe\{Z_1^2\} \\ Re\{Z_2^1\} + yIm\{Z_2^2\} - yRe\{Z_1^2\} \\ yRe\{Z_2^2\} + Re\{Z_1^1\} - yIm\{Z_1^2\} \end{bmatrix} \tag{3.14}$$

$$\begin{Bmatrix} u_x \\ u_y \end{Bmatrix} = \frac{1}{2\pi\,(\kappa+1)} \begin{bmatrix} (1-\kappa)Re\{Z_2^0\} - (\kappa+1)Im\{Z_1^0\} + 2yIm\{Z_2^1\} - 2yRe\{Z_1^1\} \\ (\kappa-1)Re\{Z_2^0\} - (\kappa+1)Im\{Z_2^0\} + 2yRe\{Z_2^1\} + 2yIm\{Z_1^1\} \end{bmatrix} \tag{3.15}$$

where

$$Z_j^0 = \int_0^a \frac{b_j(t)}{z-t}\,dt\,,\;\; Z_j^1 = \int_0^a \frac{\mu_j(t)}{z-t}\,dt\,,\;\; Z_j^2 = \int_0^a \frac{\mu_j(t)}{(z-t)^2}\,dt \tag{3.16}$$

where j = 1, 2

The integrals given in equation (3.16) can be calculated in closed form and are given in [22,23].

3.4 Satisfaction of Traction Boundary Conditions (BCs)

The unknown coefficients mentioned in equations (3.9) and (3.10) are found by satisfying the traction-free condition at the carefully chosen points on each crack in the actual boundary value (scheme to choose points is discussed in section 2.5). The tractions arising in the trivial problem (TP) of an infinite plate under far-field loading and the auxiliary problem (AP) of an infinite plate consisting of dislocation distributions along cracks must sum to zero along all crack surfaces.

$$T_{TP}^{1(i)} + T_{AP}^{1(i)} = 0, \quad T_{TP}^{2(i)} + T_{AP}^{2(i)} = 0 \tag{3.17}$$

The tractions in the TP are given as:

$$T_{TP}^{1} = n_X\sigma_{XX}^{\infty} + n_Y\sigma_{YY}^{\infty}, \quad T_{TP}^{2} = n_X\sigma_{XY}^{\infty} + n_Y\sigma_{YY}^{\infty} \tag{3.18}$$

Where T^1 and T^2 denote the tangential and normal crack-face tractions, respectively, and $i = 1 \ldots\ldots C$, where C is the total number of crack segments that can be of different length and orientation. σ∞ is the far-field stress applied to the plate and n_X and n_Y are the components of the crack surface normal.

3.5 Point Allocation Scheme

To satisfy the boundary conditions mentioned in equations (3.17) and (3.18), a point allocation scheme shown in Figure 3.6 is used. According to this, points are concentrated near wedge tips and their density is less away from the crack tip. The spacings between these allocated points are affected by the strengths of the singularities to which they are associated. These sets of points are chosen according to the distances described by Eq. (18). Figure 3.7 shows the actual location of 20 points for each set of points described by different formulations described in equation (3.17). There are 60 points in total along the crack length and it can be observed that the concentration of these points is higher at the tip of the crack as compared to the center. More details of this point allocation scheme and how unknown coefficients are determined using MATLAB can be found in [80,81].

$$\left.\begin{aligned} t_{k_1} &= a_i \left(\frac{k_1}{N_1+1}\right)^4, \; k_1 = 1,2,\ldots,N_1 \\ t_{k_2} &= a_i \left[1-\left(\frac{k_2}{N_2+1}\right)^4\right], \; k_2 = 1,2,\ldots,N_2 \\ t_{k_3} &= a_i \left(\frac{k_3}{N_3+1}\right)^1, \; k_3 = 1,2,\ldots,N_3 \end{aligned}\right\} \quad (3.19)$$

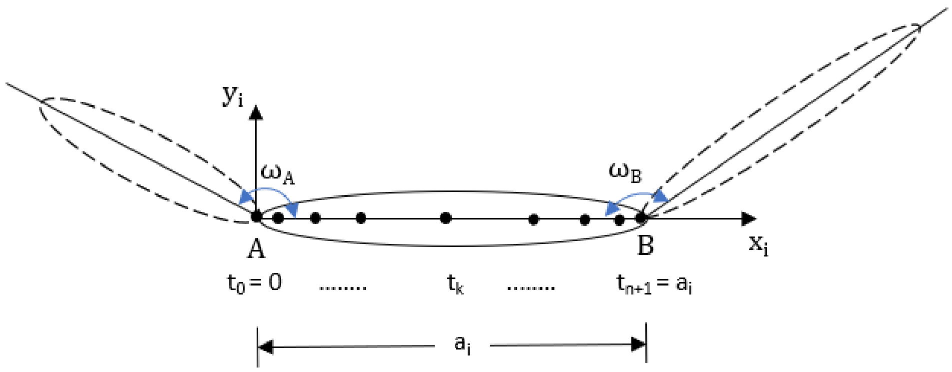

Figure 3.6 : Point allocation scheme.

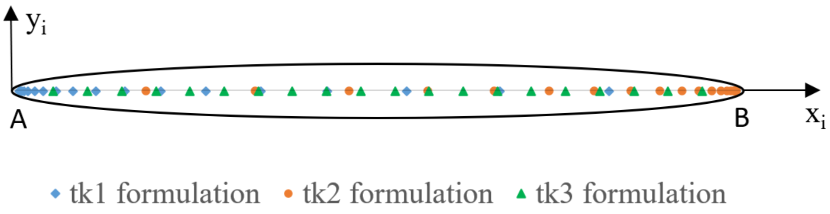

Figure 3.7 : Actual location of points along the crack line for different formulations.

3.6 Stress and Stress Intensity Factor (SIF) calculations

Once the unknown coefficients mentioned in equations (3.9) and (3.10) are calculated, all stress and displacement fields and all SIFs for crack tips and singular wedges at crack kinks can be determined. All stresses and stress intensity factors (SIFs) for mode 1 and mode 2 at the crack tip $\left(\rho\ =\frac{1}{2}\right)$ can be found from equation (3.20) and (3.21) respectively, whereas SIFs for crack kinks are given in equation (3.22).

$$\text{Stresses:}\ \begin{Bmatrix}\sigma_{xx}(X,Y)\\ \sigma_{yy}\ (X,Y)\\ \sigma_{xy}(X,Y)\end{Bmatrix}\ =\ \sum_{i=1}^{n_c}[T_i][S_i]\{U\}^{(i)} \qquad (3.20)$$

$$\text{SIFs for tip ends:}\ \begin{Bmatrix}\mathrm{K_I}\\ \mathrm{K_{II}}\end{Bmatrix}=\frac{2\mathrm{G}}{1+\kappa}\sqrt{\frac{\pi}{2\mathrm{a}}}\begin{Bmatrix}\mathrm{W}_{\frac{1}{2}20}\\ \mathrm{W}_{\frac{1}{2}10}\end{Bmatrix} \qquad (3.21)$$

$$\text{SIFs for kinks :}\ \begin{Bmatrix}K_I\\ K_{II}\end{Bmatrix}=$$

$$\frac{4G\pi}{1+\kappa}\begin{Bmatrix}\dfrac{\rho_1(1+\rho_1)}{(2\pi a)^{\rho_1}\sin\left[\frac{(\rho_1-1)(2\pi-\omega)}{2}\right]}\left[1-\dfrac{(\rho_1-1)\sin\left[\frac{(\rho_1-1)(2\pi-\omega)}{2}\right]}{(\rho_1+1)\sin\left[\frac{(\rho_1+1)(2\pi-\omega)}{2}\right]}\right]\omega_{\rho_1 20}\\ \dfrac{\rho_2(1+\rho_2)}{(2\pi a)^{\rho_2}\sin\left[\frac{(\rho_2-1)(2\pi-\omega)}{2}\right]}\left[\dfrac{(\rho_2-1)\sin\left[\frac{(\rho_2-1)(2\pi-\omega)}{2}\right]}{(\rho_2+1)\sin\left[\frac{(\rho_2+1)(2\pi-\omega)}{2}\right]}-\dfrac{\rho_2-1}{\rho_2+1}\right]\omega_{\rho_2 10}\end{Bmatrix} \qquad (3.22)$$

4. ANALYSIS PROCEDURE

The purpose of this chapter is to explain the complete analysis procedure of the proposed scheme to study the FCG using BCM. Different steps involved in modelling the geometry of the problem along with the implementation of BCM to the multiple cracks problems under fatigue loading are discussed. This chapter also describes that how the new position of the crack tip is determined after the application of cyclic loads and how the number of loading cycles required for a given crack extension are computed.

4.1 Implementation of BCM for Fatigue Crack Growth Problems

4.1.1 Modelling of the geometry

As it is mentioned in chapter 3 that in the implementation of BCM all the external boundaries of the plates and internal holes are modelled as a straight line, which are called “Cracklets”. The approximation of the holes can be adjusted by the number of sides of the polygon used to model the holes. In the following chapters, the effect of the number of sides of the polygon on the accuracy of predicting the fatigue crack growth path will be discussed in detail. To model the geometry, the coordinates of the end points of each straight line (cracklet) are entered as input. After defining the geometry of the problem, the type of cracklets is set for each straight line. For this purpose, the eigen values corresponding to the given cracklets are directly entered as input in the MATLAB codes.

4.1.2 Introduction of initial pre-cracks

After modelling the geometry, the pre-cracks are introduced into the model. The size and the orientation of each pre-crack along with their locations in the geometry are entered as input. These initial pre-cracks are inserted as C2 cracklets.

4.1.3 Estimation of SIFs and determination of new crack tip position

After the introduction of initial pre-cracks, a known stress range ($\Delta\sigma$) is applied, and mode-I and mode-II stress intensity factors (SIFs) are computed for each crack tip using BCM. This calculation of SIFs for each crack tip is done iteratively and only SIFs of one certain crack tip is calculated in each iteration. In the first iteration, SIFs for crack tip 1 are computed and in the second iteration SIFs for crack tip 2 are solved and this process goes on up to the last crack tip. These calculated stress intensity factors for mode-I and mode-II at each crack tip are used to predict the new crack kink angle by selecting a suitable criterion for the crack propagation. The details of the criteria used to predict the crack propagation angle will be discussed in section 4.3. Using the new crack kink angle the new position of the crack tip is added for a fixed crack increment size Δc. This iterative process goes on until the cracks reach up to a required crack length extension.

4.1.4 Calculation of number of loading cycles

The calculated stress intensity factor range in each iteration is used to determine the crack growth rate by applying a suitable crack growth model as discussed in section 4.2. Using this crack growth rate together with the initial cycle step size Δc, the number of cycles required for a given iteration is determined by (26). This simulation goes on incrementally with a constant incremental crack length Δc as in (27). The total fatigue life of the structure can be calculated by summing up the number of loading cycles required in each iteration.

4.2 Solution of an Example FCG Problem

The most important point in implementing the BCM to fatigue crack growth problem is that after the calculation of the initial crack orientation angle, a new small cracklet of type C2 of length Δc is added which enables us to determine the next crack orientation angle. When a new cracklet is added according to the new crack orientation angle, the type of the previous cracklet is to be changed from C2 to C3 and always the new cracklet is added with C2 cracklet type. This same technique is also explained in [90] to implement the BCM for a single crack in an infinite plate under fatigue loading.

To understand this concept, let us consider an example FCG problem in which there are two holes of radius R, separated at a distance S from each other are present in the plate and two cracks are emanating at angle $\pm\theta$ from a certain location at each hole (as shown in Figure 4.1). A constant amplitude cyclic stress σ is applied in the normal direction at the outer edges of the plate. Figure 4.2 shows the modelled geometry of the problem. The external boundary of the plate and the holes within the plate are modelled as straight lines. In this example, 16 sided polygons are used to model each hole. The corresponding cracklet types are assigned to these cracklets.

Figure 4.3 shows different iterations of the simulation. Figure 4.1(A) shows the iteration no.1 in which the first initial pre-crack is added at the given location at hole no. 1, similarly, Figure 4.3(B) shows iteration no. 2 of the simulation, and the second pre-crack is added to the model at the given location. Cracklet type C2 is given to each of these initial pre-cracks. Figure 4.3(C) shows iteration no.3 of the simulation, in which the angle of propagation for crack tip A is determined, and a new position of crack tip A is added with the given crack increment. Here, the new cracklet is added as C2 type, whereas the type of the previous cracklet is changed from C2 to C3. In Figure 4.3(D), the same procedure is shown for crack tip B. The new cracklet is always added as a C2 cracklet and the type of already present cracklet is changed from C2 to C3. The simulation goes on in a similar manner and finally, both crack tips reach up to the opposite holes and the simulation is set to be stopped. Figure 4.4 shows the FCG path after the final iteration.

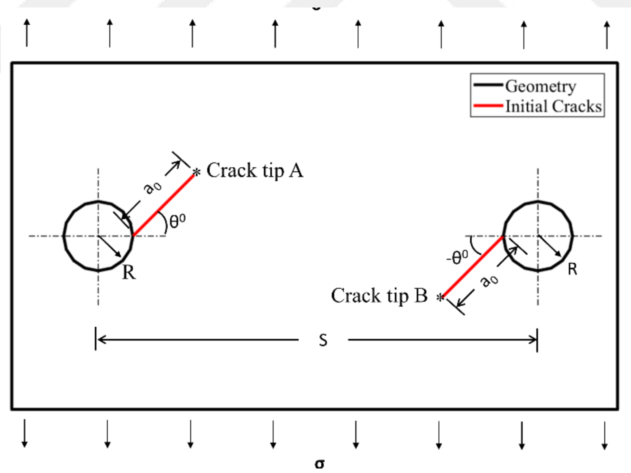

Figure 4.1 : Geometry of example problem.

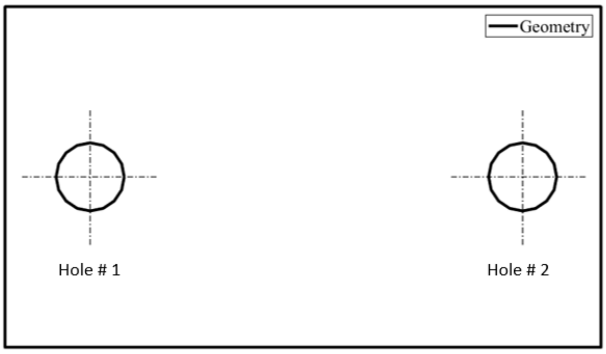

Figure 4.2 : Modelled geometry of the problem.

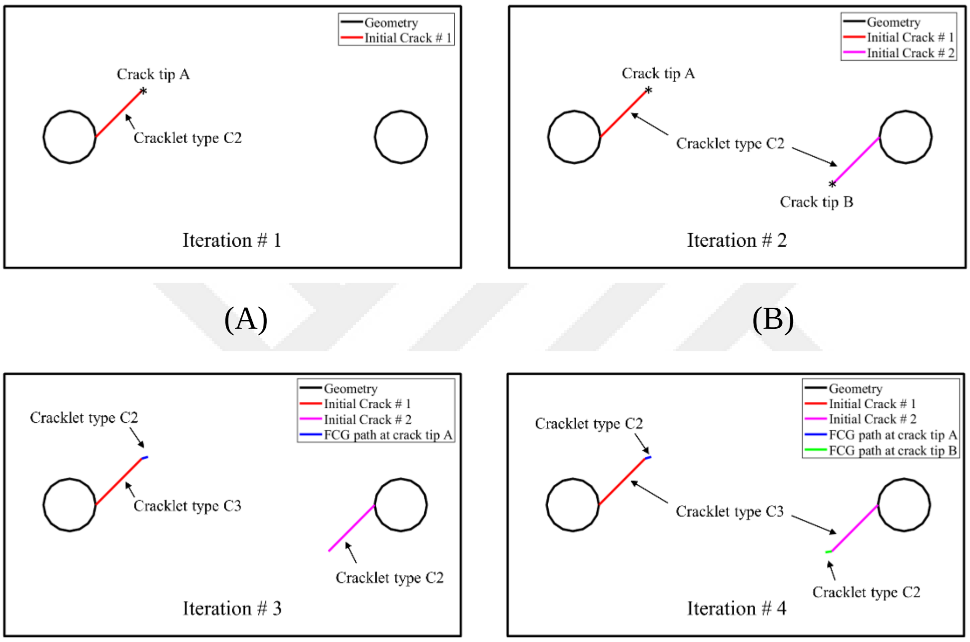

(C) (D)

Figure 4.3 : Different iteration of FCG simulation; (A) Iteration no.1, (B) Iteration no.2, (C) Iteration no.3, (D) Iteration no.4.

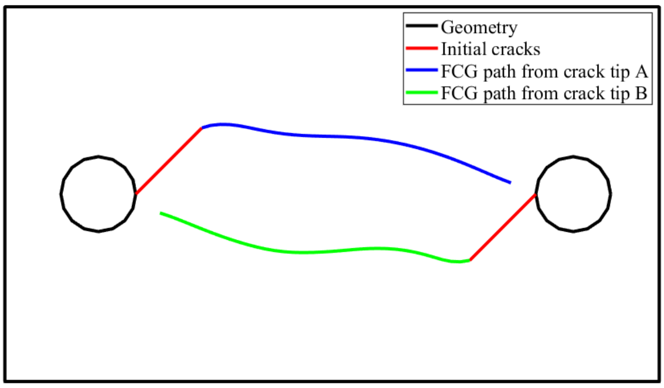

Figure 4.4 : FCG path after final iteration.

Different steps involved in the analysis of fatigue crack propagation by the proposed scheme are summarized as follows:

(1) Model the geometry using straight lines called “Cracklets”.

(2) Assign the cracklet type of each straight line and input the corresponding eigen values for the given cracklet.

(3) Add the size and orientation of every pre-crack along with their location in the model.

(4) Compute the SIFs using the boundary cracklet method for every crack tip iteratively.

(5) Determine the crack propagation angle based on the criterion mentioned in section 4.4.

(6) Add the crack extension of fixed increment along the direction computed in step 5.

(7) Using the crack growth model (mentioned in section 4.3) compute the number of loading cycles required for given crack extension.

(8) Repeat the step 4 to 7 for each crack tip until the crack reaches up to the required length.

4.3 Crack Growth Models

There is always a need of a crack growth model for calculating the size of a crack growing with the applied fatigue loading. In linear elastic fracture mechanics (LEFM), usually, the stress intensity approach is used to determine the crack-tip stress conditions in a linear elastic material. All the components of stresses at the crack tip are proportional to a constant quantity i.e. called stress intensity factor K. This SIF is a function of nominal applied stress, initial crack size and depends upon some geometric factors. Under cyclic loading, a concept of SIF range ΔK is used i.e. $\Delta K = K_{max} - K_{min}$. K_{max} and K_{min} are the SIFs values corresponding to maximum and minimum values of applied stress in a loading cycle. Figure 4.5 shows the typical curve of crack growth rate versus the stress intensity range for metals [6]. This curve is consisting of three different regions: Region I, II and III. Region I show the initiation of crack growth, here the FCG is very slow. There is a threshold value of ΔK_{th} and no crack growth is possible for $\Delta K < \Delta K_{th}$. Region II shows the propagation of the crack, where the FCG is stable and linear relation can be observed between FCG rate ΔK. Region III is the unstable region and the FCG rate rapidly increased as K_{max} reaches the K_c fracture toughness of the material.

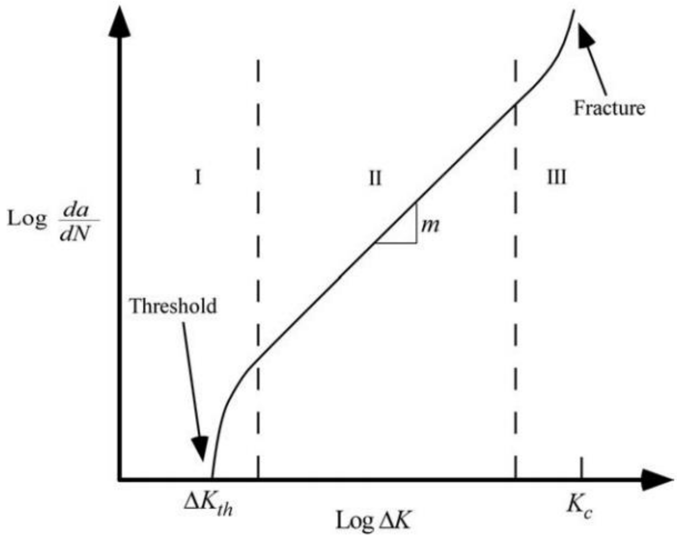

Figure 4.5 : Typical FCG curve for metals [6].

In literature, different crack growth models have been proposed to predict the rate of fatigue crack growth. Most of these crack growth models are based on Paris's law [84] proposed by Paris and Erdogan in 1960. Over time, many improvements have been made to Paris's law by different researchers. Forman et al. [85] further improved the theory presented by Paris and Erdogan by including the variation in the crack-growth rate owing to the load ratio and the instability of the crack growth when the value of the maximum stress-intensity factor approaches the fracture toughness of the material. Walker [86] modified the Paris equation to incorporate the effect of stress ratio R in the linear region of the rate of crack propagation vs crack length plot. Finally, the most general equation named NASGRO equation is developed and used in the crack growth programs AFGROW [4] and NASGRO [3] software to predict FCG behaviour in all regions of fatigue rate vs crack length plot. This model includes the stress ratio effect along with the crack closure effect.

All the above-mentioned models apply to the constant amplitude fatigue loading which is the most general type of fatigue loading in FCG analysis. In this study, the constant amplitude fatigue loading is also considered for all the studied cases. Figure 4.6 shows a constant amplitude cyclic loading having the stress ratio $R = \sigma_{min}/\sigma_{max}$ where

σ_{max} and σ_{min} are the maximum and minimum values of applied cyclic stress, respectively. The mean stress $\sigma_{mean} = \frac{(\sigma_{max} + \sigma_{min})}{2}$, the stress range $\Delta\sigma = \sigma_{max} - \sigma_{min}$ and the stress amplitude (σ_a) are also shown in Figure 4.6. In this study, Paris-Erdogan law, Walker's model and Forman's Law are used to predict the FCG behaviour and are discussed in the following sections.

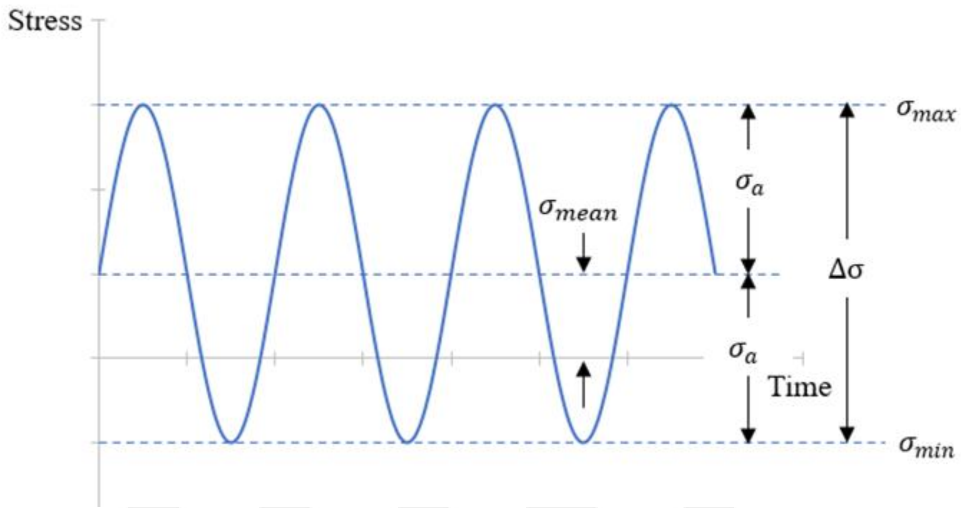

Figure 4.6 : Constant amplitude cyclic loading.

4.3.1 Paris-Erdogan's law

In 1960, Paris and Erdogan proposed that there is a linear relationship between the SIF range and the rate of fatigue crack growth on a log-log scale [84]. According to the Paris-Erdogan law, the fatigue crack growth rate can be determined by the equation (4.1).

$$\frac{da}{dN} = C\ (\Delta K)^m \tag{4.1}$$

$$\Delta \mathrm{K} = \mathrm{K}_{\mathrm{max}} - \mathrm{K}_{\mathrm{min}} \tag{4.2}$$

Where da/dN represents crack growth rate, ΔK is stress intensity range, C and m are Paris equation constants that depend on the material of the specimen.

To incorporate the mixed-mode conditions and the effect of stress ratio R, the approach of effective SIF range is used. For this purpose, a criterion proposed by Tanaka [87] is used. According to this criterion, the equivalent stress intensity factor (SIF) can be computed by the equation (4.3), and $\Delta \mathrm{K}_{\mathrm{eff}}$ is used in place of ΔK in equation (4.1) and the equation (4.4) is used to compute the rate of FCG rate.

$$\Delta K_{eff} = (\Delta K_I{}^4 + 8\Delta K_{II}{}^4)^{0.25} \tag{4.3}$$

$$\frac{da}{dN} = C\,(\Delta K_{eff})^m \tag{4.4}$$

4.3.2 Forman's Law

In 1967, Forman et al. [85] improved the theory presented by Paris and Erdogan by including the variation in the crack-growth rate owing to the stress ratio and the instability of the crack growth in region III of the FCG rate curve when the value of the maximum stress-intensity factor approaches the fracture toughness of the material. Forman proposed the relationship mentioned in equation (4.5) to determine the FCG rate.

$$\frac{da}{dN} = \frac{C\,(\Delta K)^m}{(1-R)K_c - \Delta K} \tag{4.5}$$

Where da/dN represents crack growth rate, ΔK is stress intensity range, R is the stress ratio, and m is the slope of crack growth rate v/s ΔK plot on a log-log scale and K_c is the fracture toughness of the material.

4.3.3 Walker's Model

In 1970, Walker proposed the modified form of the Paris equation by incorporate the effect of stress ratio R on FCG rate [86]. Equation (4.6) represents the proposed model of Walker, which compute the FCG rate by introducing a new parameter $\overline{\Delta K}$ that is related with the SIF range ΔK through equation (4.7).

$$\frac{da}{dN} = C\,(\overline{\Delta K}\,)^m \tag{4.6}$$

Where

$$\overline{\Delta K} = \frac{\Delta K}{(1-R)^{\gamma}} \tag{4.7}$$

After inserting the value of $\overline{\Delta K}$, Equation (4.6) takes the following form:

$$\frac{da}{dN} = C\left(\frac{1}{(1-R)^{1-\gamma}}\,\Delta K\right)^m \tag{4.8}$$

where da/dN represents crack growth rate, ΔK is stress intensity range, R is the stress ratio, and m is the slope of crack growth rate v/s ΔK plot on a log-log scale. The value γ is a material constant that indicates how strongly the stress ratio R affects the crack growth rate in the material. For most of the metals, its typical value is taken as 0.5 [6]. For R = 0, Walker's equation mentioned in equation (4.8) takes the form of Paris's equation.

4.4 Determination of Crack Growth Angle

In literature, various stress or energy-based criteria are described for crack growth direction but maximum tangential stress (MTS) criterion [88], minimum strain energy density (MSED) criterion [89] and maximum energy release rate (MERR) criterion [90] are most popular among them. In this study, MTS and MSED are used to predict the direction of crack growth angle, and the same are explained below in detail.

4.4.1 Maximum tangential stress (MTS) criterion

In this criterion, it is considered that the crack will propagate from its tip in the direction along which the maximum tangential or hoop stress $\sigma_{\theta\theta}$ will produce, so the stresses around the crack tip in polar coordinates should meet the conditions mentioned in equation (4.9).

$$\frac{\partial\sigma_{\theta\theta}}{\partial\theta} = 0\,;\ \frac{\partial^2\sigma_{\theta\theta}}{\partial\theta^2} < 0 \tag{4.9}$$

By using the stress determining equations [6] around a crack tip, differentiating it with respect to θ and applying the conditions mentioned in equation (4.9), results in equations (4.10) and (4.11), which can be solved to get the kinking angle (θ) of the propagating crack. Different forms of equations can be obtained by solving the equation (4.10), one of those forms is mentioned in equation (4.12).

$$\tan^2\frac{\theta}{2} - \frac{1}{2}\frac{K_I}{K_{II}}\tan\frac{\theta}{2} - \frac{1}{2} = 0 \tag{4.10}$$

$$-\frac{3}{2}\left\{\left(\frac{1}{2}\cos^3\frac{\theta}{2} - \cos\frac{\theta}{2}\sin^2\frac{\theta}{2}\right) + \frac{K_{II}}{K_I}\left(\sin^3\frac{\theta}{2} - \frac{7}{2}\sin\frac{\theta}{2}\cos^3\frac{\theta}{2}\right)\right\} < 0 \tag{4.11}$$

$$\theta = 2\tan^{-1}\left[\frac{\Delta K_I - \sqrt{\Delta K_I{}^2 + 8\Delta K_{II}{}^2}}{4\Delta K_{II}}\right] \quad (4.12)$$

4.4.2 Minimum strain energy density (MSED) criterion

According to the minimum strain energy density (MSED) criterion, it is considered that the crack will propagate from its tip in the direction of minimum strain energy density S and it will initiate when the strain-energy-density factor reaches a critical value S_{cr}. These two conditions are given in equations (4.13) and (4.14) respectively.

$$\left.\frac{\partial S(\theta)}{\partial \theta}\right|_{\theta=\theta_0} = 0, \qquad \left.\frac{\partial^2 S(\theta)}{\partial \theta^2}\right|_{\theta=\theta_0} \geq 0 \quad (4.13)$$

where θ_0 is the angle of crack extension and $-\pi \leq \theta_0 \leq \pi$

$$a_{11}K_I{}^2 + 2a_{12}K_IK_{II} + a_{22}K_{II}{}^2 = S_{cr}\ for\ \theta = \theta_0 \quad (4.14)$$

where

$$a_{11} = \frac{1}{16G\pi}[(\kappa - \cos\theta)(1 + \cos\theta)] \quad (4.15)$$

$$a_{12} = \frac{1}{16G\pi}\sin\theta\,[2\cos\theta - \kappa + 1] \quad (4.16)$$

$$a_{22} = \frac{1}{16G\pi}\sin\theta\,[(\kappa + 1)(1 - \cos\theta) + (1 + \cos\theta)(3\cos\theta - 1)] \quad (4.17)$$

where G is shear modulus, κ is elastic constant and equal to $(3 - \upsilon)/(1 + \upsilon)$ for plane stress and $3 - 4\upsilon$ for plane strain, where υ is the Poisson's ratio.

4.5 Estimation of Number of Loading Cycles

During the FCG analysis by the proposed method, an initial crack of known size is implemented in structure and a known stress range is applied and an effective stress intensity range ΔK_{eff} is calculated. Using that calculated stress intensity range value and crack growth model, the crack growth rate is calculated. Using this crack growth rate together with the initial cycle step size, the number of cycles required for that iteration is determined by equation (4.18). This simulation goes on incrementally with a constant incremental crack length, for the calculation of new crack length by equation (4.19) in the direction of the new angle of crack front in each iteration which is determined by suitable criterion. The total number of loading cycles required for a given crack length can be calculated by equation (4.20).

$$\Delta N_i = \frac{c_i}{(da/dN)_i} \tag{4.18}$$

$$c_{i+1} = c_i + \Delta c \tag{4.19}$$

$$N_{i+1} = N_i + \Delta N \tag{4.20}$$

Where i = 1,2,3, …. up to number of iterations.

5. VALIDATION OF THE PROPOSED SCHEME

In this chapter, the accuracy of the proposed scheme to analyse the FCG behaviour of single and as well as multiple cracks under mixed-mode loading conditions is discussed. For this purpose, different FCG problems involving single and multiple cracks in simple to relatively complex plate geometries are selected from the literature and reanalysed by the proposed method. To show the effectiveness and accuracy of the presented scheme, three different aspects of fatigue crack growth are considered for this purpose, i.e. calculation of SIFs, prediction of fatigue crack growth paths and estimation of the required number of loading cycles to produce a given crack length.

5.1 Calculation of SIFs

In this section, different problems are discussed in which mode-I and mode-II SIFs are calculated by the proposed method and computed values of SIFs are compared with those calculated by analytical methods and with those which are mentioned in the available literature.

5.1.1 An infinite plate having inclined crack under different loading conditions

Consider an infinite plate having an inclined central crack is undergoes different loading scenarios i.e. uniaxial tensile loading, shear loading and biaxial loading with different biaxiality stress ratio. Mode-I and mode-II SIFs are calculated for each case by using BCM and results are compared with the analytical results.

5.1.1.1 Under uniaxial tensile loading

The first example deals with the mixed-mode crack problem in an infinite plate with an inclined center crack under uniaxial tensile stress σ as shown in Figure 5.1. Let us assume that $2a = 1$ unit is the length of the central crack and θ is the angle between the crack and the horizontal axis. Close-formed analytical solutions [7] of mode-I and mode-II SIFs for this case are given by (5.1) and (5.2) respectively.

$$K_1 = \sigma\sqrt{\pi a}\, cos^2(\theta) \tag{5.1}$$

$$K_2 = \sigma\sqrt{\pi a}\, cos(\theta) sin(\theta) \tag{5.2}$$

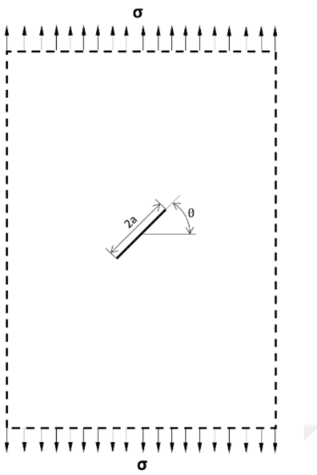

Figure 5.1 : Infinite plate having central inclined crack under uniaxial tensile stress.

Figure 5.2 shows the comparison of normalized mode-I and mode-II SIFs computed analytically with those computed by BCM for different values of crack inclination angle θ for uniaxial tension, whereas Table 5.1 shows the same comparison in tabular form. The normalized SIFs are obtained by dividing K_I and K_{II} with the term " $\sigma\sqrt{\pi a}$ ". The result shows that calculated SIFs for both mode-1 and mode-2 are very close to those calculated through analytical relationships.

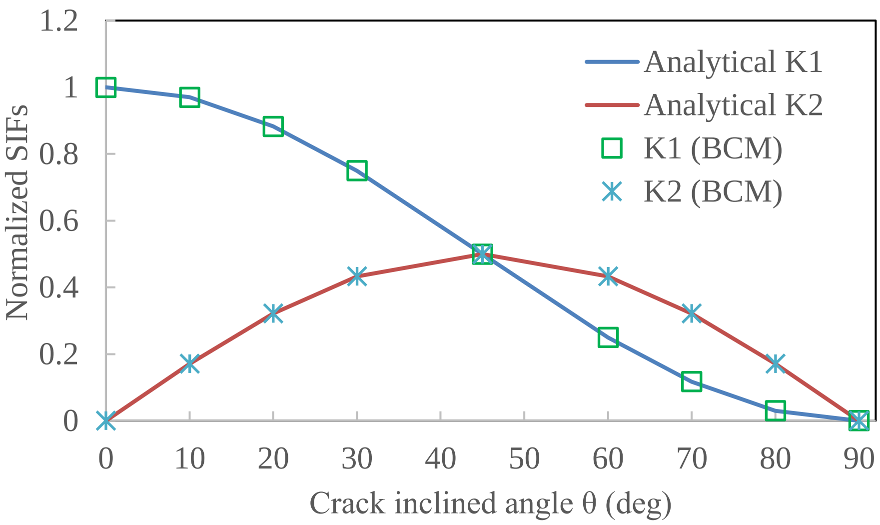

Figure 5.2 : Variation of the normalized SIFs calculated by the presented BCM in comparison with exact solution for uniaxial tensile loading.

Table 5.1 : Comparison of mode-I and mode-II SIFs (K_I, K_{II}) under uniaxial tension.

Crack angle	Mode-I SIF (K_I)		Mode-II SIF (K_{II})	
θ	Analytical	BCM	Analytical	BCM
0	1.253	1.252	0	0
10	1.216	1.214	0.214	0.214
20	1.107	1.106	0.403	0.402
30	0.940	0.939	0.543	0.542
45	0.627	0.626	0.627	0.626
60	0.313	0.313	0.543	0.542
70	0.147	0.146	0.403	0.402
80	0.038	0.038	0.214	0.214
90	0	0	0	0

5.1.1.2 Under shear loading

Figure 5.3 shows an infinite plate with an inclined central crack under shear stress τ. The length of the central crack is 2a = 1 and θ is the angle between the crack and the horizontal axis. Close-formed solutions of mode-I and mode-II SIFs for shear loading are given in Equations (5.3) and (5.4), respectively.

$$K_1 = -\,\tau\sqrt{\pi\, a}\; sin(2\theta) \tag{5.3}$$

$$K_2 = \tau\sqrt{\pi\, a}\; cos(2\theta) \tag{5.4}$$

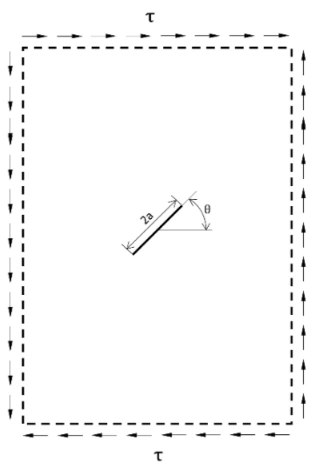

Figure 5.3 : Infinite plate having central inclined crack under shear stress.

Figure 5.4 shows the variation of normalized mode-I and mode-II SIFs (normalized SIFs are obtained by dividing K_I and K_{II} with the term " $\tau\sqrt{\pi\, a}$ ") with inclined angle θ, which are computed by analytical formulation and proposed BCM. Table 5.2 shows the comparison of computed SIFs by proposed BCM with those found out by analytical formulation for different values of crack inclination angle θ for shear loading. Results show that the computed SIFs are very close to those found by analytical formulation.

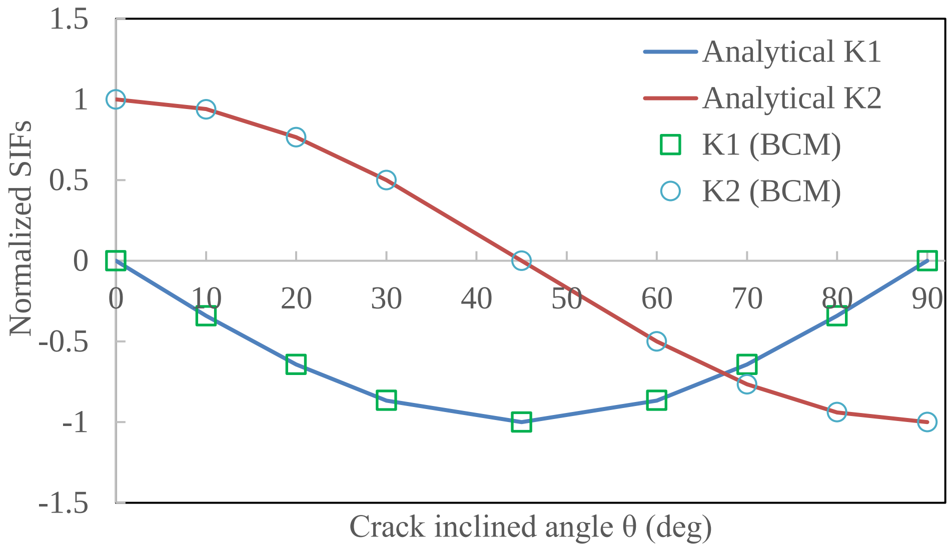

Figure 5.4 : Variation of the normalized SIFs calculated by the presented BCM in comparison with the exact solution for shear loading.

Table 5.2 : Comparison of mode-I and mode-II SIFs (K_I, K_{II}) for shear loads.

Crack angle	Mode-I SIF (K_I)		Mode-II SIF (K_{II})	
Θ	Analytical	BCM	Analytical	BCM
0	0	0	1.253	1.252
10	-0.429	-0.428	1.178	1.177
20	-0.806	-0.805	0.960	0.959
30	-1.085	-1.084	0.627	0.626
45	-1.253	-1.252	0	0
60	-1.085	-1.084	-0.627	-0.626
70	-0.806	-0.805	-0.960	-0.959
80	-0.429	-0.428	-1.178	-1.177
90	0	0	-1.253	-1.252

5.1.1.3 Under biaxial loading

This is a benchmark problem for the calculation of mode-1 and mode-2 SIFs for an infinite plate having an inclined crack under biaxial tensile loading of σ_y and $\sigma_x = \lambda\sigma_y$, where λ is the biaxiality stress ratio. Let us assume that $2a = 1$ is the length of the central crack and θ is the angle between the crack and the horizontal axis (as shown in Figure 5.5). Close-formed solutions of mode-I and mode-II SIFs for an infante plate having central inclined crack under biaxial loading [92] are given by equation 5.5) and (5.6). Table 5.3 shows the comparison of mode-I and mode-II SIFs (K_I, K_{II}) computed using BCM with those found out analytically under different values of biaxiality stress ratio (λ = -1, -0.5, 0, 0.5, 1). Results show that the computed values of SIFs by BCM under different conditions of biaxial loading are very close to those computed analytically.

$$K_1 = \sigma\sqrt{\pi\, a}\,(cos^2\theta \,+\, \lambda\, sin^2\theta) \tag{5.5}$$

$$K_2 = \sigma\sqrt{\pi\, a}\,(1-\lambda)\; cos\theta\; sin\theta \tag{5.6}$$

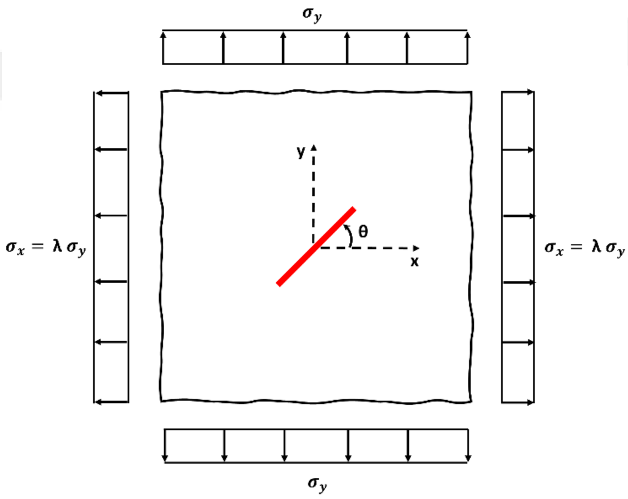

Figure 5.5 : Geometry of infinite plate having inclined crack under biaxial loading with biaxiality stress ratio λ.

Table 5.3 : Comparison of mode-I and mode-II SIFs (K_I, K_{II}) under biaxial loading for different values of λ.

Biaxiality ratio (λ)	Inclined angle (θ)	K_I		K_{II}	
		Analytical	BCM	Analytical	BCM
-1	0	1.2533	1.2535	0	0
	15	1.0854	1.0856	0.6267	0.627
	30	0.6267	0.6268	1.0854	1.086
	45	0	0	1.2533	1.254
-0.5	0	1.2533	1.2535	0	0
	15	1.1274	1.1276	0.47	0.47
	30	0.7833	0.7835	0.8141	0.814
	45	0.3133	0.3134	0.94	0.94
0	0	1.2533	1.2535	0	0
	15	1.1694	1.1696	0.3133	0.313
	30	0.94	0.9402	0.5427	0.543
	45	0.6267	0.6268	0.6267	0.627
0.5	0	1.2533	1.2535	0	0
	15	1.2113	1.2116	0.1567	0.157
	30	1.0966	1.0968	0.2714	0.271
	45	0.94	0.9402	0.3133	0.313
1	0	1.2533	1.2535	0	0
	15	1.2533	1.2535	0	0
	30	1.2533	1.2535	0	0
	45	1.2533	1.2535	0	0

5.1.2 Crack growth in an aircraft wing lug

In this problem, a relatively complex problem is solved for the determination of SIFs. A crack emanating from a circular hole from an aircraft wing lug presented in [93] is reanalysed by using the proposed method. Three different geometries of lug are considered, all dimensions of lugs are the same except ‘H’ and are shown in Figure 5.6 whereas dimension ‘H’ is mentioned in Table 5.4. The comparison of values of effective stress intensity factor (K_{eff}) calculating using FE solution [93], analytical method [5] and BCM is shown in Table 5.4. Results show that the estimated values of the stress intensity factor are very close to the analytical values as well as the values determined by FEA for different geometry of lugs.

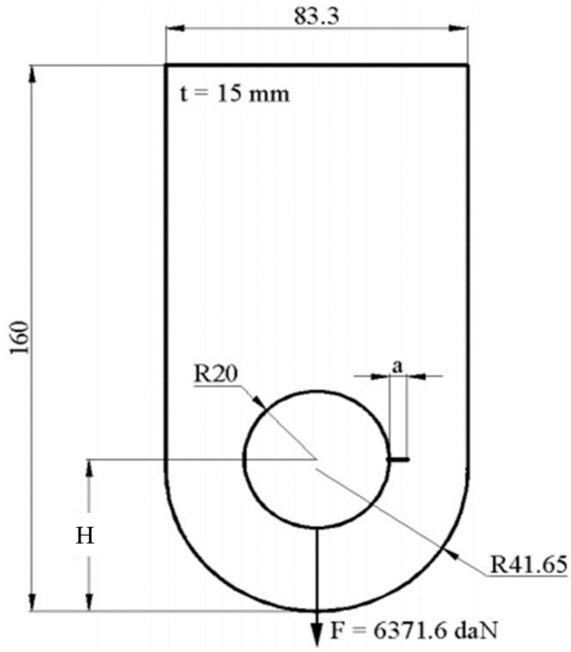

Figure 5.6 : Geometry of the aircraft wing lug [93].

Table 5.4 : Comparison of values of effective SIFs calculated using FEM, analytical approach and proposed BCM.

Lug No.	Dimension 'H' (mm)	a_0 (mm)	Eff. SIF value (MPa.mm$^{1/2}$) using		
			FEM [93]	Analytical [86]	BCM
2	44.4	5	68.78	65.62	65.91
6	57.1	5.33	68.12	70.24	71.23
7	33.3	4.16	94.72	93.64	93.39

5.2 Prediction of FCG Paths

In this section, the accuracy of the proposed method is shown by comparing the trajectories of FCG of different problems with the results presented by different researchers which were already available in the literature. Several benchmark problems are analyzed, in which single and multiple cracks in simple to relatively complex plate geometry are discussed under mixed-mode fatigue loading.

5.2.1 Crack growth from riveted holes

As a first example, FCG behaviour in a riveted plate having an initial crack emanating from one of the rivet holes is study. The geometry, material properties and other parameters are shown in Figure 5.7. Previously the same problem was solved by using the finite element method [93]. Polygons with straight lines as their sides are used to model the rivet holes in the plate. For this study, polygons with two different numbers of sides (n_pol) are used i.e. 16 and 24, to study its effect on the accuracy of the proposed method. Figure 5.8 shows the comparison of crack growth path obtained from FE solution [93] with those predicted by BCM by using 24 sides to model the holes, whereas Figure 5.9 shows the crack propagation paths obtained by using n_pol = 16 and 24. The comparison of the location of the crack tip after each solution step is given in the tabular form in Table 5.5. Results show that there is a close agreement between the crack path described by the proposed method and that is described in [93] and the accuracy of BCM can be adjusted by selecting different numbers of sides to model the holes.

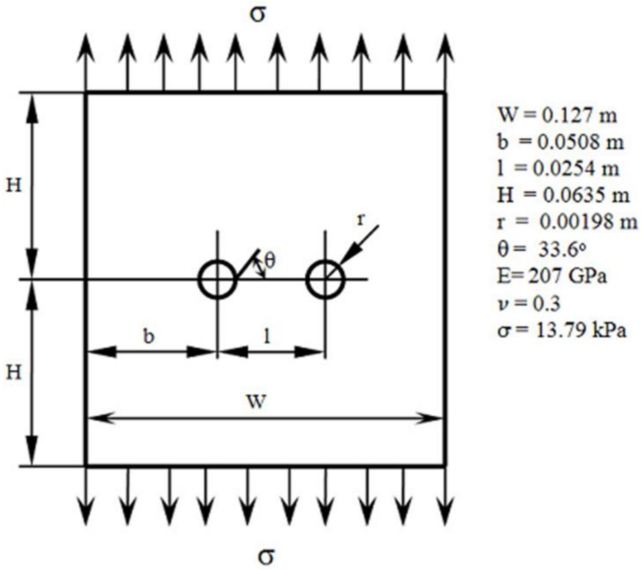

Figure 5.7 : Geometry of plate having riveted holes [93].

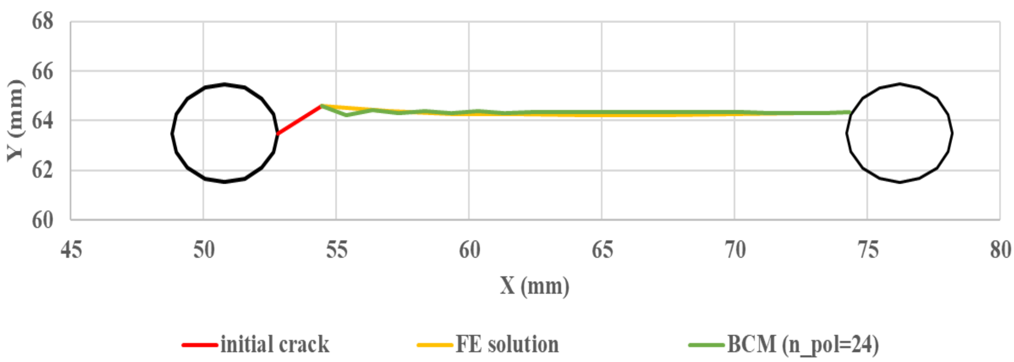

Figure 5.8 : Comparison of crack growth path for n_pol = 24.

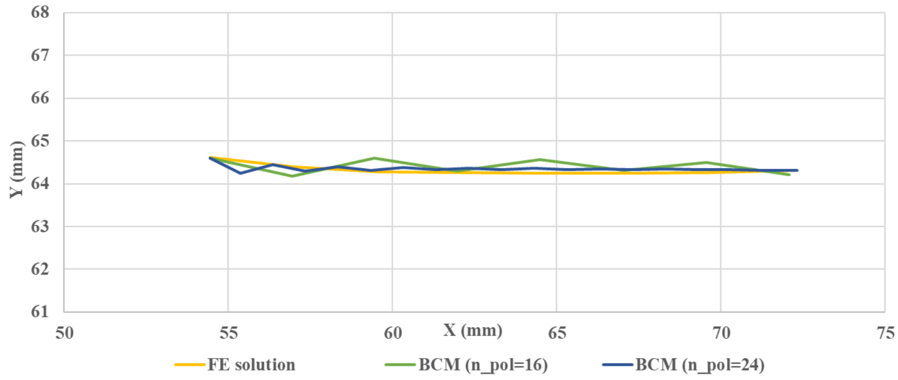

Figure 5.9 : Fatigue crack growth path with different n_pol values.

Table 5.5 : Comparison of crack tip location.

FE solution [93]		Boundary cracklet method (BCM)			
		(n_pol = 16)		(n_pol = 24)	
X (mm)	Y (mm)	X (mm)	Y (mm)	X (mm)	Y (mm)
54.458	64.618	54.446	64.607	54.446	64.606
59.525	64.287	59.452	64.599	59.332	64.315
64.605	64.247	64.500	64.559	64.326	64.360
69.685	64.27	69.562	64.502	69.325	64.331

5.2.2 FCG behaviour of cruciform specimen having central inclined crack under biaxial loading

To validate the model for the prediction of fatigue crack path under complex loading scenarios, FCG behaviour of a cruciform specimen made of aluminium alloy 7075-T651, having an inclined crack at 45^0 with the horizontal axis at the centre of the specimen is analysed under in phase biaxial loading as shown in Figure 5.10. Fatigue crack propagation paths are predicted using BCM for different values of biaxiality ratios (λ) i.e. 0, 0.5, 1, 1.5 and results are compared with the experimental results reported in [94]. Figure 5.11 shows that a good agreement is obtained between the paths predicted by BCM and experimental results [94].

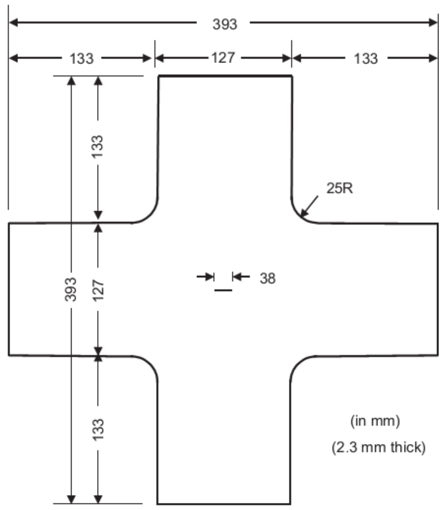

Figure 5.10 : Geometry of the problem [94] (all dimensions are in mm).

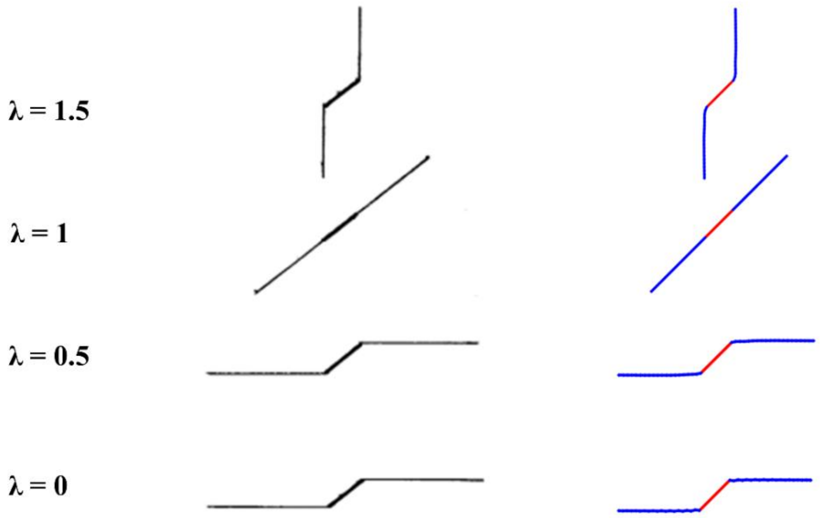

Figure 5.11 : Comparison of FCG path in cruciform specimen with a central crack at 45^0 under different values of λ; (A) Experimental results [5], (B) BCM.

5.2.3 An edge crack in a plate having a hole

In this problem, the deflection of crack propagation path due to an offset hole in a plate is discussed for two different geometries. As of **1st geometry**, a plate having a hole with a radius of 0.2 m and a pre-crack of a_0 = 0.1 m is discussed under tensile stress applied at the top and bottom edge of the plate (as shown in Figure 5.12). The plane stress conditions are assumed to be applied for this analysis. The material properties are given as follows: E = 30 GPa and ν = 0.3. In past, the same problem has been solved by many researchers e.g. Huyhn et al. [96] used polyXFEM to analyse this problem and Leonel et al. [97] solved it by using BEM formulation. Figure 5.13 shows the predicted crack propagation path using BCM and its comparison with the results proposed by Huyhn et. al. A good agreement among the paths predicted by both methods can be found.

Figure 5.14 shows a comparison of mode-2 SIF value at different crack lengths calculated using presented BCM and with the values computed by FRANC2D and BEM by Leonel et al. [97]. The results obtained from the BCM are in good agreement with those that were predicted in the reference study. Variation of K_{II} value with crack length (as shown in Figure 5.14) shows that initially, the crack grows horizontally (perpendicular to the applied normal stress), mode-1 effects are dominating and K_{II} value is very small. But when the crack propagates and deviates due to the presence of the hole (approximately at a crack length of 0.5 m), mode-II effects also start to appear and the value of K_{II} increases gradually and crack grows under mixed-mode conditions until it reaches near the hole.

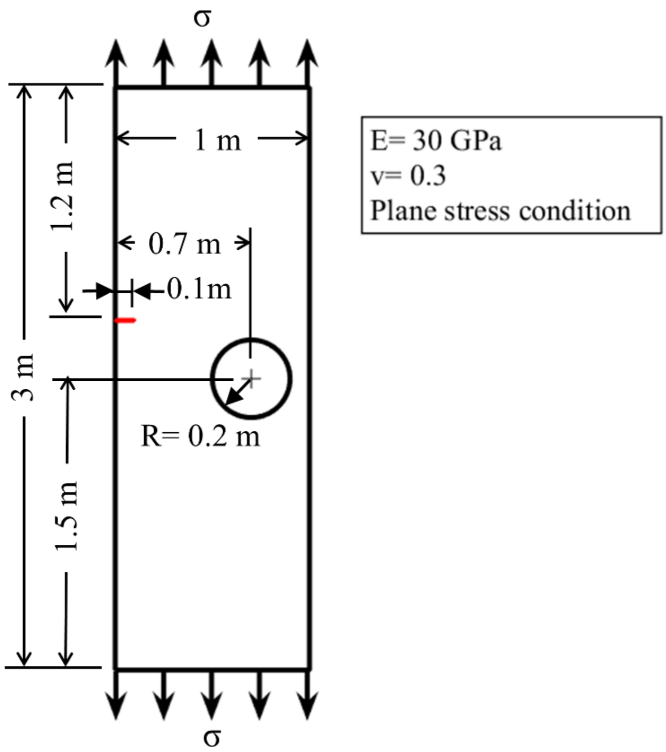

Figure 5.12 : An edge crack in a plate having a hole (1st Geometry).

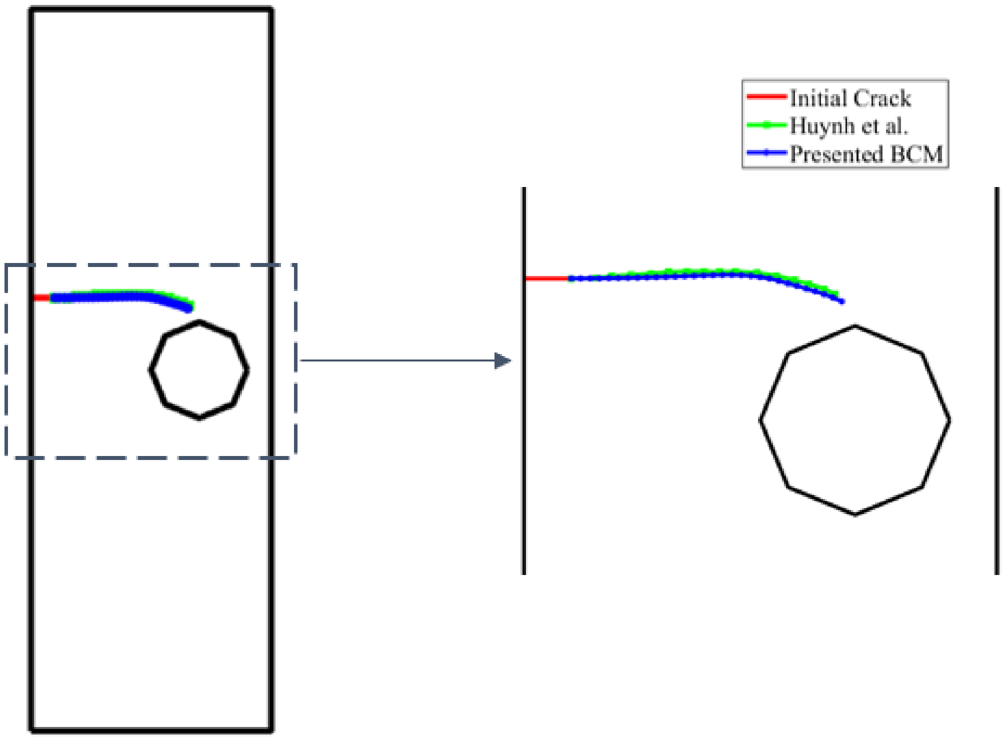

Figure 5.13 : Comparison between FCG paths predicted by BCM and that with polyXFEM [96] (green).

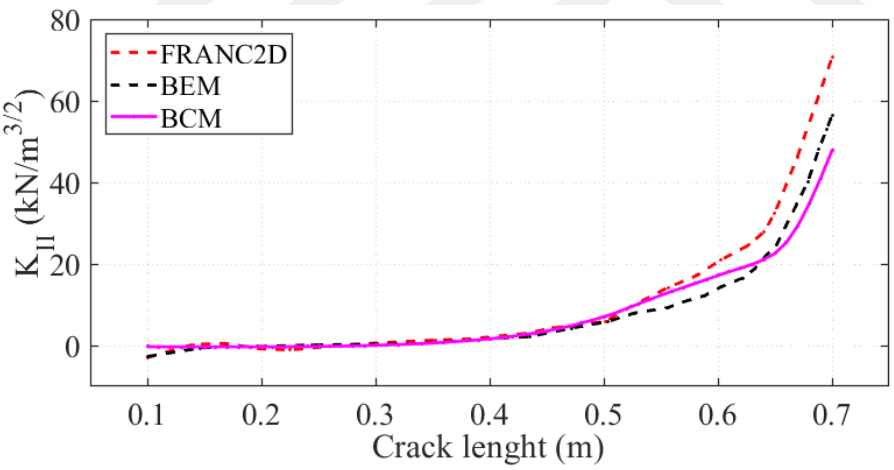

Figure 5.14 : Comparison of K_{II} using BCM, FRANC2D and BEM [97].

To study the effect of the number of sides (n) used to model the hole in the plate over the accuracy of the analysis, the same problem is repeated with different numbers of sides of the polygon (i.e. n = 4, 8, 12, 16) with fixed crack increment length of 0.02 m. Figure 5.15(A) shows a comparison of the crack propagation paths for different numbers of sides used to model the hole. The result shows that when a remarkable accuracy in predicting the FCG path is achieved, after that there is no significant effect of a further increase in the number of sides to model the hole. Table 5.6 shows the elapsed solution time for different n-values. Results mentioned in Figure 5.15(A) and Table 5.6 suggest that one can achieve reasonably good accuracy with n = 8 without compromising on solution time because the selection of n becomes critical for complex geometric problems where multiple holes are present in the model.

To investigate the effect of crack increment size (Δc) on crack propagation, the problem is also repeated with different values of Δc (i.e. 0.01 m, 0.02 m, 0.03 m, 0.04 m) using an 8-sided polygon to model the hole. Figure 5.15(B) shows crack propagation paths for different values of Δc. Results show a converged pattern of crack growth path which is also consistent with the reference path.

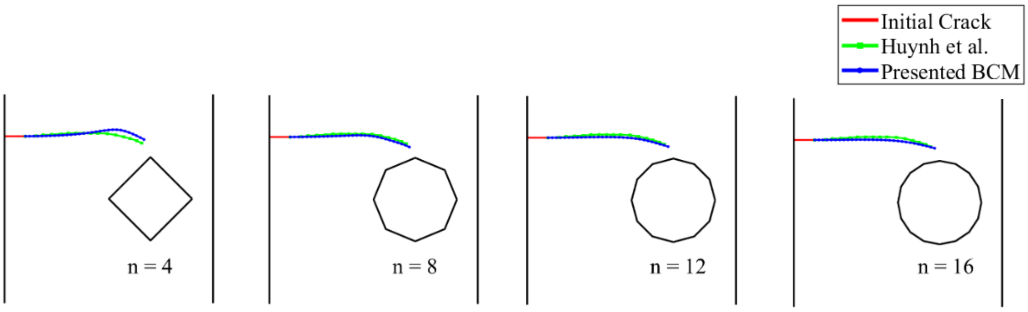

(A)

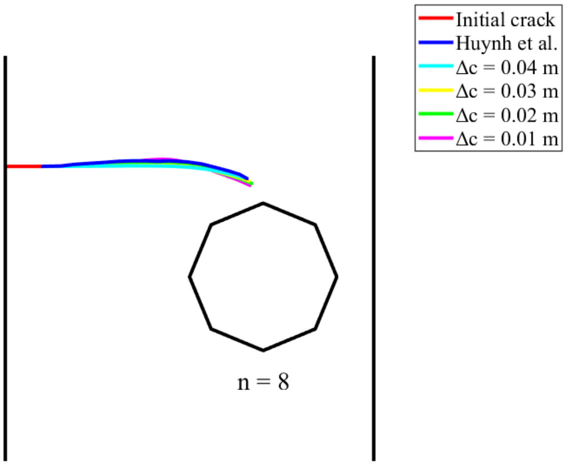

(B)

Figure 5.15 : Comparison of FCG paths predicated using BCM and polyXFEM [96]; (A) using different numbers of sides of polygon “n” used to model the hole in the plate, (B) for n = 8 with different crack increment sizes (Δc).

Table 5.6 : Solution time comparison for different numbers of sides of the polygon.

No. of sides of the polygon to model hole (n)	CPU* time (t) (sec)	CPU time comparison
4	343	t
8	464	1.35t
12	603	1.76t
16	773	2.25t

*Analyses are performed on PC of dual-core Intel Core i3-4010U with 4.00 GB RAM.

For the **2nd geometry**, a rectangular plate of 15 x 20 mm in size having an offset hole of a radius of 3.45 mm with a side edge having a pre-crack length of 2.75 mm (as shown in Figure 5.16(A)) is studied. The material is assumed to be purely elastic with Young's modulus, E = 98 GPa and ν = 0.3. Paris material constants are m = 2.39; C = 3.0e-7. The plate is subjected to uniaxial stress of 100 MPa with constant amplitude with stress ratio R = 0. Plane stress conditions are assumed. An eight-sided polygon is used to model the hole in the plate. Uniform normal stress is applied in the vertical direction at the top and bottom edge of the plate and a uniform crack incremental length of 0.55 mm (20% of a_0) is used. In past, many researchers solved the same problem, e.g. Bouchard et al. [99] used FEM with a local remeshing technique to solve it, and in 2015, Ooi et al.[100] adapted quadtree meshes in the scaled boundary finite element method to study this problem. Figure 5.16(B) shows the comparison of the predicted crack trajectory using BCM with different references. It can be observed that the crack path is deflected towards the hole initially and after it went straight towards the right edge of the plate. A close agreement is achieved in the predicted crack paths between BCM and references. The problem is solved in 23 steps and stress contours along Y-direction at different steps along with the number of loading cycles required are given in Figure 5.17.

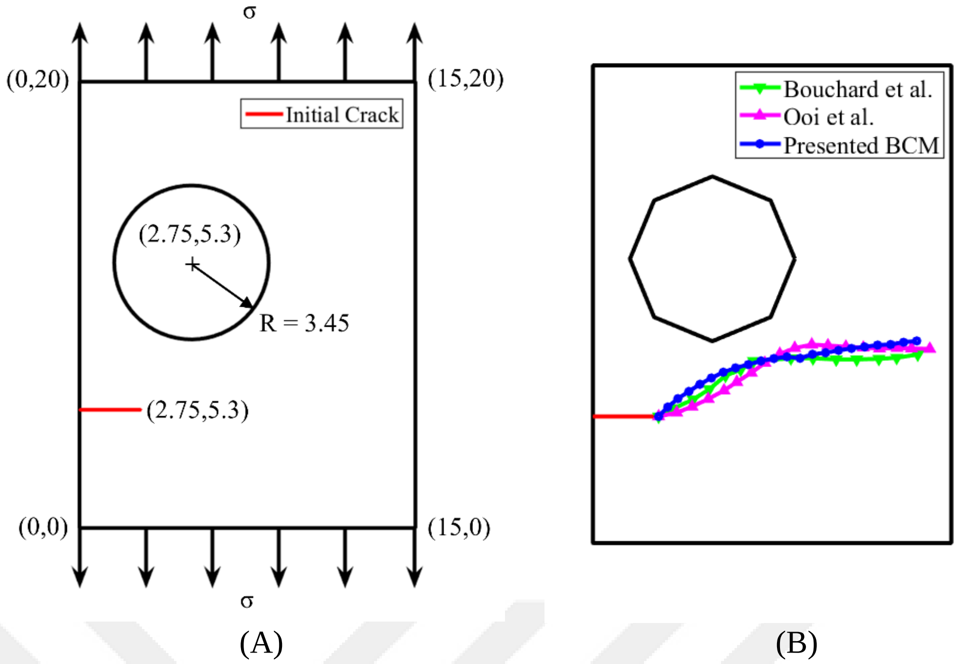

Figure 5.16 : An edge crack in a plate with a hole (2nd geometry); (A) Geometry of the problem (all dimensions are in mm), (B) Comparison of FCP paths predicted by BCM and reference studies (green [99], magenta [100]).

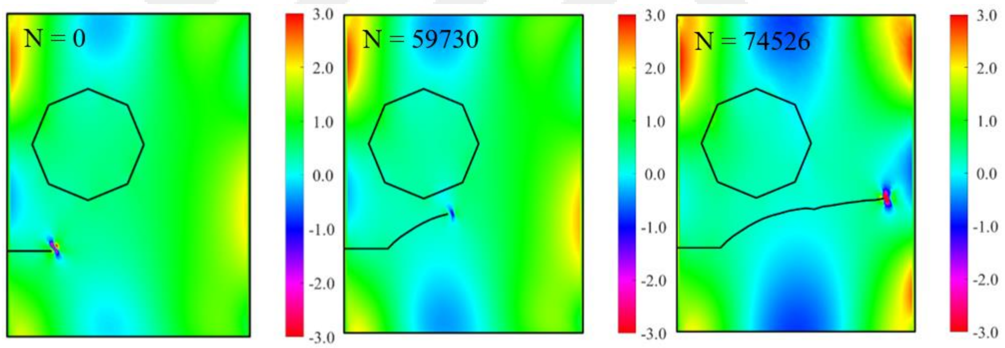

Figure 5.17 : Stress contours along Y-direction (MPa) for different loading cycles.

5.2.4 A cracked plate with four holes

In this example, the deviation of the crack propagation path due to multiple holes in a relatively complex plate geometry is discussed. For this purpose, a square plate having four holes of equal radii of 5 mm is considered. A pre-crack of a_0 = 6 mm is present at the middle of one edge of the plate as shown in Figure 5.18. Uniform stress of σ = 10 MPa is applied at the top and bottom edge of the plate. 8-sided polygons are used to model the holes in the plate. Plane stress conditions are assumed to be applied and a uniform crack increment of Δc = 1.2 mm (20% of a_0) is used to predict the crack growth path. The material properties are as follows: E = 72 GPa and ν = 0.33. The same problem is previously analyzed by Liu et al. [98] by using a fast multipole boundary element method (BEM). Figure 5.19 shows the comparison of crack propagation path using BCM and reference study [98]. A close agreement is observed between both paths. The crack path first goes towards the nearest hole then it becomes slightly horizontal and finally it goes towards the second hole.

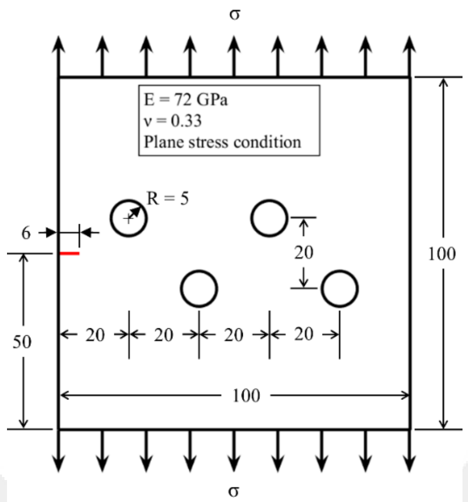

Figure 5.18 : Geometry of a cracked plate with four holes (dimensions are in mm).

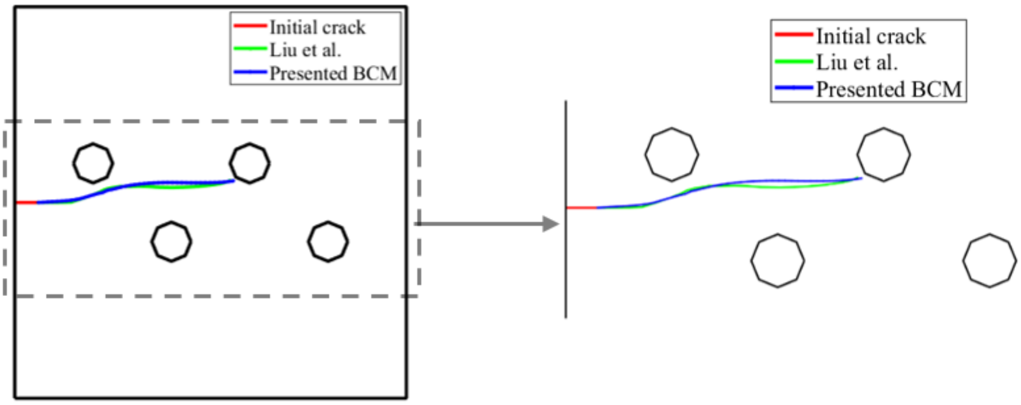

Figure 5.19 : Comparison of BCM FCG path with multipole BEM [98].

5.2.5 Double edge cracked plate with two holes

For the next problem, another classical multiple crack propagation problem is discussed which involves a plate with two holes and having two edge cracks. The geometry of the plate used for the analysis is shown in Figure 5.20. 8-sided polygons are used to model the holes. A constant crack increment of Δc = 0.5 mm is used for the crack propagation prediction. Normal traction in Y-direction is applied on the top and bottom edge of the plate. Plane stress condition is assumed to be applied in this example.

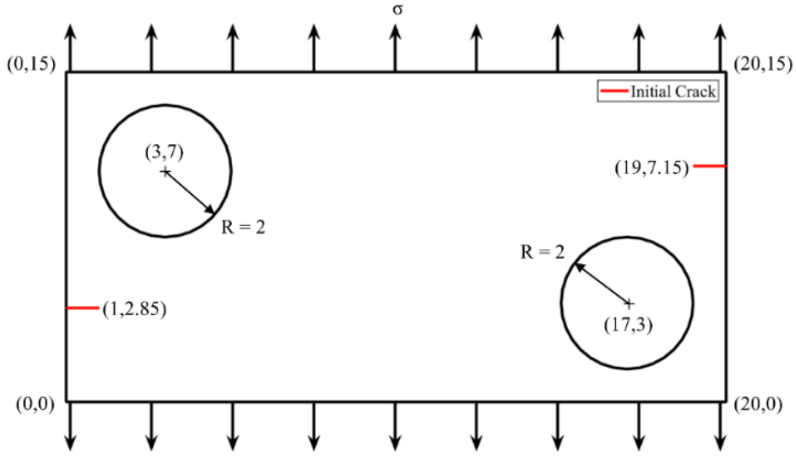

Figure 5.20 : Geometry of double edge cracked plate with two holes (all dimensions are in mm).

Previously many researchers solved the same problem using different numerical methods, e.g. Bouchard et al. [99] used a local remeshing technique with FEM and E.T. Ooi et al. [100] used a scaled boundary finite element method to solve it. Figure 5.21 shows the comparison of the predicted crack propagation path with the reference studies. Results show that a reasonably close agreement is achieved however there is slight variation even among both references but BCM shows closer interaction between crack paths which is very important to know.

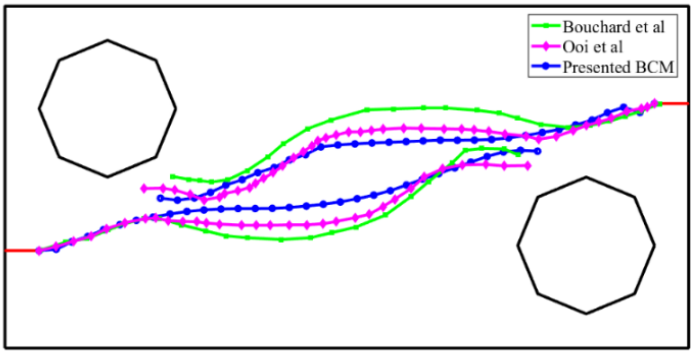

Figure 5.21 : Comparison of FCG path by BCM (blue) with reference studies; Bouchard et al. [99] (green) and Ooi et al. [100] (magenta).

5.3 Prediction of Loading Cycles

In this section, the estimation of loading cycles required for a given crack extension length is discussed. For this purpose, an example of multiple crack propagation process of two parallel cracks emanating from the outer periphery of two holes is considered from literature. Fatigue crack growth paths and the number of loading cycle required to produce the given crack length extension is compared with the reference study.

The geometry of the problem is shown in Figure 5.22. A plate having two holes, each having a radius of 2 mm separate at 25.4 mm from each other are studied using BCM under cyclic loading with two initial cracks of 5 mm emanating at $\pm 45^0$ from the outer edge of each hole. Constant amplitude force of 5 kN (stress ratio R = 0) is applied in the vertical direction as far-field loading. The elastic modulus and Poisson's ratio are 71.7 GPa and 0.3, respectively. The same problem is also studied by Zhang et al. [101] using numerical methods involving the finite element codes and results are compared with experimental ones. Plane stress conditions are assumed to be applied for the analysis. A constant crack increment $\Delta c = 1$ mm (20% of a_0) is used. Figure 5.23 shows the crack propagation path predicted using BCM in comparison with results calculated by Zhang et al. [101]. A good agreement is observed, particularly a better agreement is shown between the BCM and experimental results given in the reference study.

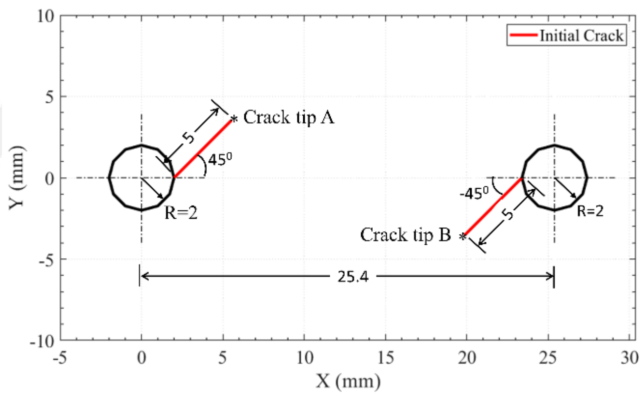

Figure 5.22 : Geometry of two parallel cracks emanating from two holes in a plate (all dimensions are in mm).

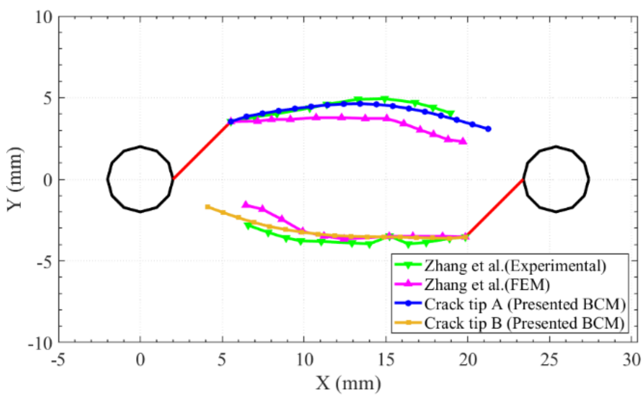

Figure 5.23 : Comparison of FCG paths by BCM with experiment and FEM[101].

For the estimation of the number of loading cycles, Paris's law is used as a crack growth model. The variation of the number of loading cycles N with the crack length computed is mentioned in Figure 5.24. Curves for both crack tips i.e. crack tip A and Crack tip B are mentioned for BCM in comparison with the average number of cycles required as computed by reference experimental and FE study [101] is also presented in Figure 5.24. Results show that implemented BCM is predicting the loading cycles very close to the reference results.

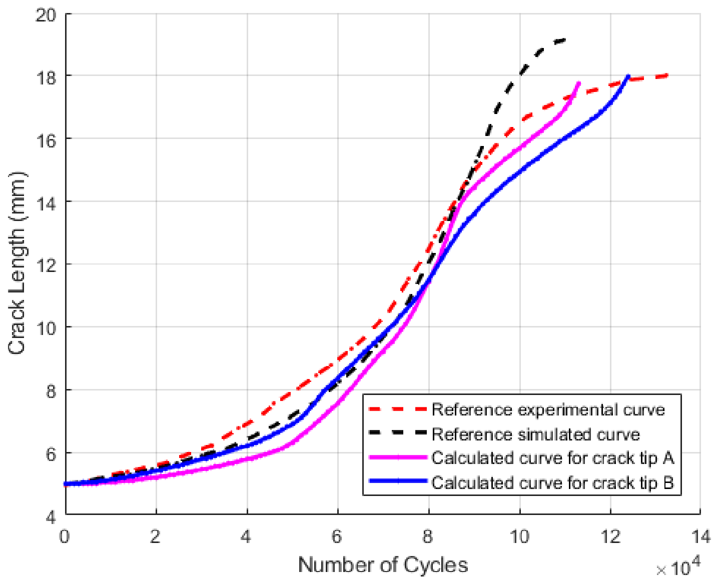

Figure 5.24 : Variation of the number of loading with crack length.

Table 5.7 shows the comparison of computed N by BCM with reference results for different crack length extensions. Percentage error for both crack tips is given in comparison of experimental as well as simulated FE results. Percentage error with experimental results is within 17 % for each crack tip, and for the simulated FE results the percentage error is within 15% for a crack length up to 15.4 mm for both crack tips, whereas for the crack length of 17.5 mm, the percentage error for crack tip B is 25.57%, which is relatively higher, this can be because at this point the crack extension is so much large and it enters in an unstable region and can give different results.

Table 5.7 : Comparison of computed N for given crack length by BCM with reference results [101].

Crack length (mm)	Reference loading cycles		Loading cycles using BCM		% Error with ref exp.[101]		% Error with ref FEM [101]	
	Exp.	FEM	Tip A	Tip B	Tip A	Tip B	Tip A	Tip B
8.8	57282	64562	67310	63130	17.51	10.21	4.26	-2.22
10.6	71152	73815	77660	75550	9.15	6.18	5.21	2.35
12.4	80696	81530	82600	83980	2.36	4.07	1.31	3.01
15.4	93583	90791	97280	104120	3.95	11.26	7.15	14.68
17.4	130372	96783	111970	121530	-14.1	-6.78	15.69	25.57

6. APPLICATIONS OF PROPOSED SCHEME TO FATIGUE CRACK GROWTH PROBLEMS

In this chapter, different applications of the proposed scheme to simulate the FCG behaviour in different plate geometries are investigated. For this purpose, three different studies are conducted to analyse and simulate the typical and complicated FCG problems of the aerospace industry which are difficult to solve by conventional methods of FCG analysis. These studies are named Study-A, Study-B and Study-C in this thesis. The findings of each study are published in different international prestigious journals.

6.1 Study-A: FCG in Plates having Rivet Holes Under Different Loading Conditions

In this problem, fatigue crack growth in a plate having two rivet holes separated at some distance and crack emanating from a certain location and orientation from one hole is analysed under three different far-field fatigue loadings i.e. loading in X-direction, loading in Y- direction and shear loading. The purpose of this study is to determine that what are the trajectories of crack propagation under different loading conditions, which kind of loading is worst for these common rivet aerospace structures and what are the effects of initial crack length on the FCG behaviour.

Figure 6.1 shows the geometry of an infinite plate having two rivet holes. The maximum tangential stress (MTS) criterion is used to predict the trajectories of crack growth. Paris's Law along with the approach of equivalent stress intensity factor is used to compute the number of loading cycles to produce a required crack length. 16-sided straight lines polygon are used to model the hole in the plate.

Following parameters are used for the analysis; E = 71200 MPa, $\upsilon = 0.3$, diameter of each hole = 4mm, spacing between holes = s = 6 mm, initial crack length = $a_0 = 0.5$ mm, angle of initial crack with central horizontal axis of hole = 33.6^o , Stress amplitude = 212 MPa and material constants are m = 3.545; C = 2.22×10^{-10} [93].

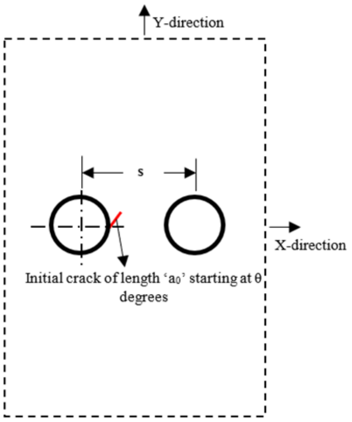

Figure 6.1 : Geometry of Infinite plate having two rivet holes.

6.1.1 Case-1: Infinite Plate under Stress in X-direction

As case-1 uniform stress is applied along X-direction. The estimated fatigue crack growth path by the proposed scheme is shown in Figure 6.2. It can be observed that the path of the crack propagation becomes perpendicular to the applied load direction after some loading cycles.

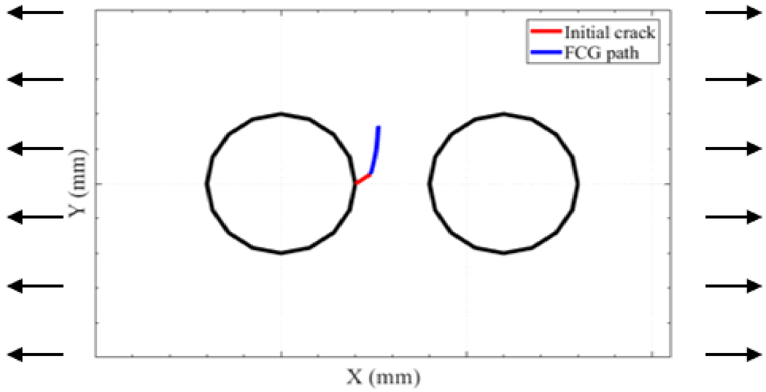

Figure 6.2 : FCG path for loading in X-direction (case-1).

6.1.2 Case-2: Infinite Plate under Shear Loading

In case-2 uniform shear load is applied as a far-field loading. The predicted fatigue crack growth path is shown in Figure 6.3.

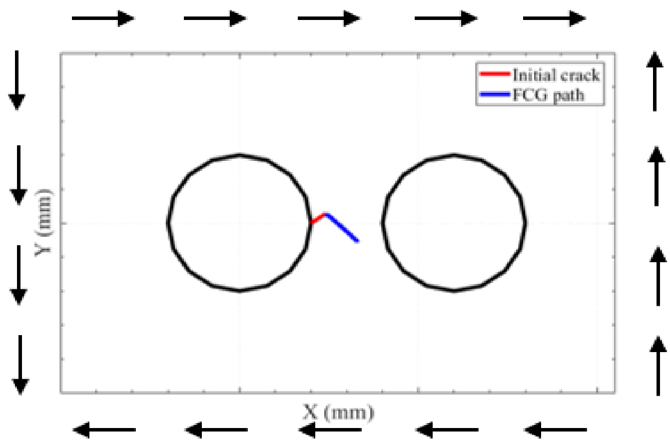

Figure 6.3 : FCG path for shear loading (case-2).

6.1.3 Case-3: Infinite Plate under uniform Stress in Y-Direction

In case-3, uniform stress is applied in Y-direction as a far-field loading. It can be observed from Figure 6.4 that similarly to the loading case-1 the crack propagation path becomes perpendicular to the far-field applied loading after some number of loading cycles.

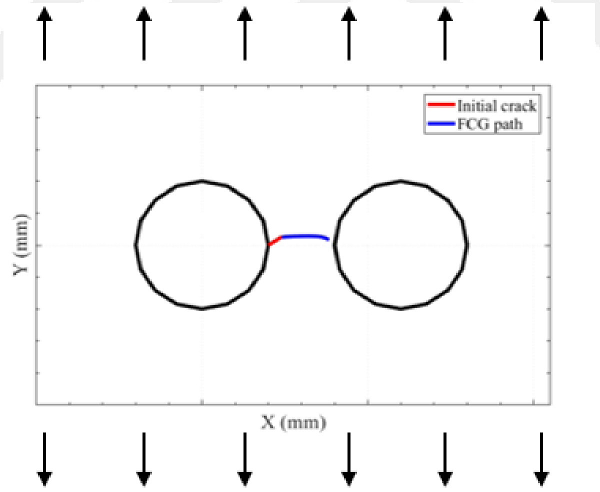

Figure 6.4 : FCG path for loading in Y-direction (case-3).

6.1.4 Discussion of results

Figure 6.5 and Figure 6.8 show the comparison of the path of fatigue crack growth under different types of loading for initial crack lengths of 0.5 mm and 1 mm, respectively. Results show that for both cases, the crack growth path becomes perpendicular to the applied loading for the tensile load whether it is in X or Y direction and similarly for the shear load it becomes perpendicular to the direction of maximum normal stress, so we can conclude that the crack growth path does not depend upon the initial length of the crack for the given loading cases at the macroscopic scale.

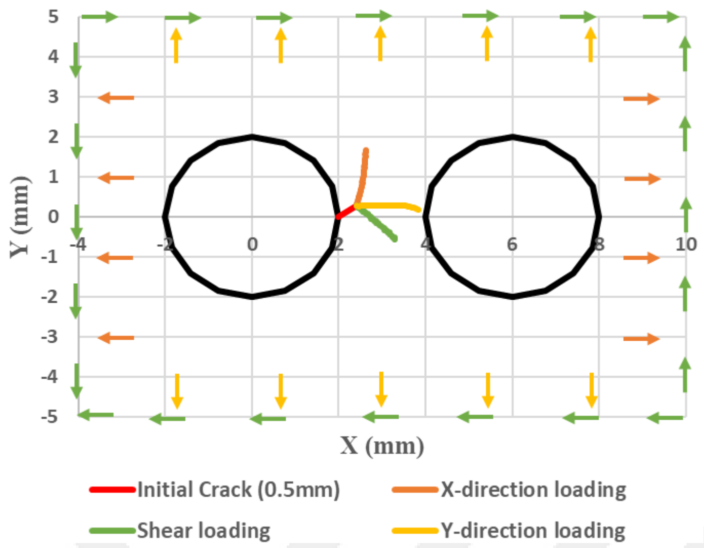

Figure 6.5 : Comparison of FCG paths under different loadings for a_0 = 0.5 mm.

In Figure 6.6, variation of ΔK_{eff} against crack length is given for each case of loading for an initial crack length of 0.5 mm. It can be observed that the highest value of ΔK_{eff} is obtained in the case of shear stress, whereas ΔK_{eff} for loading in X and Y direction are slightly different from each other.

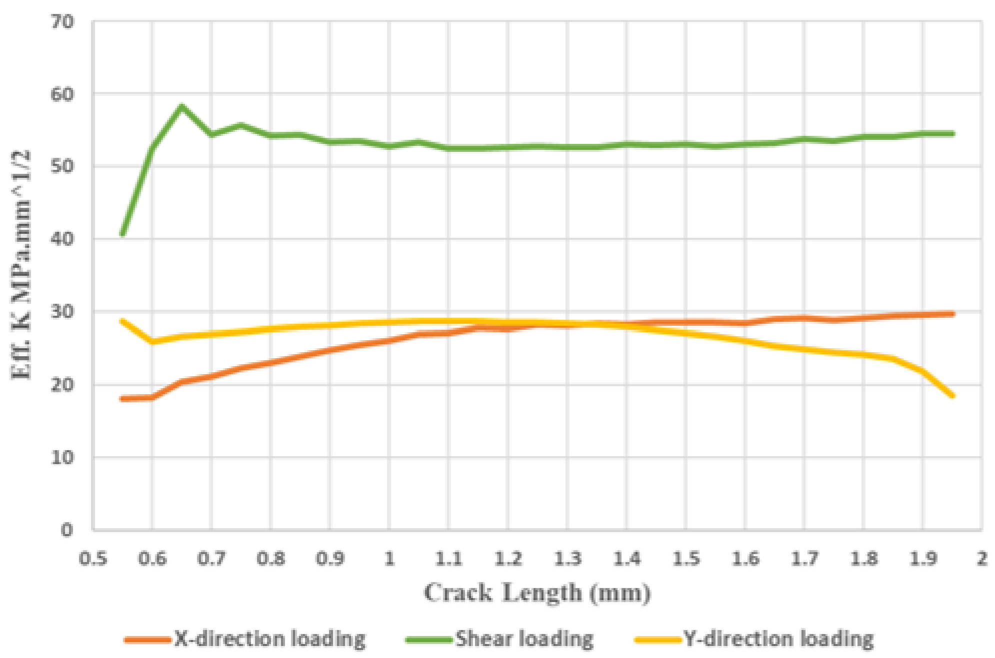

Figure 6.6 : ΔK_{eff} vs crack length plot for each loading case with a_0 = 0.5 mm.

In Figure 6.7, the variation of the number of loading cycles with the crack length for each loading case for an initial crack length of 0.5 mm is presented. It can be observed that a small number of loading cycles are required to achieve a given crack length in case of shear loading as compared to the loading either in X-direction or in the Y-direction and the rate of propagation under shear stress is almost ten times higher than that of normal stress cases.

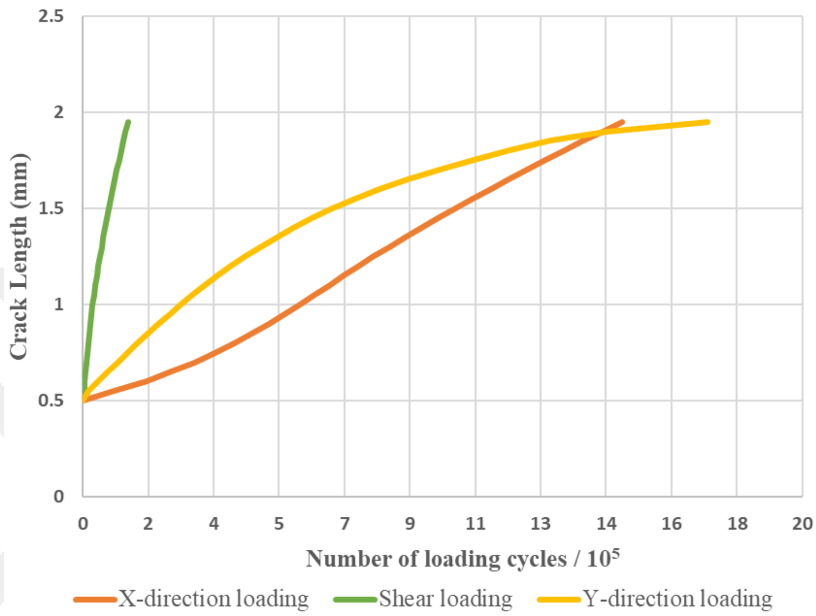

Figure 6.7 : Number of loading cycles vs crack length plot for different loading conditions for $a_0 = 0.5$ mm.

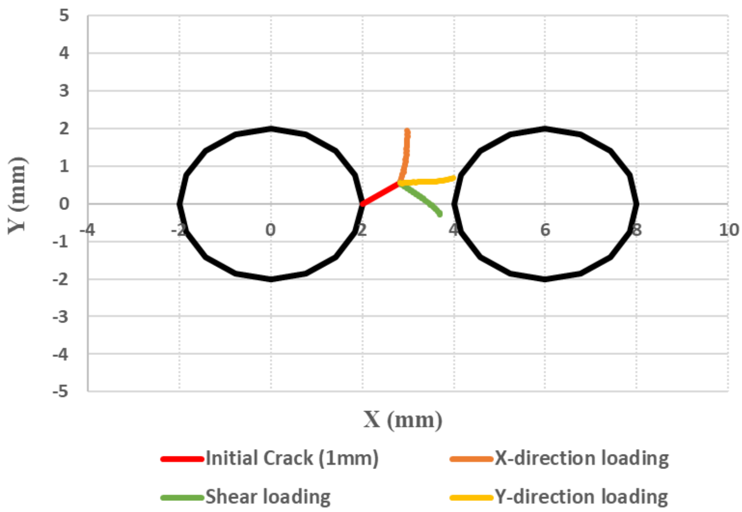

Figure 6.8 : Comparison of FCG paths under different loadings for $a_0 = 1$ mm.

Figure 6.9 shows the values of Δk_{eff} as a function of distance from the initial crack tip and Figure 6.10 shows the number of loading cycles for a given crack length, for two different initial crack sizes of 0.5 mm and 1 mm for loading along X-direction. The result shows that values of Δk_{eff} do not depend upon the initial crack size, whereas the rate of crack propagation is slightly higher in the case of small initial crack length, but this effect is not seen after a certain number of loading cycles.

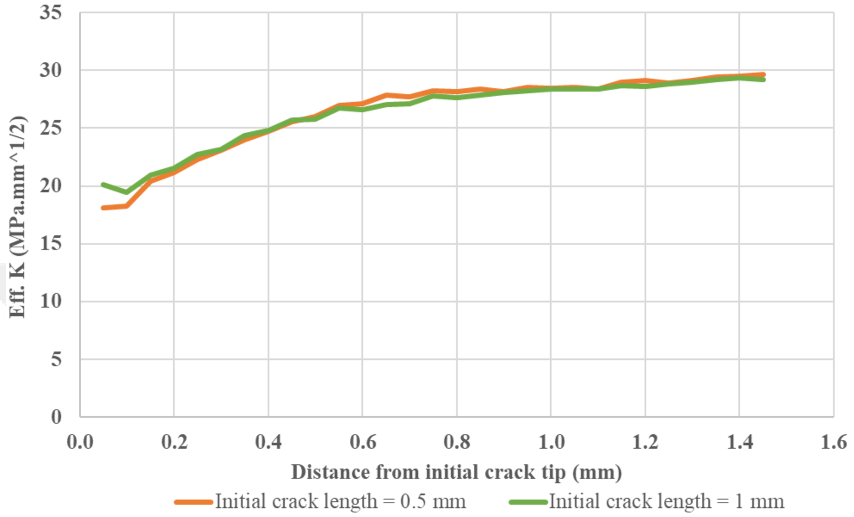

Figure 6.9 : Variation of ΔKeff with the location of crack tip for loading in X-direction for different lengths of initial crack.

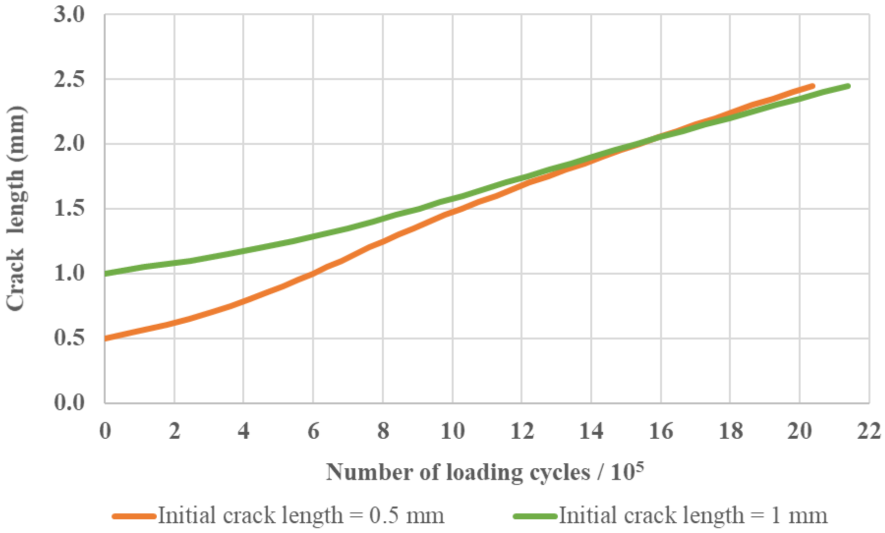

Figure 6.10 : Number of loading cycles for loading in X-direction for different initial crack lengths.

6.1.5 Conclusion of Study-A

In this study, fatigue crack growth analysis under three different far-field loading conditions with the two-dimensional Boundary Cracklet Method (BCM) is presented.

Prediction of crack growth paths and the required number of loading cycles under each loading case is done using the maximum tangential stress (MTS) criterion and the approach of equivalent stress intensity factor following Paris-Erdogan Law.

After some initial number of loading cycles, the fatigue crack growth path becomes perpendicular to the direction of applied loading in case of far-field applied tensile stress (whether in X or Y direction), and similarly, in case of shear loading, crack propagate perpendicular to the direction of maximum principal stress.

For a given geometry, the fatigue crack growth path, stress intensity factors and the number of loading cycles required for a given crack length depend only on the type of loading and do not depend upon the initial size of the crack at the global level. Effective ΔK has a higher value when uniform shear stress is applied to the plate and it has relatively less value for the loading along X or Y direction.

Almost ten times fewer loading cycles are required to reach at a certain crack size under shear loading as compared to the normal applied stress, which shows that the rate of crack propagation is ten times higher under shear stress. Therefore, it can be concluded that among the given three loading conditions shear stress is the worst case of loading for the given configuration, whereas the number of cycles for loading along X or Y direction required to reach a certain crack size is almost the same.

6.2 Study-B: Simulations of Interaction of Multiple Fatigue Cracks Growth

In this section, simulation of FCP for different cases of multiple initial cracks in a plate geometry (as shown in Figure 6.11) is discussed by using the proposed scheme. The main purpose of this study is to investigate the effects of a newly added crack in the vicinity of already present cracks on the rate of crack propagation in complex plate geometries, which are difficult to solve by conventional methods. Three different studies are conducted for this purpose and named study 1, study 2 and study 3. In study 1, cracks emanating at the different locations from the edges and middle of the given plate geometry are discussed. In study 2, two different cases of initial cracks emanating from different locations and orientations from the holes of the given geometry are presented. Finally, a combination of study 1 and study 2 is discussed as study 3, in which initial cracks are emanating from sides, middle and the outer periphery of the holes with different orientations are studied.

The used parameters for the analysis are as follows: Length and width of the plate are 100 mm and 140 mm respectively and the diameter of each hole is 10 mm. 8-sided polygon is used to model the holes. The initial length of each crack is a_0 = 6 mm. Constant amplitude cyclic loading in Y-direction with σ_{max} = 50 MPa, σ_{min} = 0 MPa and R = 0 is applied. The material properties are as follows: E = 200 GPa, ν = 0.3. Paris material constants are m = 3.73; C = 4.47e-10. Plane stress conditions are assumed to be applied in each case.

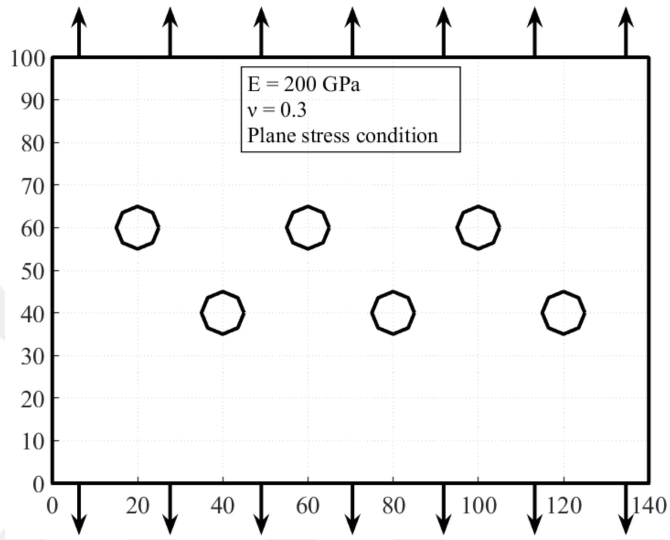

Figure 6.11 : Geometry of the problem (all dimensions are in mm).

6.2.1 Study 1: Side edge cracks at different locations and inclined cracks at the middle of the plate

In this study, three different cases of initial pre-cracks are discussed. In the first case, a two symmetric cracks system is considered, and pre-cracks are emanating from the middle of the side edge of the plate. The geometry and loading conditions are shown in Figure 6.12(A), whereas the predicted crack propagation path using BCM is shown in Figure 6.12(B). It can be observed that both crack propagation paths are symmetric and initially they propagate horizontally, then they interact with the nearest hole and tend to bend towards it, then they tend to go towards the hole of the other row in their path and finally interact with the middle hole of each row and reach up to it.

To validate the results, the same problem is also solved using the SMART crack growth module of commercial FE code ANSYS Workbench V19.2. As multiple crack interaction is not possible using ANSYS Workbench and since these two cracks are symmetric and far apart from each other and there is no interaction among them, so a single crack is modelled in ANSYS Workbench, and the trajectory of fatigue crack propagation is simulated using the adaptive re-meshing procedure. Crack growth is obtained using program-controlled incremental extensions of the crack. As the result of the crack propagation path also depends upon the mesh size used at the crack tip and different crack paths are obtained for differently used mesh size, however, strongly converging characteristics are obtained with the refinement of mesh at the crack tip. A meshed model of given geometry is shown in Figure 6.13(A) and the predicted crack propagation path is shown in Figure 6.13(B). A similar analysis is also performed for the crack on the right side edge. A comparison between the predicted crack propagation paths by BCM and ANSYS Workbench is shown in Figure 6.14.

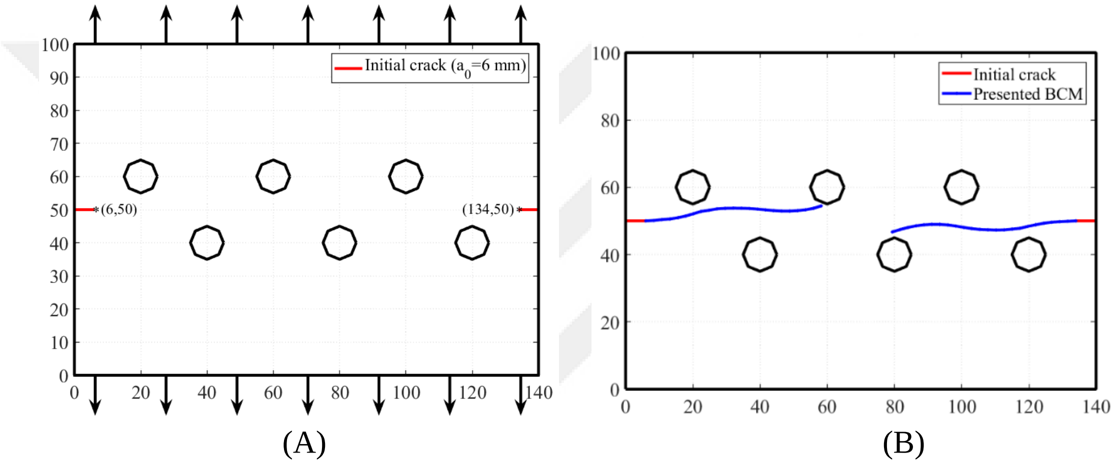

Figure 6.12 : Study 1, case-1 (BCM); (A) Geometry of problem, (B) Predicted FCG path using BCM.

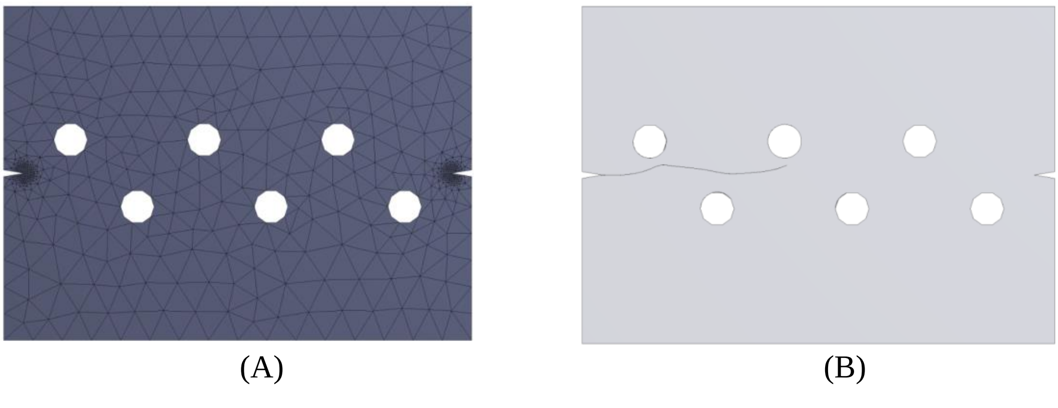

Figure 6.13 : Study 1, case-1 (ANSYS Workbench); (A) Meshed model, (B) FCG path using ANSYS Workbench.

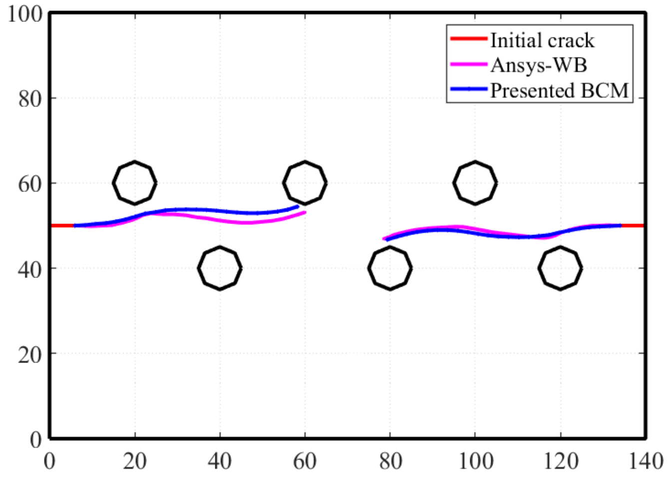

Figure 6.14 : Comparison between FCG paths using BCM and ANSYS Workbench (Study 1, case-1).

In the second case, a similar two cracks system as mentioned in the previous example is analyzed but using the initial cracks at a different location on the edges of the plate as shown in Figure 6.15(A), crack propagation path using BCM can be seen from Figure 6.15(B), whereas a comparison of crack propagation paths using BCM and ANSYS workbench is shown in Figure 6.16. It can be observed that for both these cases, the predicted crack propagation paths agree well with the FEM simulations.

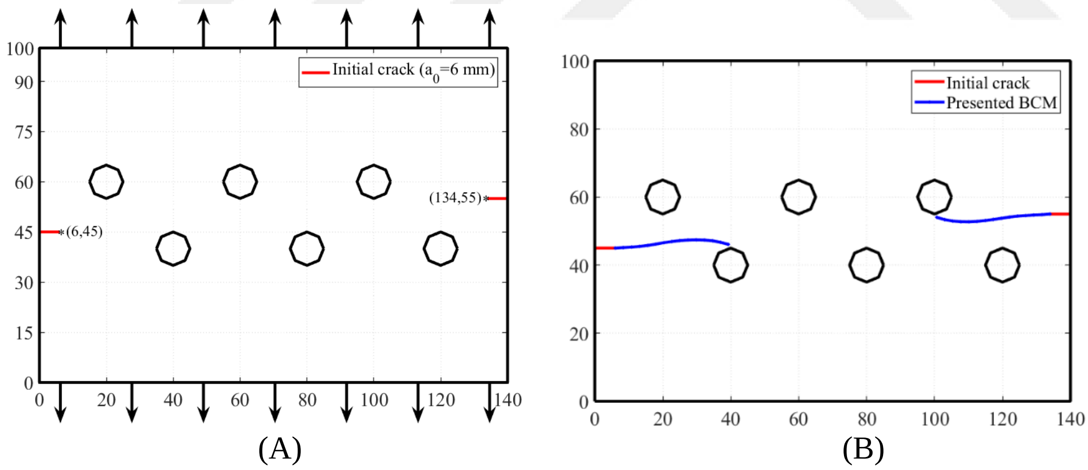

Figure 6.15 : Study 1, case-2 (BCM); (A) Geometry of the problem, (B) Predicted FCG path using BCM.

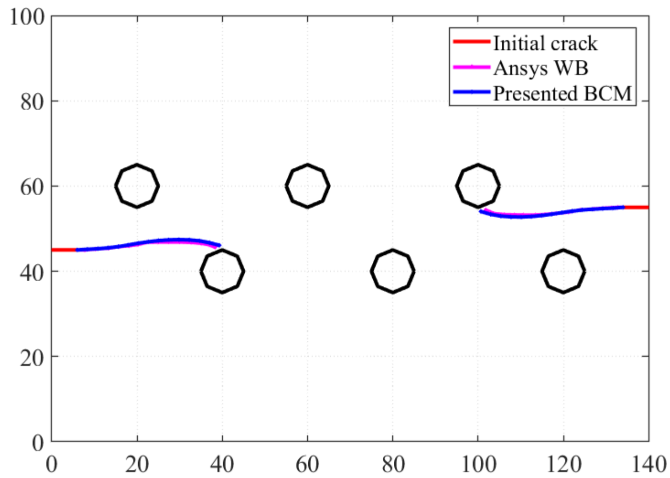

Figure 6.16 : Comparison between FCG paths using BCM and ANSYS Workbench (Study 1, case-2).

In case 3, a single crack at the middle of the plate for three different orientations i.e. 0^0, 15^0 and 45^0 is discussed. The geometry of the crack at the middle of the plate at 0^0 is shown in Figure 6.17(A), whereas Figure 6.17(B) shows the predicted crack propagation path using BCM.

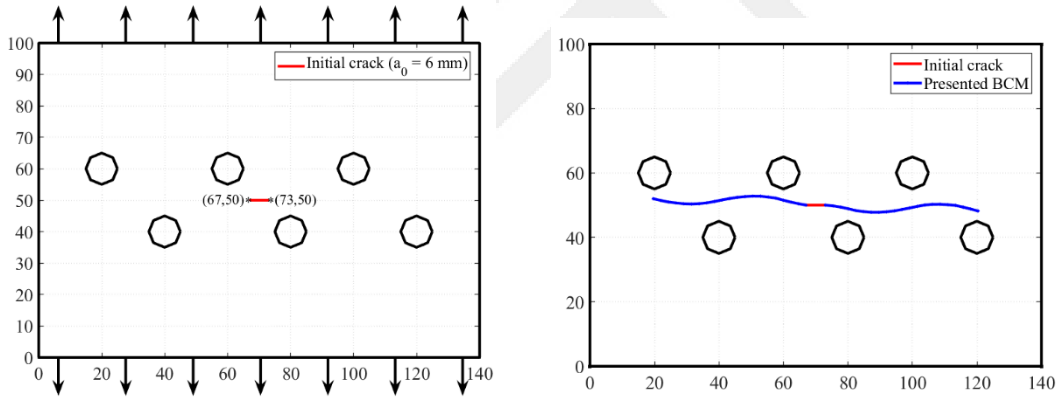

(A) (B)

Figure 6.17 : Study 1, case-3a (BCM); (A) Geometry of the problem, (B) Predicted FCG path using BCM.

The result of this study is also verified using ANSYS Workbench. The meshed model of the corresponding geometry of the problem is shown in Figure 6.18(A). As there is a limitation in ANSYS Workbench that only crack propagation can be simulated on one tip of the cracks, so two separate analyses are conducted to verify the crack propagation in either side of the crack. Figure 6.18(B) shows a close agreement between the crack propagation paths predicted by both methods. The geometry of the crack at the middle of the plate at θ^0 is shown in Figure 6.19, whereas Figure 6.20(A) and Figure 6.20(B) show the comparison of predicted crack propagation path using

BCM with that of ANSYS Workbench for crack inclination angle of 15^0 and 45^0 respectively.

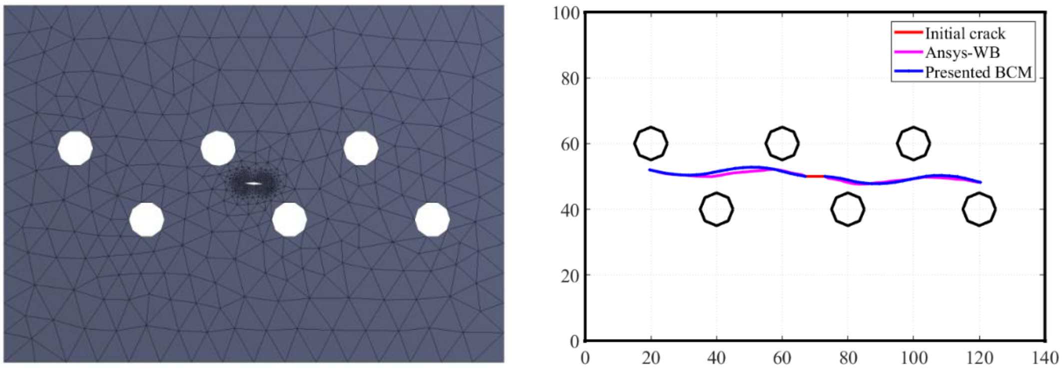

(A) (B)

Figure 6.18 : Study 1, case-3a; (A) Meshed model, (B) FCG paths comparison using BCM and ANSYS Workbench.

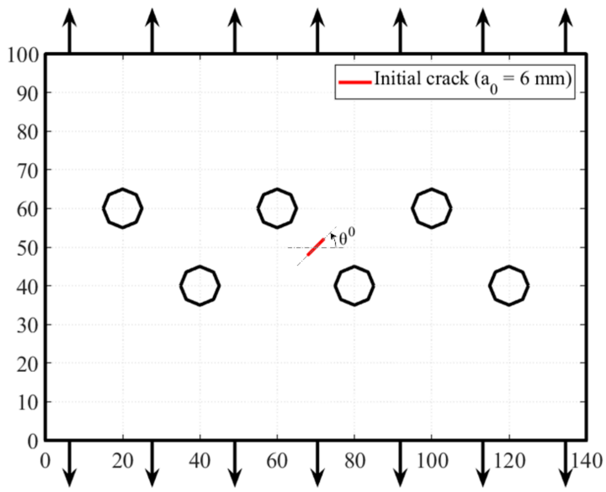

Figure 6.19 : Geometry of the problem at an angle θ^0 (study 1, case-3b).

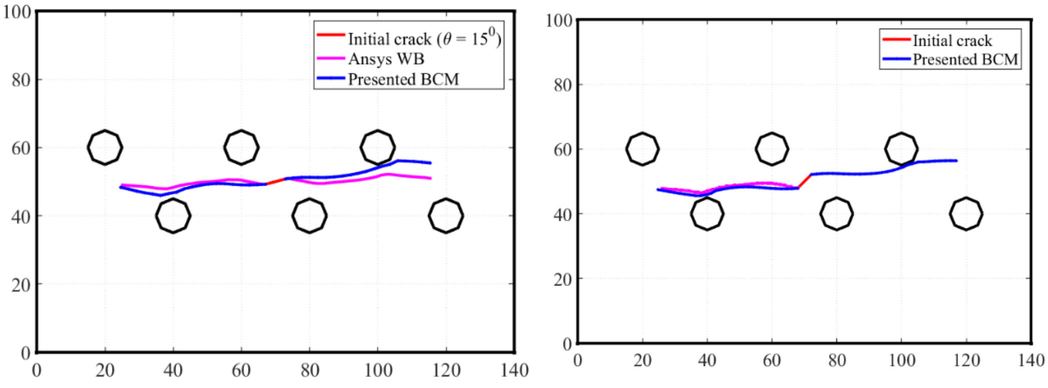

(A) (B)

Figure 6.20 : FCG paths comparison by BCM and ANSYS Workbench; (A) $\theta = 15^0$, (B) $\theta = 45^0$.

6.2.2 Study 2: Cracks emanating from holes

In this study, two different cases of initial cracks emanating from outer peripheries of holes of the given geometry are discussed under loading in the Y- direction. In case 1, cracks from 1st two holes of row 1 of the holes are emanating at -45^0, whereas the cracks from the 2nd and 3rd holes of row 2 are emanating at 45^0 (as shown in Figure 6.21(A)). The predicted crack propagation path using BCM is shown in Figure 6.21(B) for case -1. In case -2, initial cracks from 1st and 3rd holes of row 1 of the holes are emanating at -45^0, whereas the cracks from 1st and 3rd holes of row 2 are emanating at 45^0 (as shown in Figure 6.22(A)). The predicted crack propagation path using BCM for case 2 is shown in Figure 6.22(B).

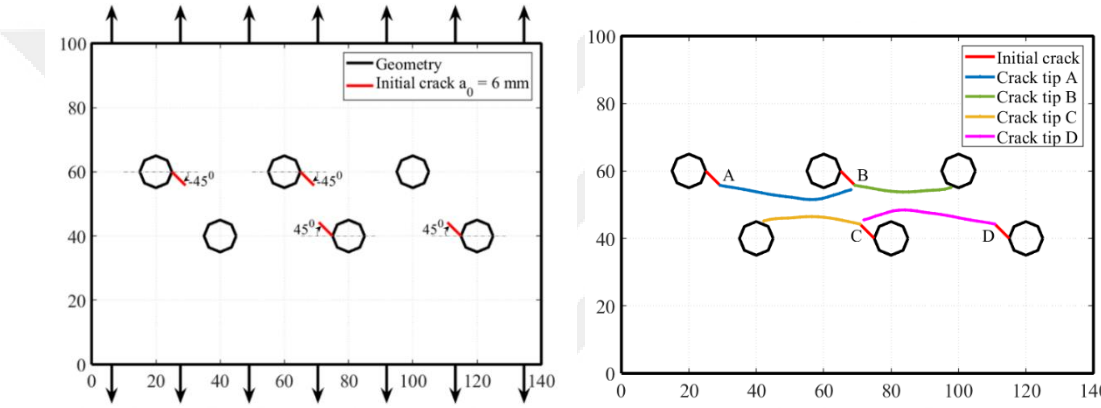

(A) (B)

Figure 6.21 : Study 2 case -1; (A) Geometry of the problem, (B) Predicted FCG path using BCM.

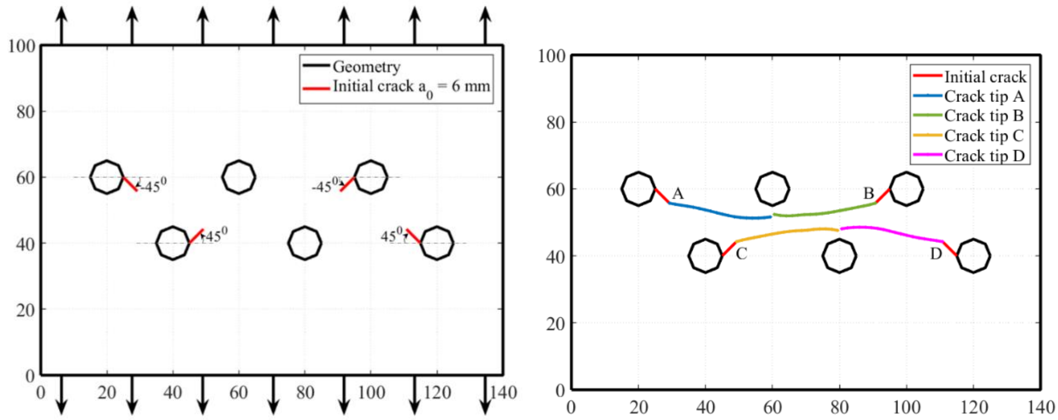

(A) (B)

Figure 6.22 : Study 2 case -2; (A) Geometry of the problem, (B) Predicted FCG path using BCM.

6.2.3 Study 3: (Crack emanating from edges and holes)

In the first three cases of this study, initial cracks emanating at different orientations from edges and holes of the plate of given geometry are discussed under loading in Y-direction. In case-1, there are four initial cracks in which two cracks are emanating from a given location on the edge of the plate and two cracks are originating from the two holes of the given geometry as shown in Figure 6.23(A). The crack propagation trajectory for this case is given in Figure 6.23(B). As the two cracks merge, it is assumed that failure has occurred, and simulation is set to stop.

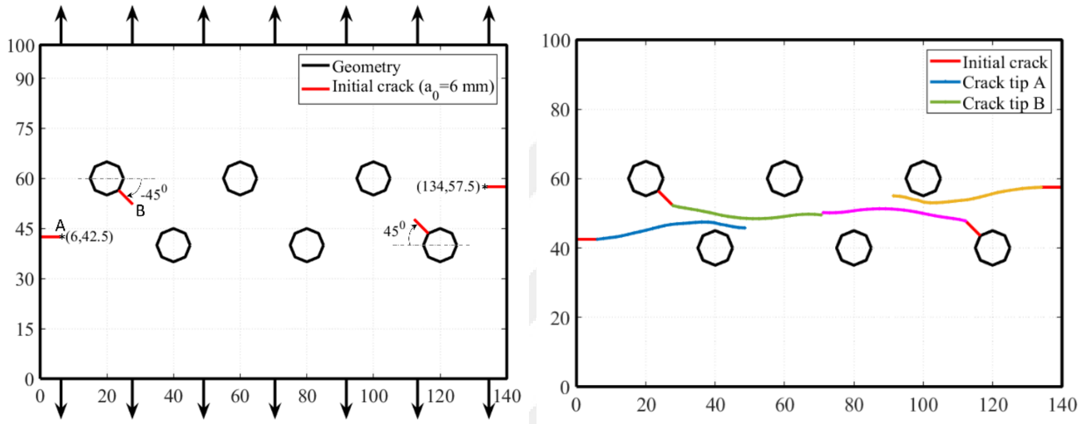

(A) (B)

Figure 6.23 : Study 3, case-1; (A) Geometry of the problem, (B) Predicted FCG path using BCM.

In case-2, there are six initial cracks in which two cracks are emanating from two opposite edges of the plate and the remaining four cracks are originating from certain origination from four different holes of given geometry (as shown in Figure 6.24(A)). Figure 6.24(B) shows the crack growth path for case 2 of study 2. In case 3, one more crack is added to the 2^{nd} case of this study at the centre of the plate at 0^0 as shown in Figure 6.25(A). The crack propagation path of case-3 is shown in Figure 6.25(B).

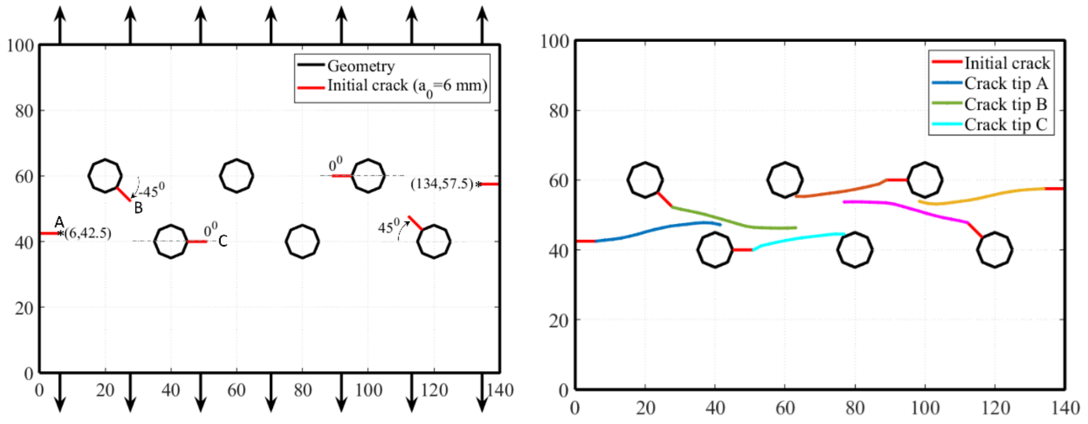

(A) (B)

Figure 6.24 : Study 3 case -2; (A) Geometry of the problem, (B) Predicted FCG path using BCM.

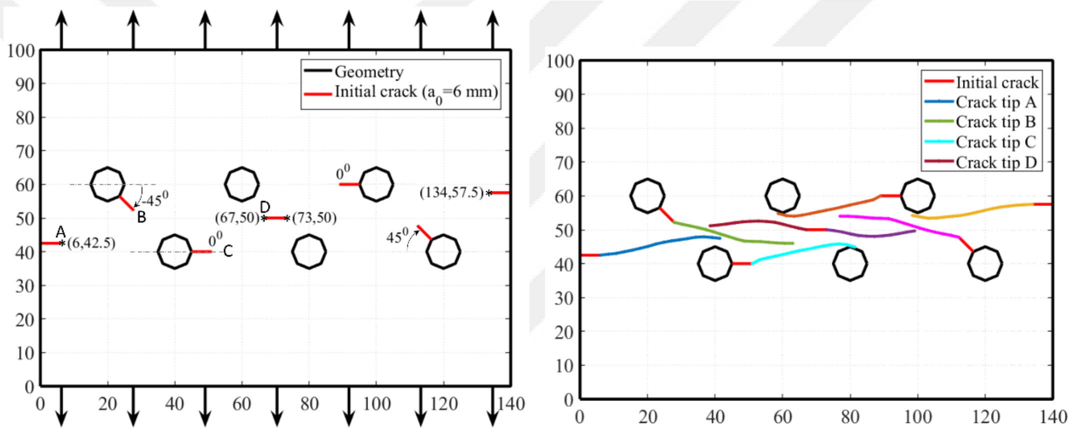

(A) (B)

Figure 6.25 : Study 3, case -3; (A) Geometry of the problem, (B) Predicted FCG path using BCM.

Figure 6.26 (A) to (C) represents the crack growth rate of different crack tips for cases 1 to 3 of study3. Although a constant crack increment is used for each crack tip in each case, the rate of crack growth for each crack is different, therefore different loading cycles are required for each crack tip to grow for the same crack length. In each case, there are symmetric cracks in the model and therefore only one set of cracks is shown in the plots. Figure 6.27(A) to (C) shows the comparison of the crack growth rate of crack tip A, B for case-1 and crack tip A, B and C for the case-2 and case-3 of study 3 respectively. These plots show that how the crack growth rate of a certain crack tip is affected by the addition of other nearby cracks to the system. In case-1 there is only one crack near the crack tip A, but in case 2 and 3 there are more cracks to interact with crack tip A, therefore the growth rate of crack tip A is relatively higher in those cases (Figure 6.27(A)). A similar effect is also observed for crack tip B and C in Figure

6.27(B) and Figure 6.27(C) respectively. It shows that when two coplanar cracks approach each other, they exhibit an over-constraining phenomenon [94], which causes the near-tip stress field to be significantly higher than that near a single crack and hence ultimately increases the rate of crack growth.

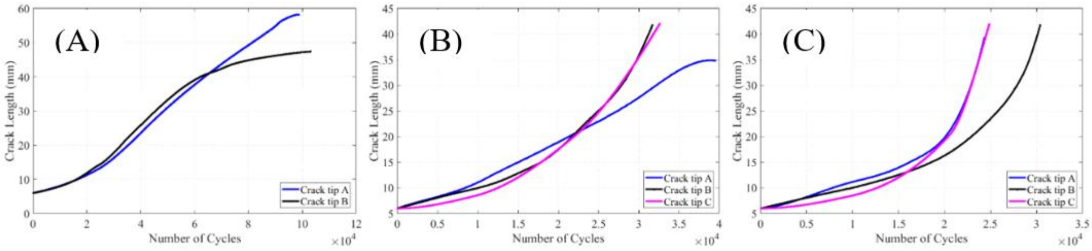

Figure 6.26 : Fatigue life curves for cracks tip A, B and C for different cases of study 2, (A) Case 1, (B) Case 2, (C) Case 3.

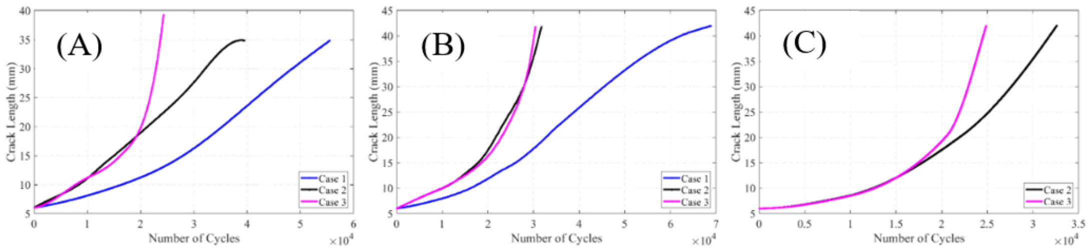

Figure 6.27 : Fatigue life curves for different cases of study 2 for different crack tips; (A) Crack tip A, (B) Crack tip B, (C) Crack tip C.

To show the versatility of the proposed method, the geometry of case-3 of study 3 is also solved for loading in X-direction and the shear and discussed as case-4 and case -5 respectively. Figure 6.28(A) shows the geometry of and the crack propagation path for loading applied in X-direction, whereas Figure 6.28(B) shows the crack propagation path of the same geometry as mentioned in case 3 under the shear loading.

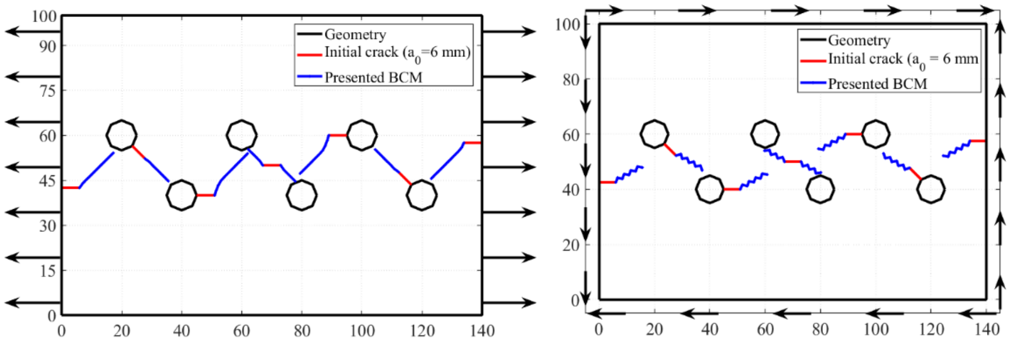

(A) (B)

Figure 6.28 : BCM Simulation of FCP (study 3, case 4 and 5); (A) under loading in X-direction (study 3, case-4), (B) under shear loading (study 3, case-5).

To show the computational efficiency of a numerical method in fatigue problems a new and very useful parameter is introduced: Yavuz's fatigue computational efficiency factor, $Y_{CF} = \mu N/t$, which is the number of computed million cycles per hour (CPU time). Table 6.1 shows the CPU time and fatigue life of each case of study 2 and study 3. Simulations are conducted on PC of dual-core Intel Core i3-4010U with 4.00 GB RAM using MATLAB R2017b. As expected, more complexity in the problem results in lower Y_{CF} because it will take more time to solve, and the number of computed life cycles will be much less per unit CPU time. BCM takes almost 15 hours to solve Study 3-case 3 with Y_{CF} = 1.66e-3 which is a very complicated problem (plate with 6 holes having 7 pre-cracks).

Table 6.1 : CPU time and fatigue life for each case.

Study	Case No.	Δc (% of a_0)	Solution time* (hours)	μN (No. of loading cycles/10^6)	$Y_{FC} = \mu N/t$ x 10^3
2	1	30	3.88	0.062	16.0
	2	30	3.95	0.057	14.6
3	1	30	8.13	0.103	12.6
	2	40	8.58	0.032	3.79
	3	40	14.9	0.025	1.66
	4	40	1.46	0.019	13.3
	5	40	2.39	0.0018	0.78

*Analyses are conducted on PC of dual-core Intel Core i3-4010U with 4.00 GB RAM using MATLAB R2017b.

6.2.4 Conclusion of the Study-B

In this study, fatigue crack growth simulation of interacting multiple cracks in perforated plates with multiple holes is discussed. To show the versatility of the proposed method, emphasis is given to study such complicated problems which cannot be solved by conventional methods. Three different studies with multiple cases of initial cracks emanating from side edges, the centre of the plate and the outer periphery of holes in the plate at different orientation are simulated and crack growth path and fatigue lives are estimated for each case. Paris's law is used as a fatigue crack growth model and the MTS criterion along with the approach of equivalent stress intensity factor is used to predict the crack tip location during crack propagation in each step under fatigue loading. The effect of a newly added crack in the vicinity of already present crack is also analyzed and concluded that when two coplanar cracks approach each other, they exhibit an over-constraining phenomenon [94], which causes the near-tip stress field to be significantly higher than that near a single crack and hence ultimately increases the rate of crack growth. To show the computational efficiency of a method in fatigue problems a new and very useful parameter is suggested: Yavuz's fatigue computational efficiency factor, $Y_{CF} = \mu N/t$, which is the number of computed million cycles per hour (CPU time). For two computational methods, the one with higher Y_{CF} is computationally more powerful.

It is also concluded through this study that the proposed scheme is an accurate tool to simulate the real cases of multiple fatigue cracks interaction in two dimensions which are the typical aerospace structures experiencing fatigue crack growth and the conventional methods of analysing FCG have limitations in solving such complex problems.

6.3 Study-C: FCG Analysis of Biaxially Loaded Hole-Edge Cracks

Aerospace structures experience different types of loading during their service life; biaxial loading is also one of them and needs significant attention for the designing of these structures. Repetitive pressurizing and depressurizing the cabin of the aircraft is one of the examples of a biaxial state of fatigue loading.

The failures due to fatigue loading usually start at small surface cracks which act as local stress raisers and propagate and interact with each other and turn into large damage-producing cracks [1]. In practice, these micro surface cracks are always likely to be present in many aircraft structural components, which are produced due to certain imperfections due to the machining processes during the manufacturing of aircraft. To produce a damage tolerance design, the most important thing is to make sure that these micro-surface cracks will not propagate and not turn into large damage-producing cracks under different loading and environmental conditions suffered by the aircraft [102]. The orientation of the micro-surface cracks specially around holes in machined structures and the nature of loading conditions can affect or even increase the rate of propagation of cracks. In such cases, the orientation of the cracks describes that whether the crack will grow in mode I, mode II or fatigue crack will grow in a mixed-mode manner. The effects of initial crack orientation under uniaxial fatigue loading are well reported in the literature but the same under the effect of different conditions of biaxial loading needs more discussion.

In the early findings of fatigue crack growth under biaxial loading, different inconsistent observations were reported. According to some researchers, in linear elastic fracture mechanics, the component of stress parallel to the crack does not affect the fatigue crack growth, whereas some others reported that the propagation rate of a fatigue crack under biaxial load is affected by stress biaxiality [103-107]. Hopper and Miller reported that compressive stress on a plane parallel to the direction of crack propagation can increase and tensile stress on the same plane can decrease the crack propagation rate [103]. In 1978, Liu and Dittmer [104] while performing different experimental tests on Al- alloys i.e. 7075-T7351 and 2024-T351 reported that crack will grow straight in a biaxial stress field when the stress component parallel to the crack is equal to or smaller than the stress component normal to the crack and biaxiality has no effect on the crack growth rates under constant amplitude loading. Anderson and Garrett [105] reported that equibiaxial tension reduces the rate of fatigue crack growth, while compressive stresses parallel to the direction of crack propagation cause a considerable increase in fatigue crack propagation rate in comparison to the uniaxial loading conditions. In 1989, Yuuki et al. [106] performed fatigue tests on stainless steel SUS 304 under various biaxial stress conditions and concluded that biaxiality ratio can affect crack growth rates only at high stresses and in the case of low stresses there is no effect of biaxiality ratio on fatigue crack growth rate. Y.C. Lam [107] investigated the fatigue crack growth of long cracks under biaxial loads and reported that when the biaxial stress ratio is much less than one, the crack grows in the direction perpendicular to the dominant stress. However, when the biaxial stress ratio is close to one then the trajectory of the growing crack depends upon the initial crack angle and is more difficult to predict.

Taylor and Lee [94] investigate the biaxiality ratio effects on the fatigue behaviour by employing cruciform specimens of aluminium alloys 1100-H14 and 7075-T651 and concluded that non-singular stress parallel to a crack affects the trajectory of crack growth and fatigue life of the structures made of mentioned aluminium alloys under both in-phase and out-of-phase biaxial loading. Misak et. al. [108] studied the crack growth behaviour of 7075-T6 under biaxial tension–tension fatigue loading. He reported that crack initiation and growth is coplanar with the initial notch under equibiaxial loading with $\lambda = 1$ and non-coplanar under $\lambda = 1.5$ [108], whereas the rate of fatigue crack growth would be higher in case of higher biaxiality ratio i.e. $\lambda = 1.5$ relative to the counterpart under uniaxial fatigue i.e. $\lambda = 0$ or biaxial fatigue with lower biaxiality ratio i.e. $\lambda = 0.5$ or 1 at a given crack driving force level in air environment [109]. Baptista et. al. [110] studied the in-plane biaxial fatigue crack growth on an optimal cruciform specimen for different initial length and angle of crack under different phase shift angle loadings of 30º, 45º, 60º, 90º and 180º and suggested that the loading phase shift angle effects the crack propagation angle. A fracture response of a finite plate having a circular hole with radial cracks emanating at different angles under biaxial loading with biaxiality ratio of 0, 1 and -1 is presented and showed how biaxiality ratio affects the mixed mode stress intensity factors (K_I and K_{II}) [111]. Recently, a complex fatigue failure under biaxial cyclic loadings where fatigue crack paths interact in complicated ways is studied using peridynamic theory and fatigue crack growth paths and fatigue lives for different initial angle of crack are predicted and verified with experimental results for different biaxiality ratios [112].

There are different possible cases of biaxial loading conditions but in this study, in-phase biaxial tension–tension cyclic loading is discussed. Fatigue crack growth behaviour of an infinite plate having two symmetric cracks emanating from certain location and orientation around a hole under far field in phase biaxial tension-tension loading is analyzed and the effects of biaxiality ratio λ, stress ratio R along with the effects of orientation of initial pre-cracks on fatigue crack growth under biaxial loads is also discussed.

6.3.1 Symmetric cracks around a hole in an infinite plate under biaxial loads

To study the effect of initial crack orientation on the FCG behaviour under fatigue loading, two symmetric cracks emanating at different locations at the outer periphery of the hole in an infinite plate are considered under in-phase tension-tension biaxial loading (as shown in Figure 6.29). The location of the initial crack is described by "crack position angle (α)" and its initial angle is determined by "crack orientation angle (β)". Analyses are done for different values of α i.e. 0^0 and 45^0 with different values of β i.e. 0^0, 15^0, 30^0, 45^0. FCG paths and the number of loading cycles for given crack length are estimated for different biaxiality stress ratio i.e. λ = 0, 0.5, 1, 1.5. The geometry of the plate is as follows: diameter of the hole is 17.5 mm and symmetric cracks of initial length $a_0 = 2$ mm is considered, and material properties are as follows: E = 73.1 GPa, ν = 0.33, m = 3, C=9.45e-11 [114]. Walker's equation is used as FCG model and MSED criterion along with the approach of equivalent stress intensity factor is used to predict the crack tip location.

6.3.2 Effect of biaxiality ratio (λ) on FCG

In this section, the effect of biaxiality ratio λ on FCG is presented for the given geometry. For this purpose, analyses with different values of λ i.e. 0, 0.5, 1, 1.5 are repeated and fatigue crack growth paths, SIFs and number of loading cycles N for a given crack length are computed for different orientations of initial pre-cracks using the proposed scheme.

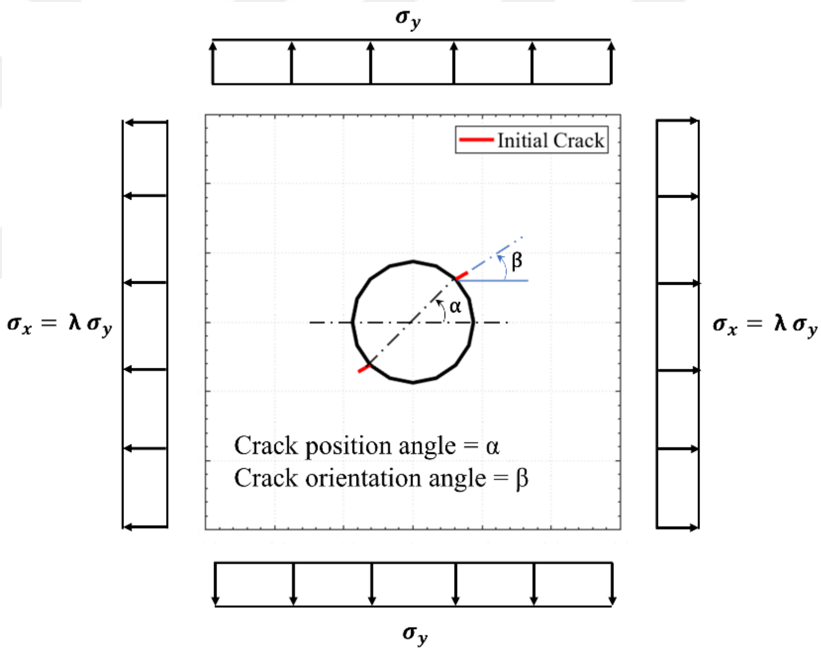

Figure 6.29 : Geometry of the infinite plate with a hole having symmetric cracks.

6.3.2.1 Effect of biaxiality ratio on fatigue crack growth trajectory

Figure 6.30 and Figure 6.31 show the FCG trajectories for symmetric cracks emanating at crack position angles α = 0^0 and 45^0 respectively for different crack orientation angles β = 0^0, 15^0, 30^0, 45^0 for λ = 0 and 0.5. Results show that for the case of uniaxial stress with λ = 0, where only σ_y is applied and σ_x is zero, cracks propagate perpendicular to the direction of the σ_y in each case of crack orientation. Similarly, for λ = 0.5, σ_y is the dominant stress among both the stress as $\sigma_x = 0.5\sigma_y$ and crack propagate perpendicular to direction of σ_y. Results show that there is no effect of the position and orientation of the pre-cracks on the trajectory of the crack growth path for λ = 0, 0.5 and it can be concluded that the FCG path is independent of initial crack location and orientation at the hole for the biaxiality ratio 0 to 0.5.

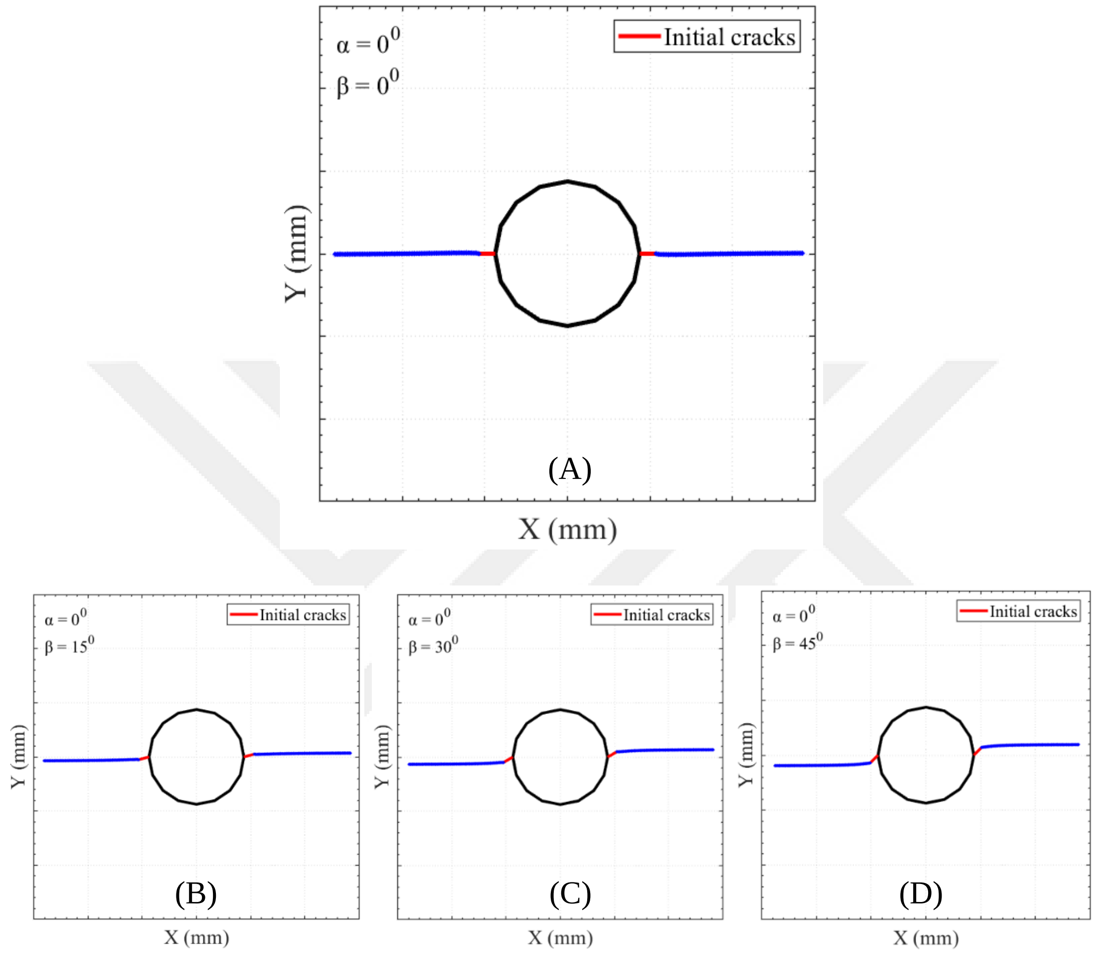

Figure 6.30 : FCG trajectories for λ = 0 and 0.5 at $\alpha = 0^0$; (A) $\beta = 0^0$, (B) $\beta = 15^0$, (C) $\beta = 30^0$, (D) $\beta = 45^0$.

Figure 6.32 and Figure 6.33 show the FCG trajectories for crack position angle $\alpha = 0^0$ and 45^0 respectively for different crack orientation angles $\beta = 0^0$, 15^0, 30^0, 45^0 for λ = 1. For λ = 1 i.e. equibiaxial loading case, results show that cracks tend to propagate diagonally in each case and their paths are sensitive with the location as well as the orientation of the initial pre-crack. In this case, there is no dominant stress direction and both stresses are equal, so crack tries to grow under the effect of both σ_x and σ_y.

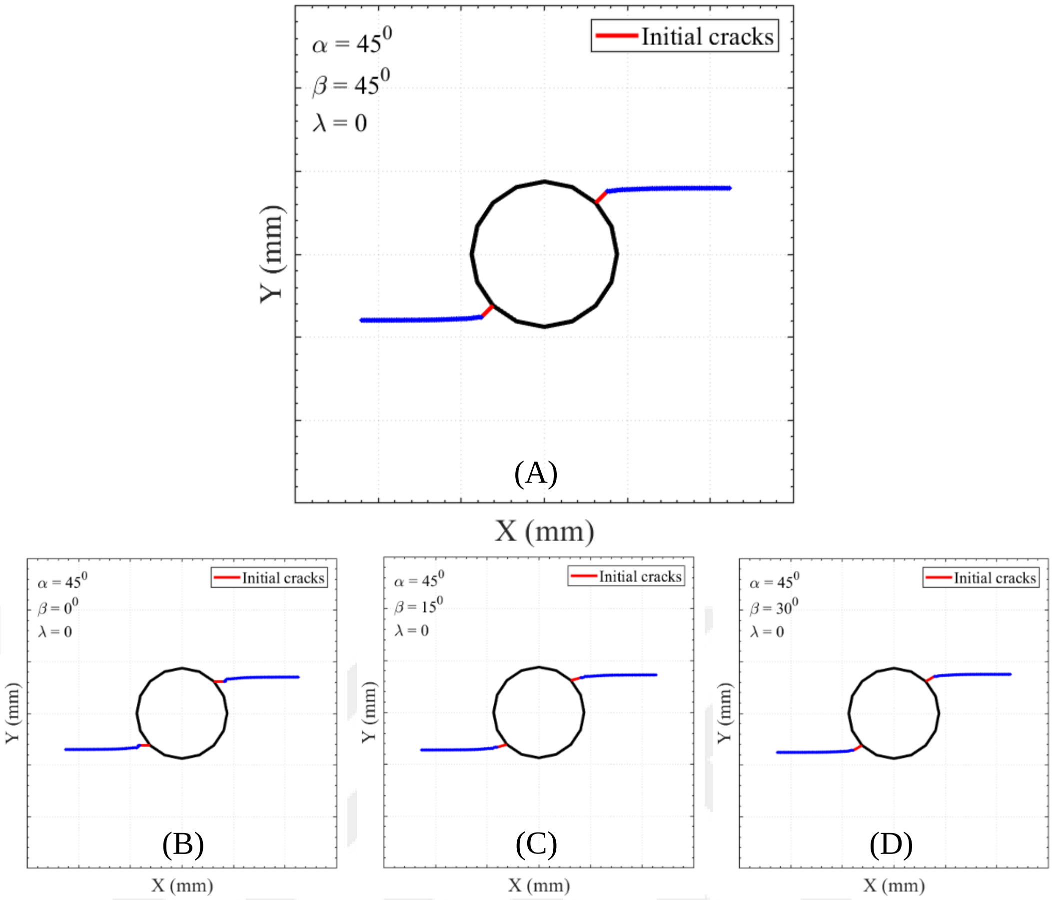

Figure 6.31 : FCG trajectories for λ = 0 and 0.5 at α = 45^0; (A) β = 45^0, (B) β = 0^0, (C) β = 15^0, (D) β = 30^0.

Figure 6.34 and Figure 6.35 show the FCG trajectories for crack position angle α = 0^0 and 45^0 respectively for different crack orientation angles β = 0^0, 15^0, 30^0, 45^0 for λ = 1.5. As in this case λ = 1.5 and σ_x is 1.5 times σ_y, therefore clearly σ_x is the predominant stress among both applied stresses, so the cracks propagate perpendicular to the direction of σ_x in each case. It is important to notice that for case where α = 45^0 and β = 0^0 (as shown in Figure 6.35(B), the crack tends to propagate perpendicular to the σ_x, but due to position and orientation of the pre-crack, it interacts with the hole and inclines towards the hole. If we keep on increasing the crack orientation angle β and when it reaches to value of 6^0 or more, then crack propagates perpendicular to σ_x like other cases e.g. as shown in Figure 6.35(C). Therefore, for this case position and orientation of the pre-crack is important and the trajectory of the path is affected by it. Results suggest that the trajectory of the FCG path under biaxial loading mainly depends upon the biaxiality ratio (λ).

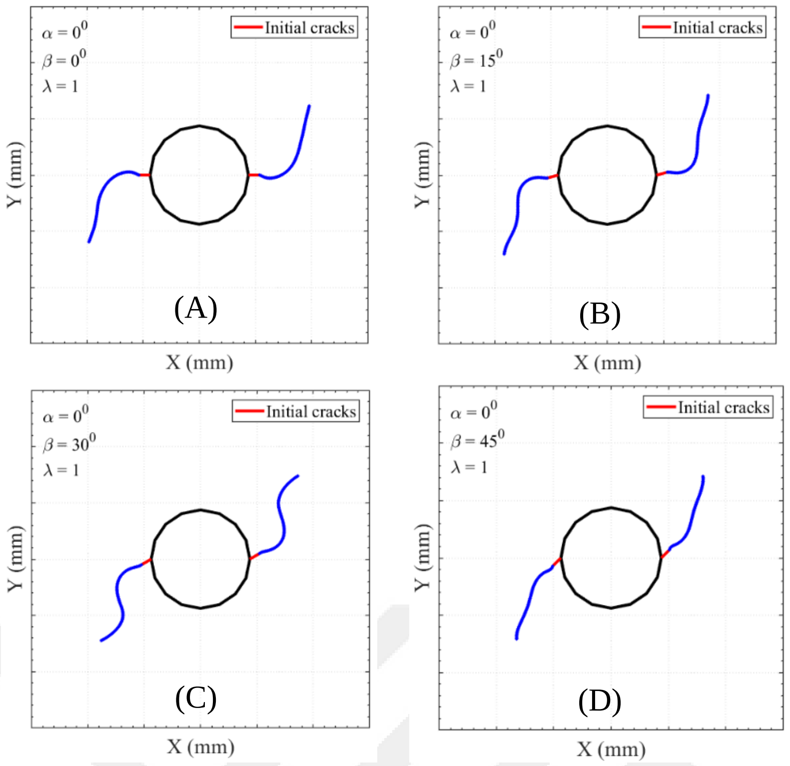

Figure 6.32 : FCG trajectories for λ = 1 at α = 0^0; (A) β = 0^0, (B) β = 15^0, (C) β = 30^0, (D) β = 45^0.

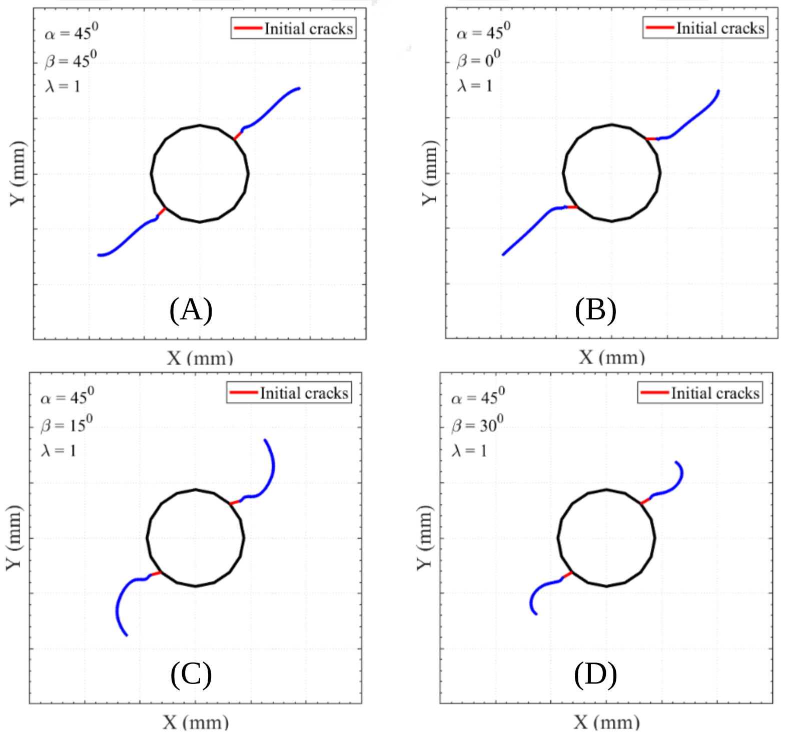

Figure 6.33 : FCG trajectories for λ = 1 at α = 45^0; (A) β = 45^0, (B) β = 0^0, (C) β = 15^0, (D) β = 30^0.

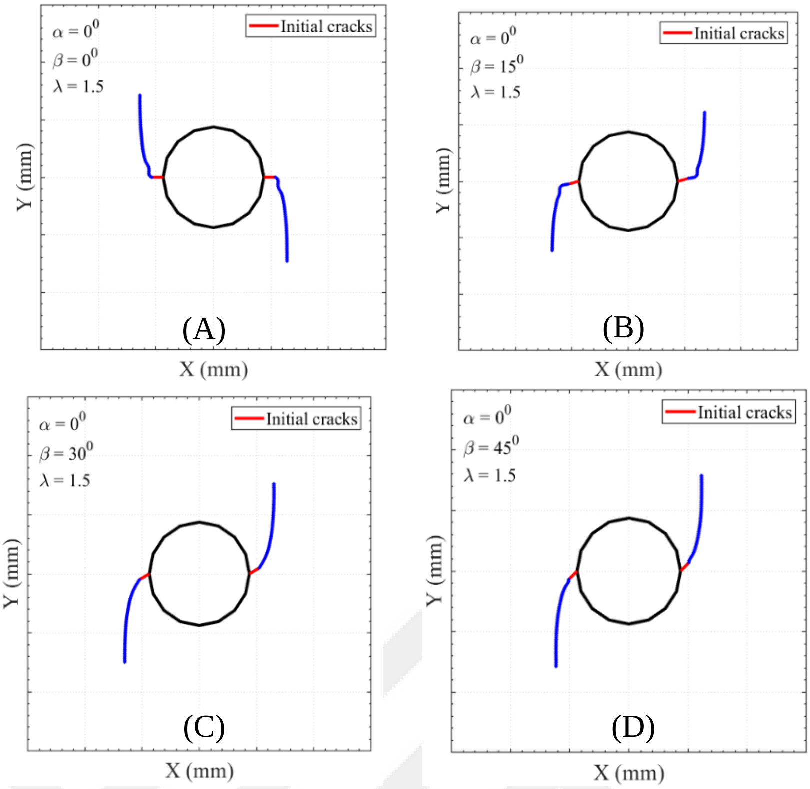

Figure 6.34 : FCG trajectories for λ = 1.5 at α = 0^0; (A) β = 0^0, (B) β = 15^0, (C) β = 30^0, (D) β = 45^0.

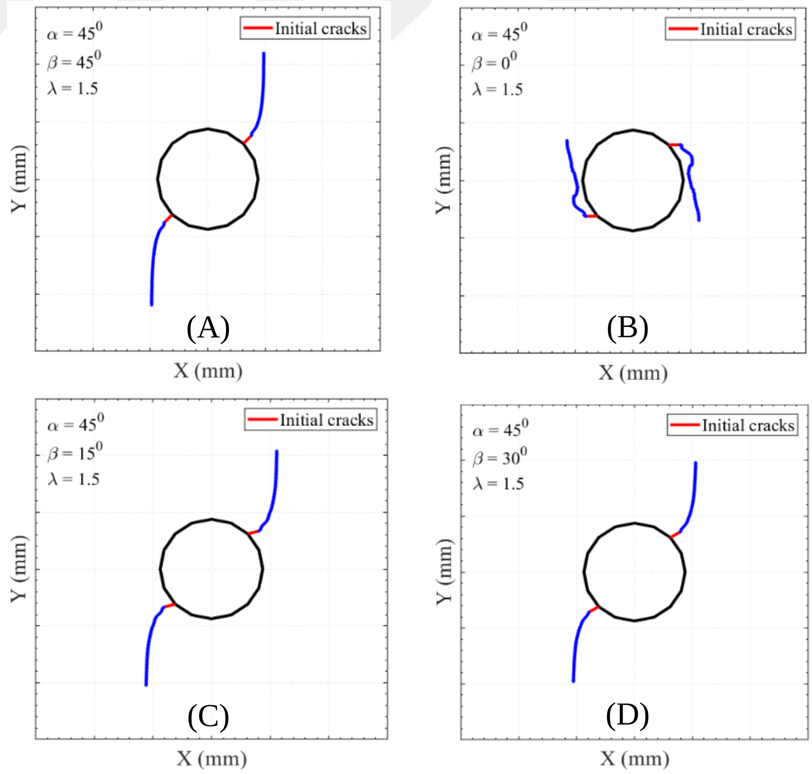

Figure 6.35 : FCG trajectories for λ = 1.5 at α = 45^0; (A) β = 45^0, (B) β = 0^0, (C) β = 15^0, (D) β = 30^0.

6.3.2.2 Effect of biaxiality ratio on initial crack tip propagation angle

Figure 6.36 shows the variation of crack tip propagation angle (with reference from the initial crack angle) of the first step of the analysis with λ for different crack orientation angles β for α = 0^0 and 45^0, respectively. Results show that the value of the initial crack propagation angle depends upon the position as well as the orientation of the pre-crack. For crack position angle α = 0^0 (Figure 6.36(A)), the initial crack propagation angle converges to the same value for λ = 0.5 regardless of the orientation angle of the crack, but the crack propagation angle varies with the orientation of the initial pre-crack for λ ≠ 0.5. A less variation in initial crack propagation angle is observed for $0 \leq \lambda \leq 0.5$ among different crack orientation angles but for $0.5 \leq \lambda \leq 1.5$ this variation is relatively high. Similarly, for crack position angle α = 45^0 (Figure 6.36(B)) the initial crack propagation angle strongly depends upon the biaxiality ratio, but in this case, variation in initial crack propagation angle for crack orientation angles decreases as the λ approaches from 1 to 1.5. From the results, it can be concluded that the initial crack propagation angle depends upon the biaxiality ratio as well as the orientation and the position of the initial pre-crack.

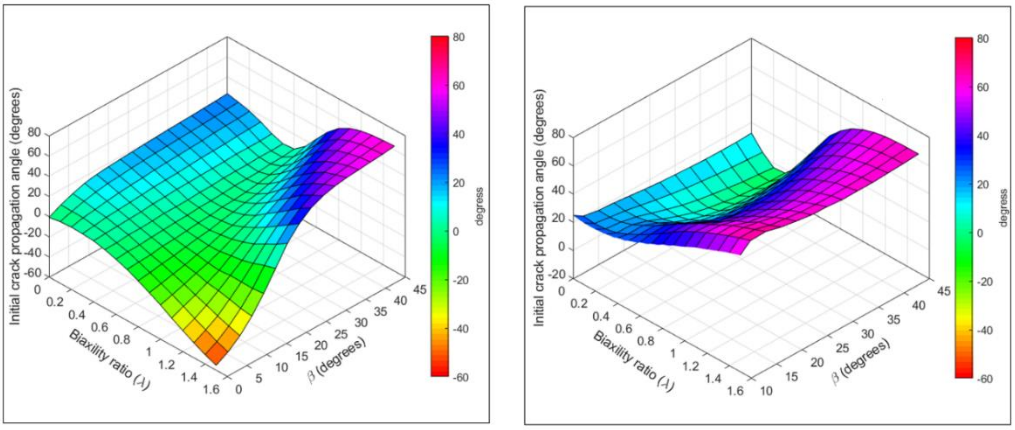

(A) (B)

Figure 6.36 : Variation of initial crack tip angle with λ; (A) α = 0^0, (B) α = 45^0.

6.3.2.3 Effect of biaxiality stress ratio on initial crack tip SIFs ratio

Figure 6.37 shows the variation of the ratio of crack tip SIFs (K_{II} / K_I) of the first step of the analysis with λ for different crack orientation angles β for α = 0^0 and 45^0, respectively. Results show that the initial crack tip SIFs ratio depends upon the position and orientation of the pre-crack and it also depends upon the biaxiality ratio. SIFs ratio increased with the crack orientation angle β at a given value of λ for both cases of crack positions (α), which means that crack tends to move under mixed-mode conditions for a higher crack orientation angle.

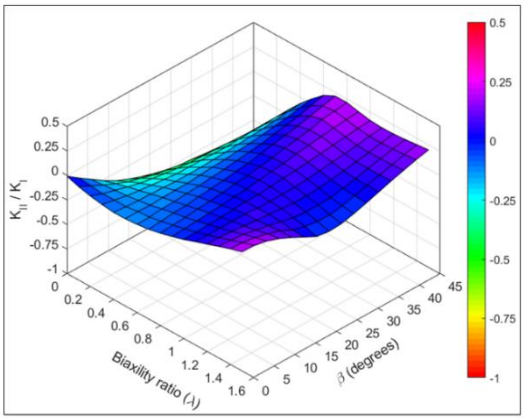

(A)

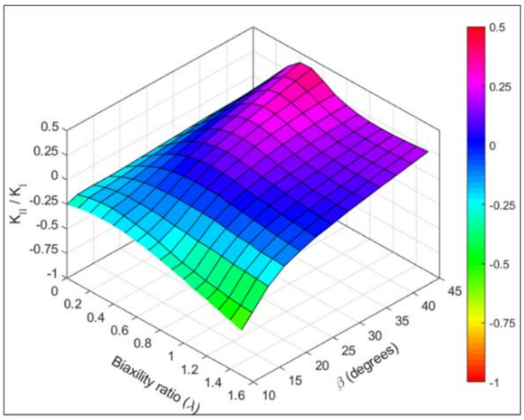

(B)

Figure 6.37 : Variation of the ratio of mode-II to mode-I SIFs (K_2/K_1) with λ.

6.3.2.4 Effect of biaxiality stress ratio on No. of loading cycles

Figure 6.38 shows the number of loading cycles required for the given crack length for each case of crack orientation angle β for $\alpha = 0^0$ and 45^0, respectively. Results show that in both cases of α, the number of loading cycles are same for λ = 0, 0.5 and 1 for each value of angle β, but for λ = 1.5 the rate of crack propagation increases, and a smaller number of loading cycles are required for the given crack length. Therefore, it can be concluded that the number of loading cycles are independent of the biaxiality ratio for $0 \leq \lambda \leq 1$ for each case of crack propagation angle and orientation, but for λ = 1.5, the rate of crack propagation increases regardless of the position and orientation of the pre-crack. Figure 6.39 also shows the same results, where a comparison of the no. of loading cycles required for a crack length of 17 mm is presented for each orientation of initial pre-crack for $\alpha = 0^0$ and $\alpha = 45^0$, respectively.

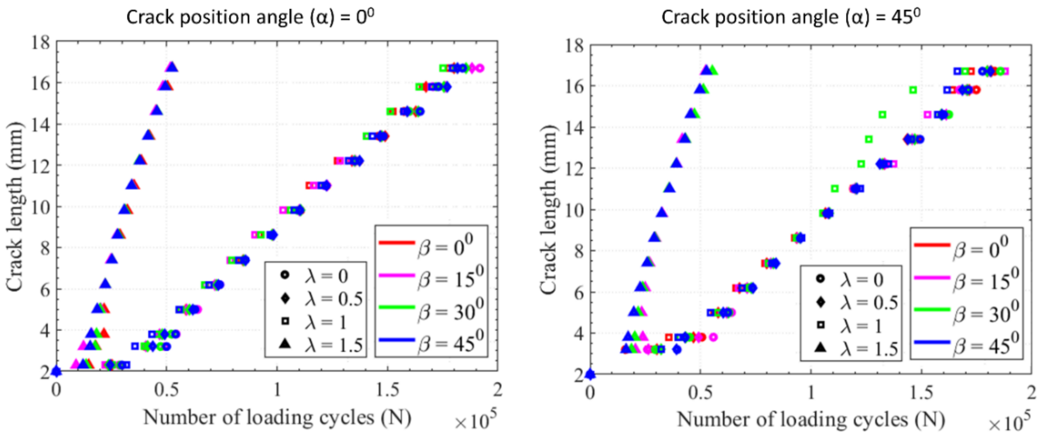

(A) (B)

Figure 6.38 : Comparison of loading cycles required for given crack length for different orientations of initial pre-crack; (A) α = 0^0, (B) α = 45^0.

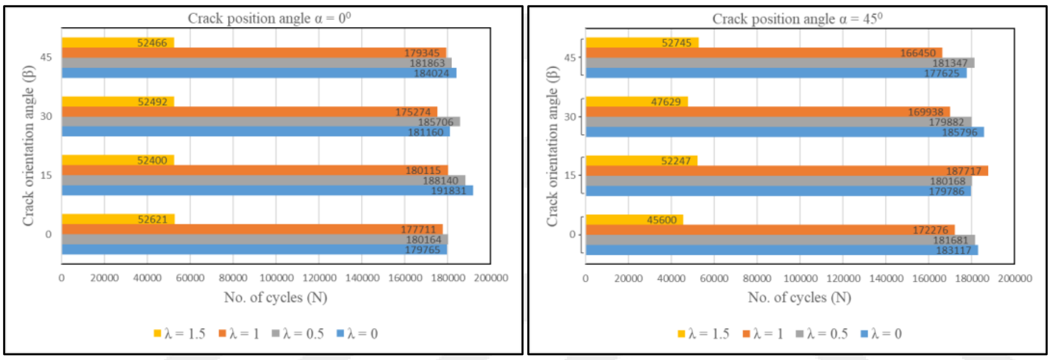

(A) (B)

Figure 6.39 : Comparison of loading cycles required for a crack length of 17 mm for different biaxiality ratio; (A) α = 0^0, (B) α = 45^0.

6.3.3 Effect of stress ratio (R) on FCG

In this section, the effect of stress ratio ($R = \sigma_{min}/\sigma_{max}$) on FCG is presented for the given geometry. Analyses with different values of stress ratio i.e. 0, 0.2, 0.4 are performed. Figure 6.40 shows the crack growth path for different values of R for the case where α = 0, β = 0, results show that there is no effect of R ratio on fatigue crack growth path. The same result is observed for every case of crack position and orientation angle for the given geometry.

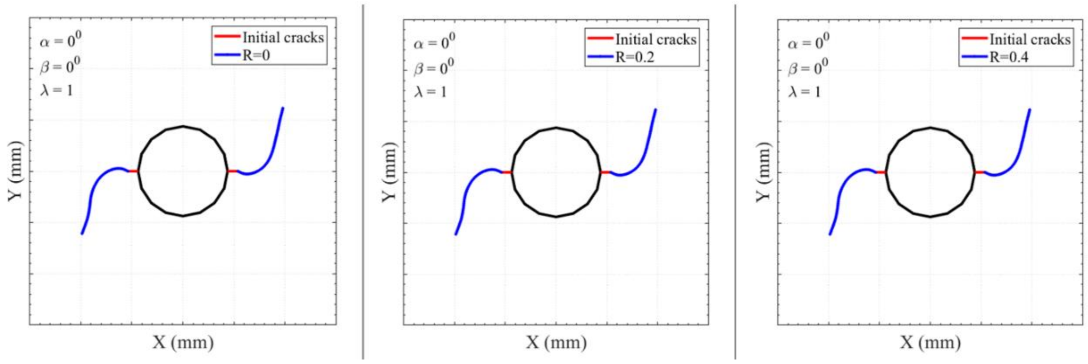

Figure 6.40 : FCG paths for different values of R for α = 0, β = 0; (A) R = 0, (B) R = 0.2, (C) R = 0.4.

Figure 6.41 shows the effect of R-ratio on the rate of crack growth rate for different values of biaxiality ratio for the geometry with α = 0, β = 0. Results show that the rate of crack growth is higher for a higher value of R ratio for a given value of ΔK_{eff}, but for a given σ_{max} the value of ΔK_{eff} is low for a higher value of R-ratio and more loading cycles are required for a given crack length.

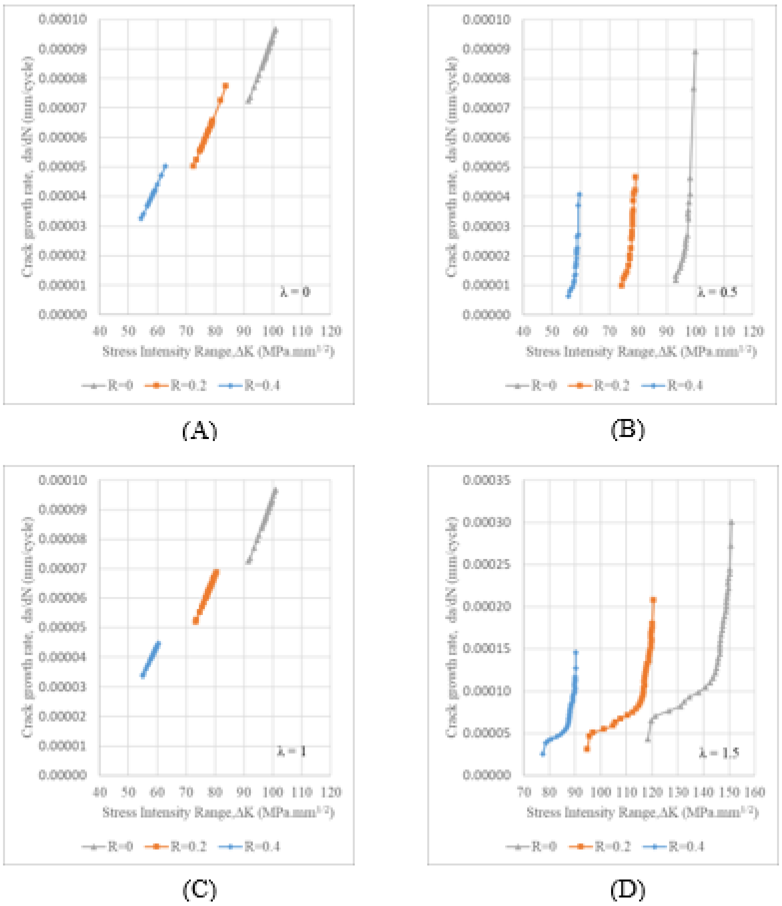

Figure 6.41 : Effect of R on FCG rates for α = 0, β = 0 for different biaxiality ratios; (A) λ = 0, (B) λ = 0.5, (C) λ = 1, (D) λ = 1.5.

Figure 6.42(A) and Figure 6.42(B) show the comparison of number of loading cycles required for a given crack length for the geometry α = 0^0, β = 45^0 and α = 45^0, β = 45^0, respectively. More loading cycles are required for a higher value of R ratio in each case of initial crack geometry. This is because at a higher R the variation of stress from maximum to minimum value is relatively less as compared to the lower value of R and it results in a lower value of ΔK_{eff} and therefore, more loading cycles are required to produce the same crack growth.

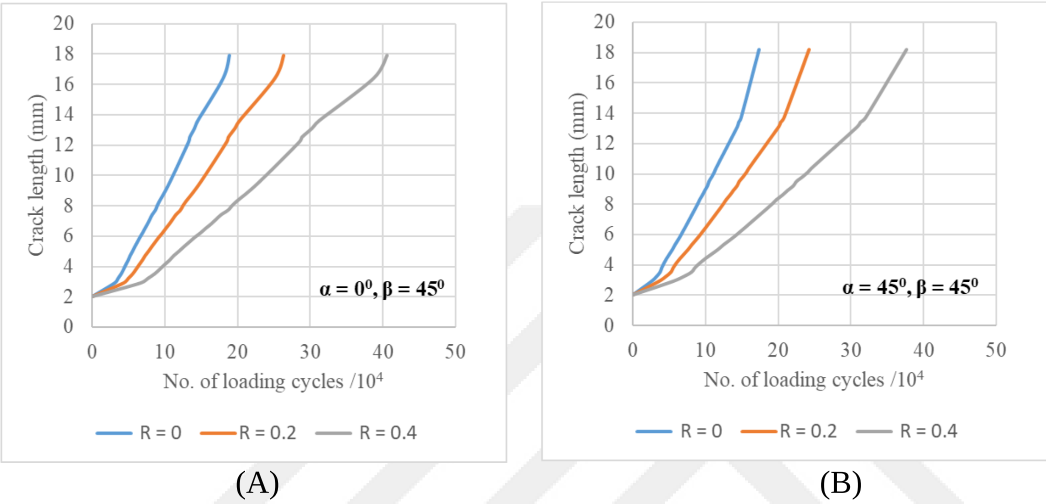

Figure 6.42 : Effect of R on fatigue life of different cases; (A) α = 0^0, β = 45^0, (B) α = 45^0, β = 45^0.

6.3.4 Conclusion of the Study-C

In this study, the analysis of fatigue crack growth in an infinite plate under biaxial loads is presented using the boundary cracklet method (BCM) in the 2-dimensional domain. Walker equation is used for the fatigue crack growth and MSED criterion along with the approach of equivalent stress intensity factor is used to predict the crack tip location during crack propagation in each step under biaxial fatigue loading. The FGC for an infinite plate having symmetric cracks, at different orientations at the hole is studied for different biaxiality stress ratios (λ = 0, 0.5, 1, 1.5) and their effect on crack propagation paths and the number of loading cycles required for given crack extension is studied. Results show that crack tends to propagate perpendicular to the direction of dominant stress in the case of biaxial load where $\lambda \neq 1$ and there is no effect of location and orientation of initial crack on the crack trajectory. For equibiaxial loading where λ =1, the crack tends to propagate diagonally, and its path depends upon the location and orientation of the initial pre-crack. As far as the number of loading cycles for a given crack extension are concerned, equal load cycles are computed for λ = 0, 0.5, 1 whereas it is concluded that for λ = 1.5, the rate of crack growth increases, and fewer loading cycles are required to produce the given crack length. To observe the effect of R-ratio on FCG, analysis with R = 0, 0.2, 0.4 are performed. It is also observed that there is no effect on crack trajectories under different R-ratio. For a given ΔK_{eff} the rate of crack propagation is increased with the increase of R-ratio, but for a given value of σ_{max} the value of ΔK_{eff} is lower for a higher R ratio value, which results in a higher number of required loading cycles to produce the same crack extension. The verification of the proposed method is done by comparing the mode-1 and mode-2 SIFs and crack growth paths computed by BCM for an inclined crack in an infinite plate under different biaxial loading conditions with those computed by the analytical formulation presented in the literature. A close agreement is achieved between the values predicted by BCM and those by the analytical method.

7. CONCLUSION AND FUTURE WORK

In this chapter conclusions drawn from this study are presented in detail. The most relevant potential studies are mentioned as well.

7.1 Conclusion

Fatigue crack growth (FCG) analysis and simulation of the interaction of multiple cracks have been a key issue for decades. There are several two-dimensional methods to investigate fatigue crack propagation such as analytical methods, finite element methods (FEM), extended finite element methods (XFEM), boundary element methods (BEM) and many more. Each one has some advantages as well as limitations and drawbacks considering the preparation of the model, the accuracy of the analysis and required computation time. Therefore, there is always room to develop new tools or schemes to simulate the FCG phenomenon accurately and efficiently.

In this study, the complex phenomenon of multiple cracks interaction under mix mode fatigue loading is analysed by using a newly developed method i.e. Boundary Cracklet Method (BCM). BCM was developed by Prof. Dr. Yavuz (co-advisor of this study) and Prof. Dr. Phoenix at Cornell University. It was developed as a semi-analytical method to calculate the overall stress field and the stress intensity factor (SIF) for crack tips under static loads before. BCM is based on a dislocation distribution approach that approximates the crack opening displacement profiles by using certain power series that satisfy the traction-free condition on crack faces. In this study, BCM is used for the first time to simulate the interacting multiple cracks under fatigue loading.

Throughout the thesis, it has been proved that BCM is an accurate method to simulate fatigue crack propagation (FCP) involving multiple cracks in complex plate geometries under different conditions of fatigue loading. The accuracy of the method was established through the results presented by different researchers which were already available in the literature. Crack tip SIFs, fatigue crack propagation paths and the number of loading cycles required to produce a given crack length extension were used as a parameter for the comparison. A good agreement among the results of each mentioned parameter was achieved for every problem.

Further, the proposed scheme is used to simulate the FCP in different plate geometries involving single as well as multiple cracks under different conditions of fatigue loading which are typical and difficult problems to solve in aerospace structural components. For this purpose, three different studies were conducted, and the findings of each study were published in different international prestigious journals.

In the first study, fatigue crack growth in an infinite plate having two rivet holes separated at some distance and crack emanating from a certain location and orientation from one hole were analysed under three different far-field fatigue loadings i.e. loading in X-direction, loading in Y- direction and shear loading. It is concluded that after some initial number of loading cycles, the fatigue crack growth path becomes perpendicular to the direction of applied loading in case of far-field applied tensile stress (whether in X or Y direction), and similarly, in the case of shear loading, cracks propagate perpendicular to the direction of maximum principal stress and there is no effect of size of initial crack on FCG behaviour. Almost ten times fewer loading cycles are required to reach a certain crack size under shear loading as compared to the normal applied stress, which shows that the rate of crack propagation is ten times higher under shear stress. Therefore, among the given three loading conditions, cycling shear stress is the worst one and needs more attention while designing the structures having rivet holes.

In the second study, fatigue crack growth simulation of interacting multiple cracks in perforated plates with multiple holes is discussed. To show the versatility of the proposed method, emphasis is given to study such complicated problems which cannot be solved by conventional methods to analyse the FCG. Three different studies with multiple cases of initial cracks emanating from side edges, the centre of the plate and the outer periphery of holes in the plate at different orientations are simulated. It has been concluded that the FCG of complicated problems e.g. plate with six holes having seven pre-cracks can be computed fast by the proposed scheme. The conventional methods of analysing FCG have limitations in solving such complex problems. Moreover, the effect of a newly added crack in the vicinity of already present crack is also analyzed and concluded that when two coplanar cracks approach each other, they exhibit an over-constraining phenomenon, which causes the near-tip stress field to be significantly higher than that near a single crack and hence ultimately increases the rate of crack growth. To show the efficiency of a computational method in fatigue problems a new and very useful parameter is also introduced: Yavuz's fatigue computational efficiency factor, $Y_{CF} = \mu N/t$, which is the number of computed million loading cycles per hour (CPU time).

In the third study, the FCG behaviour of symmetric cracks emanating at different locations at the outer periphery of the hole in an infinite plate with different orientations under in-phase tension-tension biaxial loading is shown. As the effects of initial crack orientation under uniaxial fatigue loading are well reported in the literature but the same under the effect of different conditions of biaxial loading has not been investigated. Our results show that BCM is equally effective in predicting the FCG behaviour under complex cases of fatigue loading. It is concluded that cracks tend to propagate perpendicular to the direction of dominant stress in the case of biaxial load where biaxiality ratio $\lambda \neq 1$ and there is no effect of location and orientation of initial crack on the crack trajectory. For equibiaxial loading where $\lambda = 1$, the crack tends to propagate diagonally, and its path depends upon the location and orientation of the initial pre-crack. As far as the number of loading cycles for a given crack extension are concerned, equal load cycles are computed for $\lambda = 0, 0.5, 1$ whereas it is concluded that for $\lambda = 1.5$, the rate of crack growth increases, and fewer loading cycles are required to produce the given crack length. It is also concluded that there is no change in crack trajectories under different stress ratios (R). For a given ΔK_{eff} the rate of crack propagation is increased with the increase in R, but for a given value of σ_{max} the value of ΔK_{eff} is lower for a higher R-value, which results in a higher number of required loading cycles to produce the same crack extension.

7.2 Future Work

Following are some of the recommendations for future studies.

7.2.1 Development of a BCM software to predict the FCG

As the accuracy of the proposed scheme of analysing the interaction of multiple cracks under different conditions of fatigue loads is well established with the examples available in the literature through this study, a BCM software can be developed to simulate the fatigue crack growth behaviour of complex problems having multiple cracks under mix-mode fatigue loading. Currently, most of the available software are either limited to the mode-I and mode-II loading cases only or capable of analysing a single crack only.

7.2.2 Analysing a large array of cracks

In this study, the interaction of a maximum of seven pre-cracks is simulated, but BCM can be applied to a large number of arrays of cracks. With the help of parallel computing, such problems can be solved efficiently by using supercomputers.

7.2.3 Analysing X-shaped (starred), V-shaped (kinked), Y-shaped (branched) and Z-shaped (zig-zagged) cracks

In the future, studies can be performed to study the FCG behaviour of V and Z-shaped kinked or X and Y-shaped branched cracks. There is a strong need to explore a criterion of crack branching to simulate the dynamic crack branching with BCM.

REFERENCES

[1] **Dowling, N. E.** (1993). *Mechanical behaviour of materials: engineering methods for deformation, fracture, and fatigue*. Englewood Cliffs, N.J.: Prentice Hall.

[2] **Boyer, H. E.** (1986). *Atlas of Fatigue Curves* (Ohio: ASM International)

[3] **Nasgro.** (2002). *Fracture mechanics and fatigue crack growth analysis software reference manual*. (version 4.02), NASA Johnson Space Center and Southwest Research Institute.

[4] **J. A. Harter.** (2006). *Afgrow users guide and technical manual*. AFRL-VA-WP-TR-2006, AFGROW, version 4.0011.14.

[5] **Colombo, D. & Giglio, M.** (2006). A methodology for automatic crack propagation modelling in planar and shell FE models. *Eng. Fract. Mech.*, *73*, 490-504.

[6] **Anderson, T. L.** (2005). *Fracture Mechanics: Fundamentals and Applications* (3rd ed.). Boca Raton: CRC Press.

[7] **Belytschko T & Black, T.** (1999). Elastic crack growth in finite elements with minimal remeshing. *International journal for numerical methods in engineering, 45*(5), 601-620.

[8] **Rege, K. & Lemu, H.** (2017). A review of fatigue crack propagation modelling techniques using FEM and XFEM. *IOP Conference Series Materials Science and Engineering. 276*. 012027. 10.1088/1757-899X/276/1/012027.

[9] **Chudnovsky, A. & Kachanov, M.** (1983). Interaction of a crack with a field of microcracks. *International Journal of Engineering Science, 21*, 1009–1018.

[10] **Horii, H. & Nemat-Nasser, S.** (1985). Elastic fields of interacting inhomogenieties. *International Journal of Solids and Structures*, *21*, 731–745.

[11] **Hori, M. & Nemat-Nasser, S.** (1987). Interacting micro-cracks near the tip in the process zone of a macro-crack. *Journal of the Mechanics and Physics of Solids, 35*, 601–629.

[12] **Kachanov, M., Montagut, E. L. & Laures, J. P.** (1990). Mechanics of crack-microcrack interactions. *Mechanics of Materials, 10*, 59–71.

[13] **Laures, J. P. & Kachanov, M.** (1991). Three-dimensional interactions of a crack-front with arrays of penny-shaped microcracks. *International Journal of Fracture, 48*, 255–279.

[14] **Kachanov, M.** (1994). Advances in Applied Mechanics Hutchinson. J. and Wu, T. (eds), *Elastic Solids with Many Cracks and Related Problems*. (pp. 256–426), Academic Press.

[15] **Kachanov, M.** (2003). On the problems of crack interactions and crack coalescence. *International Journal of Fracture, 120*, 537.

[16] **Bilby, B. A. & Eshelby, J. D.** (1968). In Fracture: An Advanced Treatise. H. Liebowitz ed, *Dislocations and the theory of fracture*. (pp. 99-182), N.Y.: Academic Press.

[17] **Hills, D. A., Kelly, P. A., Dai, D. N. & Korsunsky, A. M.** (1998). Solution of crack problems: The Distributed Dislocation Technique. *ASME. J. Appl. Mech, 65*(2), 548.

[18] **Chen, Y. Z., Hasebe, N. & Lee, K. Y.** (2003). *Multiple Crack Problems in Elasticity*. WIT Press, Southampton.

[19] **Bueckner, H.** (1970). Novel Principle for the Computation of Stress Intensity Factors. *Z. angew. Math. Mech, 50*(9), 125-146.

[20] **Aliabadi, M. H. & Rooke, D. P.** (1991). *Numerical Fracture Mechanics*. Kluwer Academic Publishers.

[21] **Atluri S. N.** (1997). *Structural Integrity & Durability*. Tech Science Press.

[22] **Burton, J. K. Jr. & Phoenix, S. L.** (2000). Superposition method for calculating singular stress fields at kinks, branches and tips in multiple crack arrays. *International Journal of Fracture, 102*(2), 99–139.

[23] **TerMaath, S. C.** (2000). *A two-dimensional analytical technique for studying fracture in brittle materials containing interacting kinked and branched cracks*. Ph.D Dissertation, Cornell University.

[24] **Kantorovich, L. V., & Krylov, V. I.** (1964). *Approximate Methods of Higher Analysis*. New York: Interscience Pub.

[25] **Watwood, V.B.** (1969). The finite element method for prediction of crack behaviour. *Nuclear Engineering and Design, 11*(2), 323-332.

[26] **Chan, S., Tuba, I., & Wilson, W.** (1970). On the Finite Element Method in Linear Fracture Mechanics. *Engineering Fracture Mechanics, 2*(1), 1-17.

[27] **Byskov, E.** (1970). The Calculation of Stress Intensity Factors Using the Finite Element Method with Cracked Elements. *International Journal of Fracture Mechanics, 6*(2), 159-167.

[28] **Wilson, W.,** (1973). Finite Element Methods for Elastic Bodies Containing Cracks. In Mechanics of Fracture, G. Sih, ed. Noordho International Publishing, Leyden.

[29] **Hardy, R. H.** (1974). *A High-Order Finite Element for Two-Dimensional Crack Problems*. PhD Thesis, Georgia Institute of Technology, Atlanta, GA.

[30] **Banks-Sills, L. (**1991). Application of the Finite Element Method to Linear Elastic Fracture Mechanics. *Applied Mechanics Reviews, 44*(10), 447–61.

[31] **Banks-Sills, L.** (2010). Update: Application of the Finite Element Method to Linear Elastic Fracture Mechanics. *Applied Mechanics Reviews, 63*(2), 020803.

[32] **Moës, N., Dolbow, J. & Belytschko, T.** (1999). A finite element method for crack growth without remeshing. *International Journal for Numerical Methods in Engineering, 46*(1), 131–50.

[33] **Chahine, E., Laborde, P. & Renard, Y.** (2006). Crack tip enrichment in the XFEM method using a cut off Function. *International journal for numerical methods in engineering, 00*, 1–15.

[34] **Réthoré, J., Gravouil, A. & Combescure, A.** (2005). An energy-conserving scheme for dynamic crack growth using the extended finite element method. *Int J Numer Meth Eng, 63*, 631–659.

[35] **Grégoire, D. Maigre, H., Réthoré, J. & Combescure, A.** (2007). Dynamic crack propagation under mixed-mode loading-Comparison between experiments and X-FEM simulations. *International Journal of Solids and Structures, 44*(20), 6517-6534.

[36] **Prange, C., Loehnert, S. & Wriggers, P.** (2012). Error estimation for crack simulations using the XFEM. *Int. J. Numer. Meth. Engng, 91*, 1459-1474. https://doi.org/10.1002/nme.4331.

[37] **González-Estrada, O. A., Ródenas, J. J., Bordas, S.P.A., Nadal, E., Kerfriden, P. & Fuenmayor, F.J.** (2015). Locally equilibrated stress recovery for goal oriented error estimation in the extended finite element method. *Computers & Structures, 152*, 1-10.

[38] **Sutula, D., Kerfriden, P., van Dam, T. & Bordas, S. P. A.** (2018). Minimum energy multiple crack propagation. Part I: Theory and state of the art review. *Engineering Fracture Mechanics, 191*, 205–24.

[39] **Sutula, D., Kerfriden, P., van Dam, T. & Bordas, S. P. A.** (2018). Minimum energy multiple crack propagation. Part-II: Discrete solution with XFEM. *Engineering Fracture Mechanics, 191*(September 2017), 225–56.

[40] **Sutula, D., Kerfriden, P., van Dam, T. and Bordas, S. P. A.** (2018). Minimum energy multiple crack propagation. Part III: XFEM computer implementation and applications. *Engineering Fracture Mechanics, 191*, 257–76.

[41] **Alig, Z. & Wang, H.** (2017). A fast and exact computational method for crack propagation based on extended finite element method. https://doi.arXiv (abs/1708.01610).

[42] **Cruse, T. A.** (1988). Computational Mechanics. vol. 1 of Mechanics, *Boundary Element Analysis in Computational Fracture Mechanics.* Kluwer Academic, Dordrecht, Netherlands.

[43] **Aliabadi, M. H.** (1997). Boundary element formulations in fracture mechanics. *Applied Mechanics Reviews, 50*(2), 83-96.

[44] **Dumir, P. C. & Mehta, A. K.** (1987). Boundary element solution for elastic orthotropic half-plane problems. *Computers and Structures, 26*(3), 431–438.

[45] **Silveira, N. P. P., Guimaraes, S. & Telles, J. C. F.** (2005). A numerical Green's function BEM formulation for crack growth simulation. *Engineering Analysis with Boundary Elements, 29*, 978–985.

[46] **Blandford, G. E., Ingraffea, A. R. & Liggett, J. A.** (1981). Two-dimensional stress intensity factor computations using the boundary element method. *International Journal for Numerical Methods in Engineering, 17*(3), 387–404.

[47] **Sollero, P. & Aliabadi, M. H.** (1993). Fracture mechanics analysis of anisotropic plates by the boundary element method. *International Journal of Fracture, 64*(4), 269–284.

[48] **Sollero, P., Aliabadi, M. H. & Rooke, D. P.** (1994). Anisotropic analysis of cracks emanating from circular holes in composite laminates using the boundary element method. *Engineering Fracture Mechanics, 49*(2), 213–224.

[49] **Pu, J.** (2004). A doubly iterative BEM for solving crack closing in an elastic body. *Computers & Structures*, *82*(1), 25-33.

[50] **Crouch, S. L. & Starfield, A. M.** (1983). *Boundary Element Methods in Solid Mechanics.* George Allen and Unwin, London, UK.

[51] **Shen, B. & Stephansson, O.** (1994). Modification of the G-criterion for crack propagation subjected to compression. *Engineering Fracture Mechanics, 47*(2), 177–189.

[52] **Shi, J., Shen, B., Stephansson, O. & Rinne, M.** (2014). A three-dimensional crack growth simulator with displacement discontinuity method. *Engineering Analysis with Boundary Elements*, *48*, 73-86.

[53] **Portela, A., Aliabadi, M. H. & Rooke, D. P.** (1992). Dual Boundary element method: efficient implementation for crack problems. *International Journal of Numerical Methods in Engineering, 33*, 1269-1287.

[54] **Yan, X.** (2006). A brief evaluation of approximation methods for microcrack shielding problems. *ASME Journal Applied Mechanics, 73,* 694-696.

[55] **Kebir, H., Roelandt, J. M. & Chambon, L.** (2006). Dual boundary element method modelling of aircraft structural joints with multiple site damage. *Engineering Fracture Mechanics, 73*, 418-434.

[56] **Leonel, E. D. & Venturini, W. S**. (2010). Dual boundary element formulation applied to analysis of multifractured domains. *Engineering Analysis with Boundary Elements, 34,* 1092-1099.

[57] **Leonel, E. D. & Venturini, W. S.** (2010). Non-linear boundary element formulation with tangent operator to analyses crack propagation in quasi-brittle materials. *Engineering Analysis with Boundary Elements, 34*, 122-129.

[58] **Yan, X.** (2005). Microdefect interacting with a finite main crack. *Journal of Strain Analysis Engineering Design, 40,* 421-430.

[59] **Kumar, V. & Mukherjee, S.** (1997). Boundary-integral equation formulation for time dependent inelastic deformation in metals. *International Journal of Mechanical Sciences, 19*(12), 713–24.

[60] **Poon, H., Mukherjee, S. & Bonnet, M.** (1998). Numerical implementation of a CTO-based implicit approach for solution of usual and sensitivity

problems in elasto-plasticity. *Engineering Analysis with Boundary Elements, 22*, 257-269.

[61] **Botta, A. S., Venturini, W. S. & Benallal, A.** (2005). BEM applied to damage models emphasizing localization and associated regularization techniques. *Engineering Analysis with Boundary Elements, 29*, 814-827.

[62] **Leonel, E. D. & Venturini, W. S.** (2010). Non-linear boundary element formulation with tangent operator to analyse crack propagation in quasi-brittle materials. *Engineering Analysis with Boundary Elements, 34*(2), 122-129.

[63] **Yan, X.** (2007). Automated simulation of fatigue crack propagation for two-dimensional linear elastic fracture mechanics problems by boundary element method. *Engineering Fracture Mechanics*, *74*(14), 2225-2246.

[64] **Nikishkov, G. P., Park, J. H. & Atluri, S. N.** (2001). SGBEM-FEM alternating method for analyzing 3D non-planar cracks and their growth in structural components. *Comput. Model. Eng. Sci., 2,* 401-22.

[65] **Yang, Z.** (2006). Fully automatic modelling of mixed-mode crack propagation using scaled boundary finite element method. *Eng. Fract. Mech., 73* 1711-31.

[66] **Yang, Z. J., Wang, X. F., Yin, D. S. & Zhang, C.** (2015). A non-matching finite element-scaled boundary finite element coupled method for linear elastic crack propagation modelling. *Computers and Structures, 153,* 126–36.

[67] **Bordas, S., Rabczuk, T. & Zi, G.** (2008). Three-dimensional crack initiation, propagation, branching and junction in non-linear materials by an extended meshfree method without asymptotic enrichment. *Eng. Fract. Mech, 75*, 943-60.

[68] **Tanaka, S., Suzuki, H., Sadamoto, S., Imachi, M. & Bui, T.Q**. (2015). Analysis of cracked shear deformable plates by an effective meshfree plate formulation. *Engineering Fracture Mechanics, 144*, 142-57.

[69] **Khosravifard, A., Hematiyan, M. R., Bui, T. Q. & Do, T. V.** (2017). Accurate and efficient analysis of stationary and propagating crack problems by meshless methods. *Theoretical and Applied Fracture Mechanics, 87*, 21-34.

[70] **Nguyen-Xuan, H., Liu, G.R., Bordas, S., Natarajan, S. & Rabczuk, T.** (2013). An adaptive singular ES-FEM for mechanics problems with singular field of arbitrary order. *Computer Methods in Applied Mechanics and Engineering, 253*, 252-73.

[71] **Liu, G. R., Nourbakhshnia, N. & Zhang, Y. W.** (2011). A novel singular ES-FEM method for simulating singular stress fields near the crack tips for linear fracture problems. *Engineering Fracture Mechanics, 78*(6), 863-76.

[72] **Liu, Z., Zheng, H. & Sun, C.** (2016). A domain decomposition-based method for two-dimensional linear elastic fractures. *Engineering Analysis with Boundary Elements, 66*, 34-48.

[73] **Zhang, H. H., Li, L. X., An, X. M. & Ma, G. W.** (2010) Numerical analysis of 2-D crack propagation problems using the numerical manifold method. *Engineering Analysis with Boundary Elements, 34*(1), 41-50.

[74] **Mirsayar, M. M.,** (2015). Mixed mode fracture analysis using extended maximum tangential strain criterion. *Materials & Design, 86*, 941–7.

[75] **Griffith, A. A. & Eng, M.** (1920) “VI. The phenomena of rupture and flow in solids. *Philosophical Transactions of the Royal Society of London Series A, Containing Papers of a Mathematical or Physical Character, 221*(582–593), 163-198.

[76] **Griffith, A. A.** (1924). The theory of rupture, *Proc. 1st Intern. Congr. Appl. Mech.*, Delft, 55–63.

[77] **Irwin, G. R.** (1957). Analysis of stresses and strains near the end of a crack traversing a plate. *J. Applied Mechanics, 24*, 361–364.

[78] **Chang, K. J.** (1981). On the maximum strain criterion – a new approach to the angled crack problem. *Eng Fract Mech,14*, 107-24.

[79] **Dowling, N. E. & Begley, J. A.** (1976). Fatigue Crack Growth During Gross Plasticity and the J-Integral. *ASTM STP 590, American Society for Testing and Materials*, Philadelphia, PA, 82–103.

[80] **Yavuz, A. K., Phoenix, S. L. & Termaath, S. C.** (2006). An accurate and fast analysis for strongly interacting multiple crack configurations including kinked (V) and branched (Y) cracks. *International Journal of Solids and Structures, 43*, 6727-6750.

[81] **Yavuz, A. K. & Phoenix, S. L.** (2009). Easy Handling of Complex Multiple Crack Interactions by Boundary Cracklet Method (BCM). *Collection of Technical Papers - AIAA/ASME/ASCE/AHS/ASC Structures, Structural Dynamics and Materials Conference.* 10.2514/6.2009-2627.

[82] **Yavuz, A. K., Phoenix, S. L. & TerMaath, S. C.** (2006). Multiple crack analysis in finite plates. *AIAA Journal, 44*(11), 2535-2541.

[83] **Williams, M. L.** 1952. Stress singularities resulting from various boundary conditions in angular corners of plates in extension. *ASME Journal of Applied Mechanics 19,* 526–528.

[84] **Paris, P. C. & Erdogan, F.** (1960). A critical analysis of crack propagation laws. *J. Basic Eng., 85*(4), 528-534. https://doi.org/10.1115/1.3656900.

[85] **Forman, R. G., Kearney, V. E. & Engle, R. M.** (1967). Numerical Analysis of Crack Propagation in Cyclic-Loaded Structures. *ASME. J. Basic Eng., 89*(3), 459–463.

[86] **Walker, K.** (1970). *The Effect of Stress Ratio During Crack Propagation and Fatigue for 2024-T3 and 7075-T6 Aluminum. In STP462-EB Effects of Environment and Complex Load History on Fatigue Life*. ed. M. Rosenfeld, West Conshohocken, PA: ASTM International, 1-14.

[87] **Tanaka, K.** (1974). Fatigue crack propagation from a crack inclined to the cyclic tensile axis. *Engineering Fracture Mechanics, 6*(3), 493-507.

[88] **Erdogan, F. & Sih, G. C.** (1963). On the Crack Extension in Plates Under Plane Loading and Transverse Shear. *ASME. J. Basic Eng., 85*(4): 519–525.

[89] **Sih, G. C.** (1978). Strain-energy-density factor applied to mixed mode crack problems. *International Journal of Fracture, 10*, 305-321.

[90] **Hussain, M., Pu, S. & Underwood, J.** (1974). Strain Energy Release Rate for a Crack Under Combined Mode I and Mode II, in Fracture Analysis. *Proceedings of the 1973 National Symposium on Fracture Mechanics,* Part II, ed. G. Irwin (West Conshohocken, PA: ASTM International, 2-28.

[91] **Yavuz, A. K., Senalp, A. D., Turkmen, H. S., & Phoenix, S. L.** (2012). Interacting Fatigue Crack Growth Analysis with Boundary Cracklet Method. *Advanced Materials Research, 445*, 1017–1022.

[92] **Eftis, J. & Subramonian, N.** (1978). The inclined crack under biaxial load. *Engineering Fracture Mechanics, 10*(1), 43-67.

[93] **Stamenković, D., Maksimović, K., Nikolić-Stanojević,V., Maksimović, S., Stupar, S., Ivana, V. & Serbia, T.** (2010). Fatigue life estimation of notched structural components. *Journal of Mechanical Engineering, 56127*, 620-178.

[94] **Seah, T. T. & Qian, X.** (2018). An interaction factor to estimate the over-constraining effect in plates with co-planar cracks. *Engineering Fracture Mechanics, 199*, 13-28.

[95] **Lee, E. U. & Taylor, R. E.** (2011). Fatigue behaviour of aluminum alloys under biaxial loading. *Engineering Fracture Mechanics, 78*(8), 1555-1564.

[96] **Huynh, H. D., Nguyen, M. N., Cusatis, G., Tanaka, S. & Bui, T. Q.** (2019). A polygonal XFEM with new numerical integration for linear elastic fracture mechanics. *Engineering Fracture Mechanics, 213*, 241-263.

[97] **Leonel, E. D. & Venturini, W. S.** (2011). Multiple random crack propagation using a boundary element formulation. *Engineering Fracture Mechanics, 78*(6), 1077-1090.

[98] **Liu, Y. J., Li, Y. X. & Xie, W.** (2017). Modeling of multiple crack propagation in 2-D elastic solids by the fast multipole boundary element method. *Engineering Fracture Mechanics, 172*, 1-16.

[99] **Bouchard, P. O., Bay, F. & Chastel, Y.** (2003). Numerical modelling of crack propagation: automatic remeshing and comparison of different criteria. *Computer Methods in Applied Mechanics and Engineering, 192*(35-36), 3887-3908.

[100] **Ooi, E. T., Man, H., Natarajan, S. & Song, C.** (2015). Adaptation of quadtree meshes in the scaled boundary finite element method for crack propagation modelling. *Engineering Fracture Mechanics, 144*, 101-117.

[101] **Zhang, X., Wang, J., Wei, W., Ji, X., Chen, B. & Fang, G.** (2019). Simulation of fatigue cracks growth processes of two parallel cracks in thin plate pulled by the constant amplitude cyclic loading. *Journal of*

the Brazilian Society of Mechanical Sciences and Engineering, 41(374).

[102] **Mouritz, A. P.** (2012). Introduction to Aerospace Materials. *Fatigue of aerospace materials.* Woodhead Publishing, pp. 469-497.

[103] **Hopper, C. D. & Miller, K. J.** (1977). Fatigue Crack Propagation in Biaxial Stress Fields. *J. Strain Anal., 12*(1), 23–28

[104] **Liu, A. F., & Dittmer, D. F.** (1978). *Effect of Multiaxial Loading on Crack Growth*, Vol 1–3, Air Force Wright Patterson, Aeronautical Lab, Ohio, (Report No. AFFDL-TR-78-175).

[105] **Anderson, P. R. G. & Garrett, G. G.** (1980). Fatigue Crack Growth Rate Variations in Biaxial Stress Fields. *International Journal of Fracture, 16*, 111–116.

[106] **Yuuki, R., Akita, K. & Kishi, N.** (1989). The Effect of Biaxial Stress and Changes of State on Fatigue Crack Growth Behaviour. *Fatigue and Fracture of Engineering Materials and Structures, 12*, 93-103.

[107] **Lam, Y. C.** (1993). Fatigue Crack Growth Under Biaxial Loading. *Fatigue Fract. Eng. Mater. Struct., 16*(4), 429–440.

[108] **Misak, H. E., Perel, V. Y., Sabelkin, V. & Mall, S.** (2013). Crack Growth Behaviour of 7075-T6 under Biaxial Tension–Tension Fatigue. *Int. J Fatigue, 55*, 158-165.

[109] **Misak, H. E., Perel, V. Y., Sabelkin, V. & Mall, S.** (2014). Biaxial Tension-Tension Fatigue Crack Growth Behaviour of 2024-T3 under Ambient Air and Saltwater Environments. *Engineering Fracture Mechanics, 118*, 83-97.

[110] **Baptista, R., Cláudio, R. A., Reis, L., Madeira, J. F. A. & Freitas, M.** (2016). Numerical study of in-plane biaxial fatigue crack growth with different phase shift angle loadings on optimal specimen geometries. *Theoretical and Applied Fracture Mechanics, 85* (Part A), 16-25.

[111] **Khatri, K. & Lal, A.** (2018). Stochastic XFEM based fracture behaviour and crack growth analysis of a plate with a hole emanating cracks under biaxial loading. *Theoretical and Applied Fracture Mechanics, 96*, 1-22.

[112] **Liu, Y., Deng, L., Zhong, W., Xu, J., & Xiong, W.** (2020). A new fatigue reliability analysis method for steel bridges based on peridynamic theory. *Engineering Fracture Mechanics, 236*, 107214.

[113] **Eftis, J. & Subramonian, N.** (1978). The inclined crack under biaxial load. *Engineering Fracture Mechanics, 10*(1), 43-67.

[114] **Boljanović, S., Maksimović, S. & Posavljak, S.** (2020). Analysis of two symmetric cracks at a hole under cyclic loading. *Acta Technica Corvininesis Jul-Sep 2020- Bulletin of Engineering, 13*(3), 67-70.

CURRICULUM VITAE

Name Surname **:** Talal AHMED

Place and Date of Birth **:**

EDUCATION:

- **B.Sc.:** 2005, University of Engineering and Technology, Taxila, Pakistan. Mechanical Engineering Department
- **M.Sc.:** 2010, University of Engineering and Technology, Taxila, Pakistan. Mechanical Engineering Department

PROFESSIONAL EXPERIENCE AND REWARDS:

- Completed B.Sc. engineering with Honours.
- 2006-2017 worked as design engineer in different R & D organizations.

PUBLICATIONS FROM THE THESIS:

- Yavuz, A. K., **Ahmed, T**. & Türkmen, H. S. (2020). Computer Simulation of Fatigue Crack Growth under Different Loading Conditions using Boundary Cracklet Method (BCM). *Advances in Science and Engineering Technology International Conferences (ASET), Dubai, UAE, 2020*,1-6. DOI: 10.1109/ASET48392.2020.9118170

- **Ahmed, T.**, Yavuz, A. K. & Türkmen, H. S. (2020). Fatigue crack growth simulation of interacting multiple cracks in perforated plates with multiple holes using boundary cracklet method. *Fatigue Fract. Eng. Mater Struct*, 1–16. DOI: org/10.1111/ffe.13359

- **Ahmed, T.**, Yavuz, A. K. & Türkmen, H. S. (2021). Fatigue crack growth analysis of biaxially loaded hole edge cracks using boundary cracklet method (BCM), submitted to a peer-reviewed journal and is under review process.